Feedback Control of Transient Smoke Emissions from Compression Ignition Engines

by

Guang Hong

A Dissertation
Submitted to the University of Cambridge for the
Degree of Doctor of Philosophy

Trinity College

November, 1988

To my motherland

Keywords

Smoke Sensor, Diesel Particulates, Engine Emissions, Engine Modelling, Parameter Estimate, Feedback Control, Engine Smoke Control, Self-tuning control

Summary

The smoke emission from diesel engines is now regarded as a very significant problem because of greater public consciousness of environment damage, and in some countries legislation is now in force limiting the particulate generation. This thesis describes work on the feedback control of diesel smoke, in which a new smoke sensor was used to make real-time smoke detection feasible during engine transients. Experimental results demonstrated that this control system significantly reduced the smoke 'puff' normally generated by a sudden power demand.

An advanced identification method is presented, which models the engine based on experiments. This method is dependent on an understanding of the sampling action of the fuel injector on a diesel engine and utilizes a synchronization technique for acquiring the information of the engine dynamics. Parameter estimation was used to derive the models of speed-to-fuel rack and smoke-to-fuel rack. The nonlinearity of the model of smoke-to-fuel rack was investigated in a preliminary way.

Two kinds of controllers, non-adaptive controllers and self-tuning controllers, were developed and implemented on a real engine. The non-adaptive controllers, designed with a combination of PI control algorithm and optimisation of the engine performance, were of relatively low complexity and had the ability to work effectively at light-load engine conditions. The self-tuning controllers associated with a smoke predictor were applied to solve the problems of the system nonlinearity and enable the control system to work in a wider range of engine operations. The problem associated with self-tuning controllers were demonstrated but the possibility of using such controllers was proven.

Preface

The work described in this dissertation was carried out by the author at the Cambridge University Engineering Department between April 1985 and October 1988, under the supervision of Dr. N. Collings. The research work was carried out in part fulfillment of the requirements for the Degree of Doctor of Philosophy. This dissertation presents the original work of the author except where otherwise stated and has not been submitted for a degree or other qualification at any other university.

I would like to express my sincere gratitude to my supervisor, Dr. N. Collings, for introducing me to this subject and his encouragement and continued guidance during the period of research. Many thanks are due to Dr. Steve Williams for his kindness of discussing my work and providing valuable suggestions.

Thanks must also go to the research students and staff in Heat Laboratory for their help in reading the manuscript of my thesis and technical assistant in the experiments.

Financial supports from Chinese government, Trinity College and Cambridge University Engineering Department are gratefully acknowledged.

Trinity College
Cambridge

Guang Hong
November, 1988

Contents

List of Principle Symbols

$a_{i(j)}$	the ith parameter of the denominator in model j
$A(z^{-1})$	denominator of the transfer function in Z domain
$b_{i(j)}$	the ith parameter of the numerator in model j
$B(z^{-1})$	numerator of the transfer function in Z domain
$C_j(z^{-1})$	transfer function of controller j
$G(s)$	transfer function in s domain
$G(z^{-1})$	transfer function in Z domain
J	objective function in optimisation
k_i	integral gain
k_p	proportional gain
n_a	order of the denominator in the transfer function
n_b	order of the numerator in the transfer function
nd	sample intervals taken by the time delay
Nm	Newton force–meter
p	pole in the characteristic equation
q^{-1}	back shift operator
r	system input
RPM	revolutions per minute
$R(z^{-1})$	system input in Z domain
t	time
T_c, T_s	sample interval
T_r	rise time
T_{st}	settling time
$T(z^{-1})$	polynominator in the designed characteristic equation
u	control actuation
v	white noise sequence
W	estimate gain
$\mathbf{W}$	matrix of the estimate gains
y	system output
$Y(z^{-1})$	system output in Z domain
z	z transform operator
$\bar{\alpha}$	factor matrix in parameter estimate

$\bar{\beta}$	factor matrix in parameter estimate
θ	vector of the parameters in a model
Θ	matrix of the parameters in the models
$\hat{\theta}$	estimated θ
ϕ	vector of the sampled actuation inputs and outputs
Φ	matrix of the sampled actuation inputs and outputs
ω	frequency

Chapter One

Introduction

1.1 Motivation

Although diesel engines have a higher thermal efficiency than gasoline engines, and can be more easily made in large displacements, they are not without emissions problems. Gasoline engines have three principle noxious emissions — nitrous oxide, carbon monoxide and unburnt hydrocarbons. The latter two are normally a result of running close, or richer than stoichiometry although hydrocarbons can also be a problem at over-lean conditions. In the diesel, the mixture is always lean overall, and it is nitrous oxide and particulates which are the primary emissions. The generation of particulates is a complex process, but essentially results from the fact that combustion in a diesel takes place as a diffusion flame, i.e., the flame is rich.

The particulate emissions normally appear as black smoke, and not only cause air pollution but also with serious overfuelling result in reduced fuel economy. Table 1[B1] shows that a comparison of a typical diesel engine exhaust with a typical

Table 1.1 Typical emission levels from Diesel and Petrol engines

	Diesel engine	Petrol engine
Particulate matter	0.5 g/m^3	0.01 g/m^3
Carbon Monoxide	<0.1% by volume	<10% by volume
Hydrocarbons	<300 ppm	<1000 ppm
Oxides of Nitrogen	1000-4000 ppm	2000-4000 ppm

petrol engine is favourable to the diesel engine except for particulate matter (smoke).

Much effort has been concentrated on understanding the particulate production, and how reductions might be made by improving the engine design. In addition particle collection in the exhaust by means of the traps requires a detailed knowledge of the particulates' size distribution, composition etc. Particle emission depends on whether the fuel burns completely or not. Two types of factors can be identified that affect diesel particulate production:

(a):	(b):
chamber type and proportions (pre/main)	injection timing
chamber shape	injection period
stroke/bore ratio	inlet air temperature and pressure
cylinder size	exhaust back pressure
compression ratio	A/F ratio
fuel quality	swirl velocity
injection pressure	cold start

The factors in (a) are mainly decided by the engine design which can be treated as static factors. The factors in (b) are active in a dynamic system and thus it may be important to control these to enable the engine to perform better. This is because they determine the mixture of air and fuel in the burning process, and then the real-time particulate production.

Electronic feedback control is a novel technique for real-time smoke detection by controlling the dynamic factors in (b). Much work has been done on electronic control of IC engines, but feedback control of diesel smoke is still a new area of research. The reason is that a sensor with a sufficiently fast frequency response to be the basic

transducer component in the closed loop has not previously been available. The widely-used closed loop control system cannot be utilised without a suitable sensor to get accurate information about the controlled factor. Thus realising a sensor and then some routine to control the diesel smoke is exciting the minds of many researchers.

1.2 Literature review

1.2.1 Diesel particulate generation

For regulatory purposes, diesel particulates are defined as solid or liquid matter that collects on an absolute filter in a diluted exhaust stream at a temperature equal to or less than 52^0C. A typical particulate sample includes solid material (carbon) and volatile material consisting of unburned hydrocarbon compounds and sulfates [A3]. Smoke is defined as carbon or soot concentration, which is the nonvolatile portion of the particulates [G5].

Essentially the generation of a soot particle in the flame can be divided into three phases under all normal combustion conditions: 1) formation of precursors, 2)growth of the nuclei into soot particles by the chemical reactions of aggregation and dehydrogenation, and 3) physical coagulation of these first particles. Formation of the first particles from the precursors, and the initial aggregation of the former, are both very rapid processes occurring in the hotter zone of the flame. After emission from the hottest zones of the flame, the small but fully formed soot particles continue to grow into bigger units by coagulation [B3].

In a diesel engine, the carbon generated in a diffusion flame is either completely consumed, or some of it may be released as soot. This means that the carbon formation and carbon combustion will be occurring simultaneously during the heat release period. The concentration of carbon particles at the end of the major part of heat re-

lease will be the net soot release. This may be further consumed during the expansion stroke before finally finding its way into the engine exhaust [K2].

The formation of smoke in a diesel engine is mainly determined by the mixing process, which controls the spatial and temporal history of the fuel-air mixture and temperature. There are many variables affecting the formation of the smoke through their effect on fuel-air mixing; here the emphasis will be put on dynamic ones.

1) Fuel injection timing

A variation in injection timing has a number of effects[K2]. First, the ignition delay changes with timing. This in turn changes the proportion of fuel that burns as a diffusion flame.

In DI (direct injection) engines, turbulence is generated prior to combustion, and the smoke level increases with the advance of timing[K2,I1]. Advanced timing results in longer delay periods which allows more fuel vapour and small droplets to be carried away with the swirling air, more fuel injected before ignition, higher temperatures in the cycle, and an earlier ending of the combustion process. All these reduce the smoke intensity in the exhaust. Some experimental results in [K3] showed that the smoke level increased with an advance in timing up to a given point (small angles before TDC), beyond which further advance reduced exhaust smoke. Khan[K4] suggested that one of the factors that contributed to the reduction in smoke at retarded timing was the reduced rate of formation at the lower diffusion flame temperature occurring later in the expansion stroke.

In an IDI (indirect injection) engine, turbulence is combustion-generated. The effect of injection timing on IDI engines is different from that of DI ones — smoke levels increase with timing advance especially under heavy load [G5,A2]. Thus, the basic smoke characteristic with respect to injection timing is the reverse of that for

DI engines. The exhaust smoke becomes less and less sensitive to changes in injection timing as the efficiency of air-fuel mixing is increased [K3].

2) Air/Fuel ratio

Diesel engines produce a serious smoke problem if operated at a low enough A/F ratios. A typical diesel characteristic [S1] shows that smoke density at any given RPM increases with decreasing A/F ratio. This is due to soot formation when fuel-rich mixtures are subjected to a high temperature. The soot formation has a strong dependence on temperature and on lack of oxygen (low A/F ratio) while soot oxidation has a strong dependence on temperature and needs excess oxygen (high A/F ratio). The more fuel-rich the mixture, or the higher the temperature, the greater the yield of soot from the carbon available in the fuel. The emission of soot is therefore associated with the main part of the injected fuel and in particular with that part which is injected after the ignition delay period. Fuel injected before ignition has time to mix to leaner conditions before the temperature rises. This means that in a sense A/F ratio in the cylinder is related to the injection timing.

3) Engine speed

At a middle engine speed point, the concentration of particulates is minimum [I1]. Smoke thus becomes worse with an increase or decrease in speed [M6]. Above the speed point with minimum smoke, the level increases due partly to a decrease in air charge (reduced volumetric efficiency) and partly incomplete burning owing to a shorter burning period. The higher smoke level at lower speed occurs because the air motion generated in the combustion chamber tends to mismatch the fuel motion, resulting in a deterioration of the smoke level.

4) Air swirl ratio

Some of the results pertaining to the effect of air swirl are given in [K4]. The

swirl ratio in these experiments was adjusted with a shrouded valve. The smoke level tends to reduce when the swirl ratio becomes high, but at the higher engine speeds the smoke verses swirl ratio curves flatten out or turns upward at the higher end of the swirl ratio range. The effect of injection pressure and injector design are closely related to the air flow. The objective is to produce a spray which will penetrate the air charge fully, but not wet the piston or cylinder walls. This is complicated problem to achieve at a full range of operating conditions.

5) Temperature

It is generally said that higher temperatures during the combustion process always increase the soot released. Increase of air inlet temperature will increase the end of compression temperature and hence the rate of soot formation [G5]. The effect of cooling water is examined in [I1,A2]. Coolant temperature did not significantly influence the gaseous emissions. In general, and especially at the high loads, increasing the coolant temperature caused a modest decrease in the smoke and particulate emissions, i.e. a similar trend, as far as smoke is concerned, caused by inlet air temperature changes.

1.2.2 Engine control

Current research on electronic engine control

Cross [C12] described a versatile diesel fuel injection system for a direct injection engine, which offered electronic control of injection timing, fuel metering, and injection pressure. The controller design for the injection system was based on hybrid analog/CMOS logic which implemented the timing and fueling schedules varied with the engine operating conditions. He showed that this injection system was able to make full range fueling or timing adjustments between successive injections to meet the targets of engine transient behaviour and emissions.

A comparison of closed loop and open loop control techniques for electronic diesel injection systems was presented in [T3]. The closed loop control exhibited accuracy, response time and disturbance input rejection characteristics while offering the potential of relaxed actuator specifications.

Single point electronic fuel injection system technology was reviewed by Toyoda et al [T2]. They pointed out the potential of this system as a future important fuel supply system for spark ignition engines and showed an example describing how the control algorithm or the basic tables for control could be adjusted according to environmental changes or system deterioration by learning control, which is a powerful tool to compensate for offsets in the control points.

A/F ratio control is essential for the efficient operation of a three-way catalyst (for HC, CO and NOx control) system. In these systems, the engines are normally controlled by a microprocessor using feedback from an oxygen sensor in the engine exhaust to maintain the A/F ratio at close to stoichiometry [C1].

Closed-loop control of A/F ratio has attracted much research since the late 60's. Aquino [A1] put the emphasis on examining the various possible causes of A/F excursions to quantify their relative importance and to compensate the controller. Bosch's engine management system, on the other hand[G4], introduced an adaptive A/F ratio control system which was an open-loop control system used to resolve the problem that the engine was run lean at lower loads and rich at higher loads.

Engine emission control is normally a part of the hybrid control on engine performance. Much work has been done on controlling the emissions to meet the specified requirements on the pollutants HC, CO and NOx. In the work of S ell et al [S6], the closed-loop control of carbon monoxide was based on direct detection of the emission, in contrast to the normal CO control by means of a $\lambda = 1$ zirconia oxygen sensor and three way catalyst.

The recirculation of exhaust gases has been employed in light duty diesel engines to reduce the formation of NOx [R6]. The formation of NOx was reduced by lowering the combustion temperatures, which effectively reduced the oxygen concentration in the charge. The proportion of exhaust gases which were recirculated was varied in accordance with changes in engine operating conditions and ambient atmospheric pressure. In the electronically controlled EGR emission system, the control signal for the EGR valve was obtained from the signals derived from engine fuel/load signal and the engine speed signal. In addition, EGR control was automatically compensated with barometric pressure changes.

Reams et al. [R2] developed an experimental diesel electronic fuel control system by modification of the transient fueling characteristics and used it to assess the effects of the fuel system on diesel vehicle emissions and smoke levels. Modified governor characteristics were shown to obtain a 37 percent reduction of particulate emissions. The system is an open-loop control of EGR and injection with the benefit of reducing smoke.

Engine optimal control

The problem of optimization of engine performance can be simply stated: minimizing fuel consumption while meeting emission limits with acceptable driveability.

The approaches for solving optimization of engine performance fall into two categories: off and on-line. In the off-line approaches, previous researchers[R1,P3,A4,W6] have developed steady-state models relating fuel consumption and emissions to engine operating conditions and engine controls. The optimum calibration was obtained at fixed speed-load points.

Cassidy [C2] and Doher [D2] optimised the engine controls on-line. They did not use engine models but instead used the engine itself to evaluate performance and to

determine search directions in the optimization procedure.

Different techniques for optimization have been employed. The disadvantage of the classical indirect methods is that it makes the problem solution hard to implement. Some of these procedures require detailed physical models of the engine and its operation. The problem of developing a physical model of a multicylinder engine is a very time consuming and complex task.

Cassidy [C2] employed an on-line technique in which a minicomputer, connected to an engine and programmed with an optimisation algorithm, automatically determined the calibrations for the best possible fuel economy performance at a specified level of emissions.

Dohner [D2] presented an optimisation procedure which replaced the mathematical system model with the process itself and used experimental measurements to solve the optimal control problem. The procedure synthesised a set of optimal feedback control functions which maximised fuel economy for specified emission and driveability constraints and dealt with the engine-vehicle system during transient operation, including the cold-start portion of the emission test and the catalytic converter transient emission signature.

The geometric programming method was used to determine optimum engine control settings by Dehghani and Sehitoghi [D1]. This technique converted a non-linear problem into a set of linear equations, and this made the problem easier to resolve. In contrast to the classical methods, the technique first found the optimum value of the objective function instead of the optimum independent variables. After the optimum value of the objective function was found it was a relatively simple task to calculate the optimal independent variables. This method is especially effective in fuel economy problems where the constraints are highly non-linear.

A control system used on a 6-cylinder, 2.8-litre petrol engine was developed by the Nissan Motor Co., Ltd., which employed a microprocessor to electronically control four factors of the automotive engine: fuel injection, spark timing, exhaust gas recirculation and air intake during idling [I2]. The optimum performance was achieved through correlative control of the respective factors in transient conditions. The evaluation functions and the restrictions to achieve the optimum performance were determined through mapping at different engine operation conditions.

Engine adaptive control

Recently, adaptive control has begun to be used in engine control system. Zanker and Wellstead[Z1] applied self-tuning to a turbo-charged diesel engine to the regulation of engine speed associated with direct digital control. Three forms of self-tuning controllers were designed and tested: minimum variance, de-tuned(tailored) minimum variance and pole-shifting. Of the three, de-tuned minimum variance gave the most satisfying results. The performance of the self-tuning digital controller was compared with a fixed-term electronic analogue controller, which had previously been developed for the engine. Both the self-tuning and electronic controllers could span the entire operating range of the engine. The good transient responses typical of the electronic controller were equaled in some of the self-tuning runs, but the general transient behaviour of the self-tuning controller was poorer than that of the electronic controller. Additionally, re-tuning transients occurred in self-tuning runs. However, the experiments of this work showed the possibility of such an approach and aspects of self-tuning control on engines.

Another approach using self-tuning regulators was the simulation work done by Olsson et al[O1]. In their work, the extended Least-Square method was used for system identification and the minimum variance method was used as the control algorithm to overcome problems connected with unknown bias of the the engine dynamics,

slowly varying engine parameters and excess oxygen sensor characteristics. The simulation results showed the feasibility of self-tuning in comparison with conventional PI controllers.

In [M5], Mihelc and Citron developed an idle mode control system which adaptively adjusted the idle operating points in response to the changes in engine operating and environment conditions. This was accomplished by operating at an idle speed which gave the maximum acceptable level of engine roughness and had the best compromise of fuel economy, idle quality and emission levels.

1.2.3 Engine modelling for control system design

How to get the models of the system is important and critical to a design of a control system. The models are required in order to apply the tools of control system simulation and analysis. Two general classes of engine model have been developed for the purpose of control:

1. Physical models

Based on mass balance energy balance and momentum, this kind of model has the advantage that the governing equations are expressed in terms of physical parameters, so that the model can be used to evaluate the control performance in the range of operating conditions, engine sizes and alternative configuration prior to hardware implementation [A1,M8,W3]. In [D3], the model was formulated in a modular manner which recognised the physical processes that occurred in the engine. Use of normalized parameters and a modular structure allowed for simulation of different engines, changing engine component performance characteristics and adding new model features. But the problem of this kind of model is that it is considerably more complex with many involved variables which may not be those to be controlled or necessary input/output factors.

2. Empirical Models

Most engine control systems have been developed using an approach that is empirical. This class of engine models have been used as the basis for current engine control system. They are synthesised from measured data with obvious advantages: independence from any physical model and analysis, accurately representing the engine performance under special test conditions, employing mathematical forms much less complex then those of physical models of the same fidelity.

1) A mapping technique has long been used to present the relationship of the variables of the engines [G6,I2]. Usually a three dimensional surface was used for determining the controlled factors in terms of two input factors. Here the problem is that if the functional relationship of the entire control and performance variables are linear, then time average performance measures can be readily deduced from steady state information. Unfortunately, the highly nonlinear nature prohibits such a simplification.

2) A dynamic modelling technique is based on the application of the test signal to the system. The application of modern control theory to design the engine control system has led to the research on a dynamic modelling technique used for engine control. Up to date, the modelling techniques which have been used for engine control are frequency response, time response, statistic and parameter estimation methods.

The detail review of the engine modelling will be represented later in the first section of Chapter 3.

1.3 Objective

As mentioned above, engine smoke control is getting more and more attention due to more stringent emission requirements. Two main techniques have been used to address the problem of excessive particulate emissions. One is to make some improvement on the engine design such as combustion chamber, inlet manifold, fuel pump, injector and so on. The alternative is processing the particles in the exhaust with an effective particle trap. But of these methods, the first cannot resolve the dynamic problems when engine is operating and the second has not been established; serious technological problems still exist. So it is clear that dynamic smoke control is important.

Through the survey of engine control, it can be found that electronic control of engine emissions has normally resulted in the auxiliary benefit of hybrid engine control.Transient control of diesel engines might be expected to have similar spin-off effects.

Generally speaking, the major problems for improved diesel engine control are following:

1) Sensors and actuators with adequate accuracy, reliability and cost effectiveness for control system performance.

2) Application of control theory to the analysis of control system.

3) Techniques of engine dynamics modelling for use in control systems synthesis.

4) Implementation of the control algorithms.

In contrast to the steady-state engine operation, real engine operation, such as engines of motor vehicles and motor trucks, involves a large number of transient conditions which are of considerable importance for certain engine-pollution control

systems.

The fact that operating conditions strongly affect particulate emissions is true for acceleration. During hard acceleration particles can be seen emerging from the exhaust. The composition of the particulates in the exhaust is still somewhat of an open question. It may be carbon-rich particles from the rich mixture or may be combustion-chamber deposits broken loose by thermal shock due to the transient change in cylinder pressure and temperature. Mckee and McMahon[S10] showed that with increasing engine speed (from idle to 50 mph) the amount of particulate matter emitted from a diesel engine increased considerably. The emission rate further increased during acceleration. A similar effect on gasoline engines was observed by Hirschler et al(pp. 196, [S10]) who found that during acceleration the amount of lead emitted was several times higher than the amount of lead consumed when lead was used with the fuel to control combustion in engine.

Thus the objective of this research is to develop an engine control system which maintains the engine operation at a predetermined smoke level and meets the speed requirement during transients.

Chapter Two

Diesel engine apparatus

Fig. 2.1 is a schematic of the engine control system. This system has five main components:

1. the diesel engine to be controlled;
2. the computer which processes the information from the sensors and sends commands to the actuator;
3. the sensors which monitor the operating conditions of the engine, and give feedback signals to the computer;
4. the signal processing circuits which process the raw signals before digitization;
5. the actuator which receives commands from the computer to control the position of the fuel rack.

In order to describe the relevant features of this system, it is convenient to consider each component in isolation.

2.1 Diesel engines

Two diesel engines were used in this study. Both were four-stroke engines and installed in the test cells at the Engineering Department in Cambridge University. Details of the engine specifications are given below.

a) Ricardo E16 diesel engine

Type:	Indirect injection combustion chamber
Number of cylinders:	1

Bore:	120.70mm
Stroke:	139.70mm
Compression ratio:	13.8:1
Maximum speed:	1800RPM

b) A.E.C. Engine

Type:	Direct injection combustion chamber
Number of cylinders:	1
Bore:	105.00mm
Stroke:	130.00mm
Compression ratio:	14.7:1
Maximum speed:	1800RPM
Maximum torque:	66Nm (at 1000RPM)
Fuel pump:	C.A.V. 8mm element, no governor fitted

These engines were loaded by electrical dynamometers. The load due to the dynamometer could be varied from 0 to 130Nm.

The characteristics of the engine at steady-state torque and speed condition with constant fuel rack position can be understood by remembering that the fuel per firing is proportional to rack position, hence fuel per unit time is proportional to rack position times engine speed. Assuming a constant indicated efficiency, the engine brake power is proportional to fuel per unit time minus losses due to frictional loads. When the losses are proportional only to engine speed (i.e. constant friction torque), the torque-speed curves are flat, and the engine can maintain any speed at a constant rack position, i.e. the rack position-speed characteristic is that of a integrator. When the losses dominate the torque-speed curves slope off, the rack position-speed characteristic shifts from pure integrator to first order lag, slow and stable at high speed and high load, unstable at low speeds.

2.2 Smoke sensor

2.2.1 Operation principle

The sensor is designed to utilise of the fact that some of the particulates emitted from a diesel engine are charged. The reason for the charge is somewhat obscure, but the phenomena itself has been observed and studied in the previous study[M8].

Although this work was not centrally concerned with the dependent of the sensor itself, new sensor design was developed, and calibration was undertaken. Early work with the sensor[C10] had aimed to produce a high performance ring sensor, which would have a high sensitivity, but it was found that insulation problems, and difficulties in insertion, limited the usefulness of this design.

Fig. 2.2 shows the design[C10] developed for the present work, which is very simple. By using a circuit(Fig. 2.6) on which there are integrators with virtual earth input, the effect of a varying leakage path to ground is almost negligible until the resistance to ground becomes very low. The problem of leckage effects and net charge transfer to the detector is avoided by negative feedback of a low pass version of the signal output from the first stage integrator.

Although the sensor is simple, it is very difficult to get an exact explanation of sensor's behaviour. Some suggestions for the sensor's behaviour were given in [C10], where it was concluded that:

1) the smoke has a net charge, especially during exhaust blow down

2) the net charge on the smoke as it passes the sensor is of the same sign(except at very high smoke levels when the signal reverse polarity)

3) the origin of the charge is contact electrification effects between the the particulates and the exhaust valve.

The operation of the smoke sensor is that the charged particulates are issued from a diesel engine, and this charge can be detected by measuring the image charge induced in the probe.

The characteristics of this smoke sensor are as follows:

1) It is different from other instruments measuring the smoke as it gives an electronic output which can be used as feedback in a closed-loop control system.

2) It can work as a real time smoke detector in diesel engine.

3) The structure of it is simple and it is easy to install on a engine.

2.2.2 Smoke signal and signal processing

The signals obtained from the sensor are mainly during the blow down phase. Typical sensor response is shown in Fig. 2.3. It consists of a sharp pulse of positive charge followed by a wider pulse with a smaller peak of negative charge. Significant cyclic dispersion, not normally associated with diesel engines, is present in the real time smoke signals. This is due to the 'noise' in the difference between two large quantities — smoke generation and consumption in the cylinder.

The smoke signals enter a processing circuit(Fig. 2.6) to be amplified and integrated over a 'window' period which is typically between 130 and 200 degrees after firing top dead center, the period of exhaust valve opening during which the signal is present. so the instantaneous level of output from the signal processing circuit corresponds to the total charge sensed by the smoke sensor up to that point in the engine cycle. If the signal does not return, after the exhaust event, to the level which it had before the exhaust event, this is due to charge transfer between the smoke and the sensor. In practice this transfer can be of either sign, and is usually small with respect to the main signal amplitude.

The operation of the smoke sensor is that the charged particulates are issued from a diesel engine, and this charge can be detected by measuring the image charge induced in the probe.

The characteristics of this smoke sensor are as follows:

1) It is different from other instruments measuring the smoke as it gives an electronic output which can be used as feedback in a closed-loop control system.

2) It can work as a real time smoke detector in diesel engine.

3) The structure of it is simple and it is easy to install on a engine.

2.2.2 Smoke signal and signal processing

The signals obtained from the sensor are mainly during the blow down phase. Typical sensor response is shown in Fig. 2.3. It consists of a sharp pulse of positive charge followed by a wider pulse with a smaller peak of negative charge. Significant cyclic dispersion, not normally associated with diesel engines, is present in the real time smoke signals. This is due to the 'noise' in the difference between two large quantities — smoke generation and consumption in the cylinder.

The smoke signals enter a processing circuit(Fig. 2.6) to be amplified and integrated over a 'window' period which is typically between 130 and 200 degrees after firing top dead center, the period of exhaust valve opening during which the signal is present. so the instantaneous level of output from the signal processing circuit corresponds to the total charge sensed by the smoke sensor up to that point in the engine cycle. If the signal does not return, after the exhaust event, to the level which it had before the exhaust event, this is due to charge transfer between the smoke and the sensor. In practice this transfer can be of either sign, and is usually small with respect to the main signal amplitude.

2.2.3 Calibration

Tests were conducted to calibrate the sensor on the Ricardo E16, single-cylinder, IDI engine.

Independent smoke measurements were made using a Hartridge Smoke-meter MK30 which measures the opacity of the exhaust gas. The smoke-meter was connected by a sample pipe and a sample probe to the diesel exhaust system. The exhaust sample pressure was adjusted to be correct by altering the position of the probe or exhaust pressure, and the temperature was controlled by heating the tube in the smoke-meter.

The signal processing of the smoke sensor was described previously. The final signal, the output voltage of the processing circuit, is the total charge which has passed the probe up to the present time. They are digitized through the A/D converter which samples at a frequency of 10 Hz, then averaged over 30 samples and stored by a program for data acquisition.

Calibration tests are carried on at three speeds(700, 800, 900RPM). The torque was varied between 45 and 130 Nm at each speed. The results of these tests are shown in Fig. 2.4. A correlation coefficient of 0.87 confirms a good correlation between the average sensor signal and Hartridge smoke units.

Transient smoke levels were measured during the period of the engine transients. The output of the Hartridge smoke-meter was converted to a voltage which was recorded by a chart recorder. The result of the smoke sensor was also recorded by the chart recorder. Comparison of two kinds of measurements in Fig. 2.5 shows that the tendencies of two traces are well agreed.

2.3 The computer

The computer used for control is PDP11/23-PLUS. The main characteristic of this 16-bit microcomputer is that it can address up to one megabyte of parity MOS MSV11-P memory while offering full PDP-11 processor functionality.

The CPU module of PDP11/23-PLUS contains diagnostic and bootstrap ROM, a memory management unit, line-time clock, two asynchronous serial lines, and three sockets for the Commercial Instruction Set(CIS) and Floating Point Instruction Set options.

This kind of computer was designed with a system distribution panel that simplifies access, installation, reconfiguration, and relocation of all serial line and option connections.

2.3.1 Physical Specification

Physically, the PDP11/23-PLUS consists of a single unit containing the microcomputer hardware itself, a keyboard, and a visual display unit(VDU). External devices, floppy disk units and printer, can be connected to the computer. The main features are following:

a) There are two DLV-11 type serial line units for the system console, and an additional terminal or line printer.

b) Extended LSI-11 Bus interface supports a full megabyte of memory. The LSI-11 Bus provides vectored priority interrupts, programmed I/O transfers, and DMA I/O data transfers. All modules operate asynchronously at their highest possible speed.

c) The four-level interrupt bus structure allows the priority of bus options for each level to be conveniently determined by their physical locations on the bus.

2.3.2 A/D and D/A conversions

The Analogue-to-Digital and Digital-to-Analogue converters are on an AXV11-C circuit board. The board accepts up to 16 single-ended inputs, or up to 8 differential inputs, either unipolar or bipolar, and has a programmable gain on these inputs of 1, 2, 4, or 8 times the input voltage.

The AXV11-C also has two separate digital-to-analogue converters(DACs). Each DAC has a write-only register that provides 12-bit input data resolution. On receiving the data, the AXV11-C changes the data to an analogue output voltage.

The process of A/D or D/A conversion can only be realized by assembly language. The time of A/D conversion is 25μs and D/A conversion 65μs.

2.4 Actuator and engine speed measurement

The actuator used to receive the command signal from the computer and drive the fuel rack is a servo motor modified from the FP-S34 made by FUTABA Corporation of U.S.A. The output torque of the servo is 112.6 oz·in (8kg·cm) and operating speed is 0.19 sec/60^0. This servo motor has a polyacetal resin precision servo gear which can operate smoothly and provide positive neutral and virtually no backlash.

The servo motor is connected mechanically with the engine fuel rack and electrically with a driving circuit which replaced the initial electronics control system of the servo. The command signal from the D/A converter enters the circuit, and then is compared with the output signal of the servo which moves the fuel rack while rotating. The error signal resulted from the comparison passes through an amplifier and output to make the servo's operating angle up to be the right position. So the operating angle of the servo is a linear function of the voltage level of the command signal.

The fuel rack travels from minimum fuel supply position to maximum fuel supply position when the operating angle of the servo changes from 0^0 to 180^0. The range of the voltage from the D/A converter to the servo is -10V. to $+10$V.

The engine speed signal is taken from a techogenerator on the crankshaft. This ac signal is rectified before A/D converter.

2.5 Discussion on the output of smoke sensor

The description of the smoke sensor in section 2.2 shows that the output of the smoke sensor is related to the exhaust particle concentration. The test results of calibration give a good agreement between the output of the smoke sensor and the Hartridge Units. The use of this smoke sensor in a transient smoke control system will be evaluated through the performance of control system discussed in Chapter 4 and 5.

In this section the behaviour of the smoke signals such as cyclic variation, independency and origin of the sensor response, and how these affect the sensor's application will be discussed.

1. Cyclic variation

The problem of cyclic variation was found early in the work at Ricardo[R3] and later by Schweimer[S5] . This was also investigated in the work of Collings, et al[C10]. The smoke signal used for smoke feedback control is a processed one of the pulse generated by the imbalanced charge brought with the particles. The pulses are sampled by a 'window' and integrated, so the smoke signal before A/D converter is actually a voltage level which is related directly to the total charge in the pulse up to a particular time. If the pulse smoke signal keeps unchanged from cycle to cycle, the smoke level will be smooth with time invariance. So, the cyclic variation of the pulses results in the oscillation of the smoke level. However, when the fuel supply increases suddenly(a big

step input to the fuel rack), the smoke pulse becomes much bigger than that at steady-state condition. Comparing to the high smoke level at transients, the oscillation of the smoke signal resulted from cyclic variation at steady-state is very small. Hence, the cyclic variation of the smoke signals is ignored in the smoke feedback control system.

2. Speed dependency

The dependency of the smoke signals can be investigated with the calibration between smoke and other coefficients of engine. The calibration was conducted in three engine speed points. The sample 'window' for processing the smoke signals was produced by a circuit which processed the pulses from crankshaft and camshaft. When the engine speed decreased, the 'window' becomes a little wider, this means that the integral time for the smoke signal became longer. If the smoke signal had a relatively high offset, the width of the 'window' would affect the integrated results very much. However, the offset of the raw smoke signal was removed by the simple electronic circuit described in section 2.2.1 before the signal was processed. The variation of the width of the sample 'window' did not show much effect to the smoke level held after the integrators. Early work in Ricardo[R3] gave the observations that the response of the probe(for smoke sensing) was speed dependent. In our work, no special investigation has been done for this. However, the correlations(Fig. 2.4) separately at three different speed points show that the general speed dependency of the smoke level is not very significant

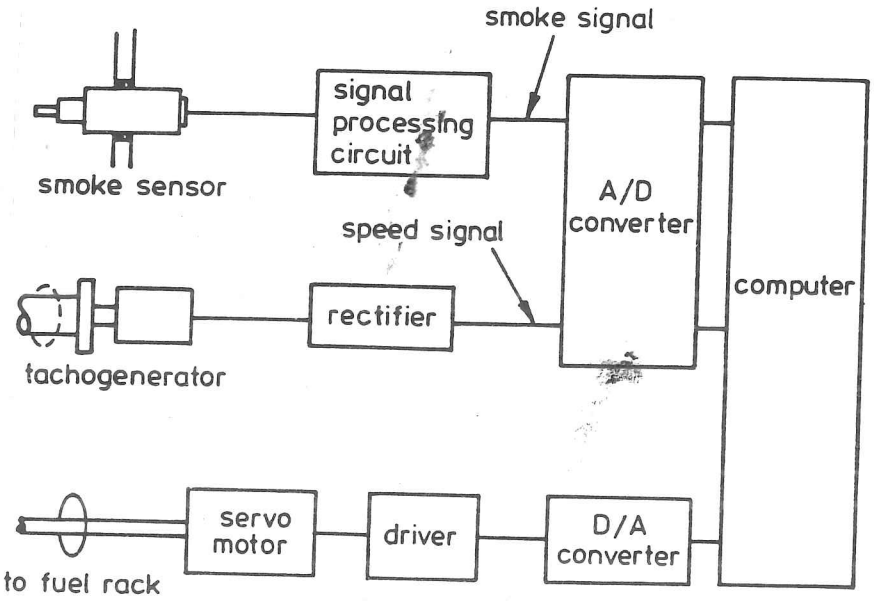

Fig. 2.1 Schematic of engine control system

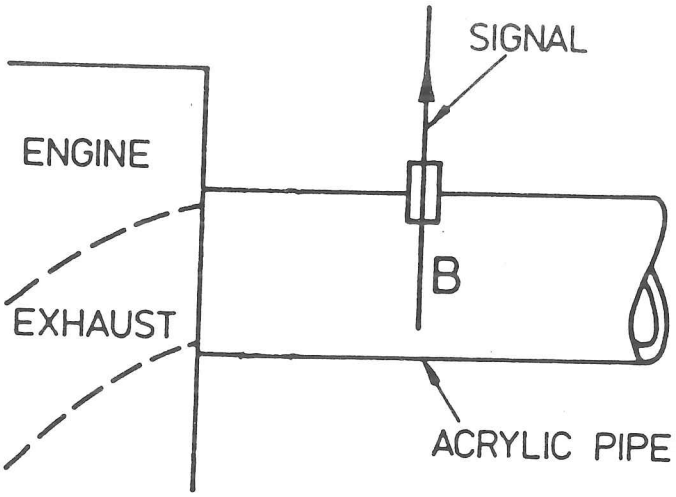

Fig. 2.2 Smoke sensor device

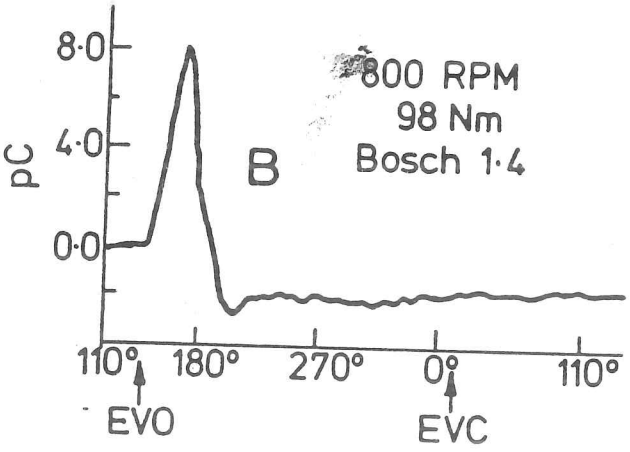

Fig. 2.3 Output signal of smoke sensor

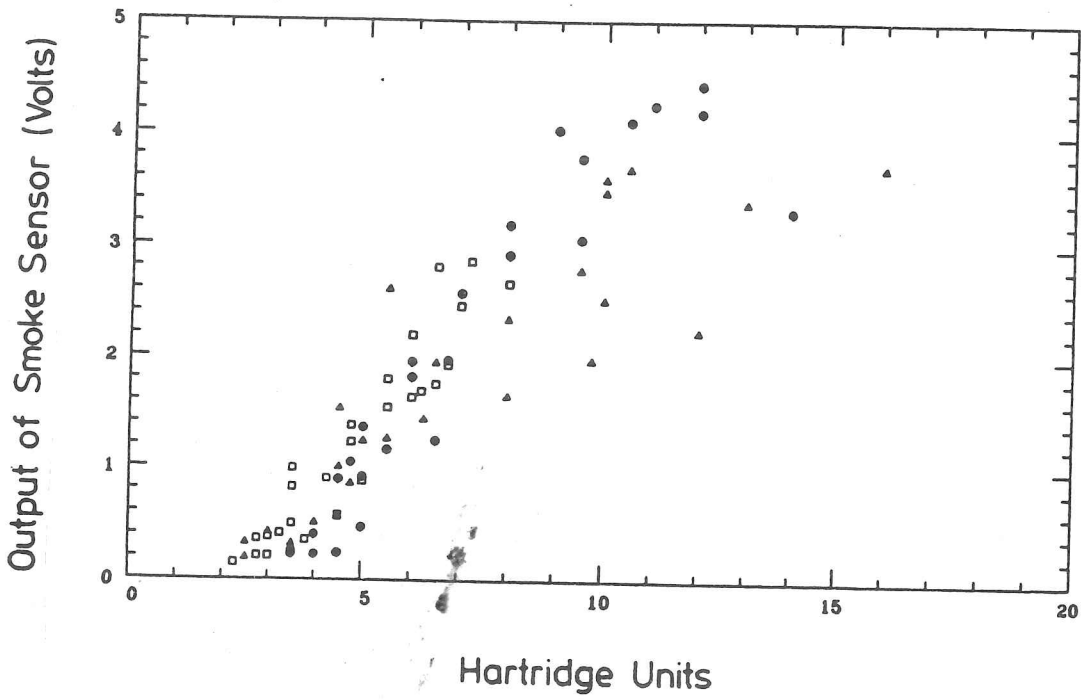

Fig. 2.4 Calibration of outputs of the smoke sensor and Hartridge Units

▲ — 700RPM, ● — 800RPM, ▫ — 900RPM

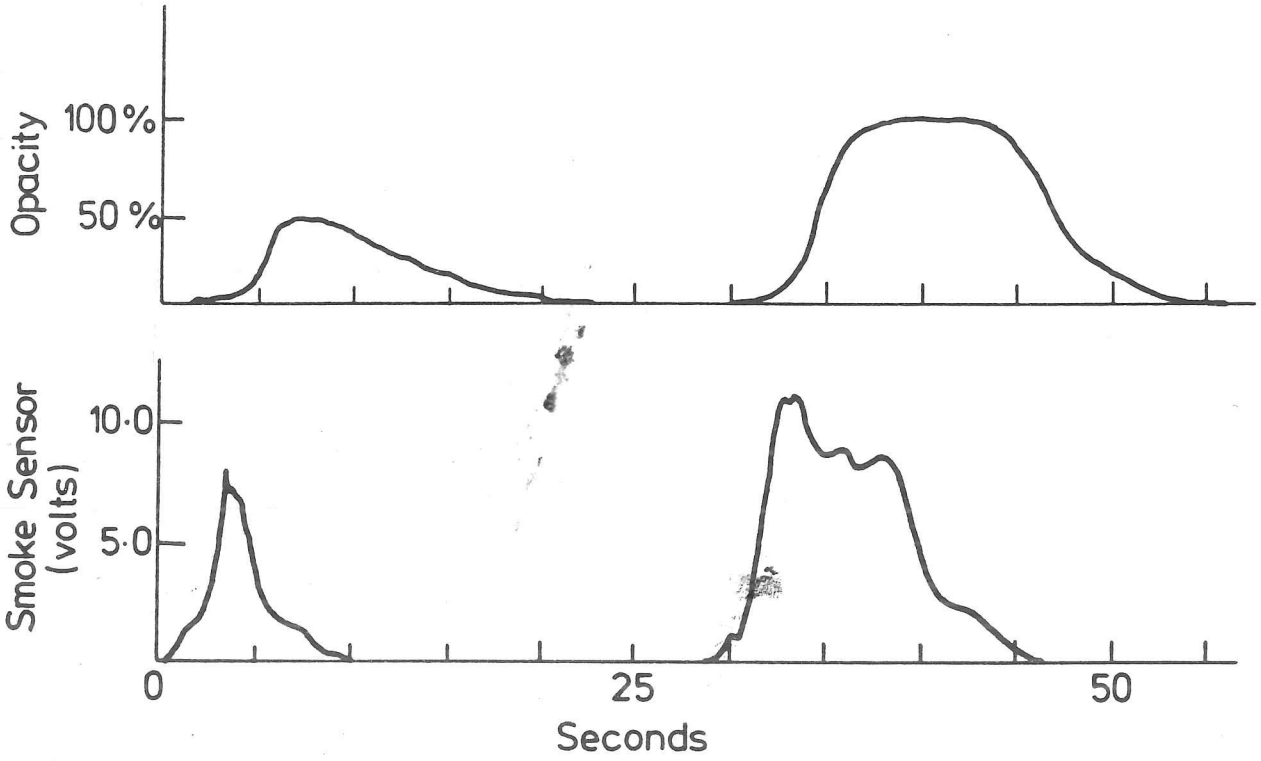

Fig. 2.5 Comparison of transient outputs of smoke sensor and

Hartridge smoke meter

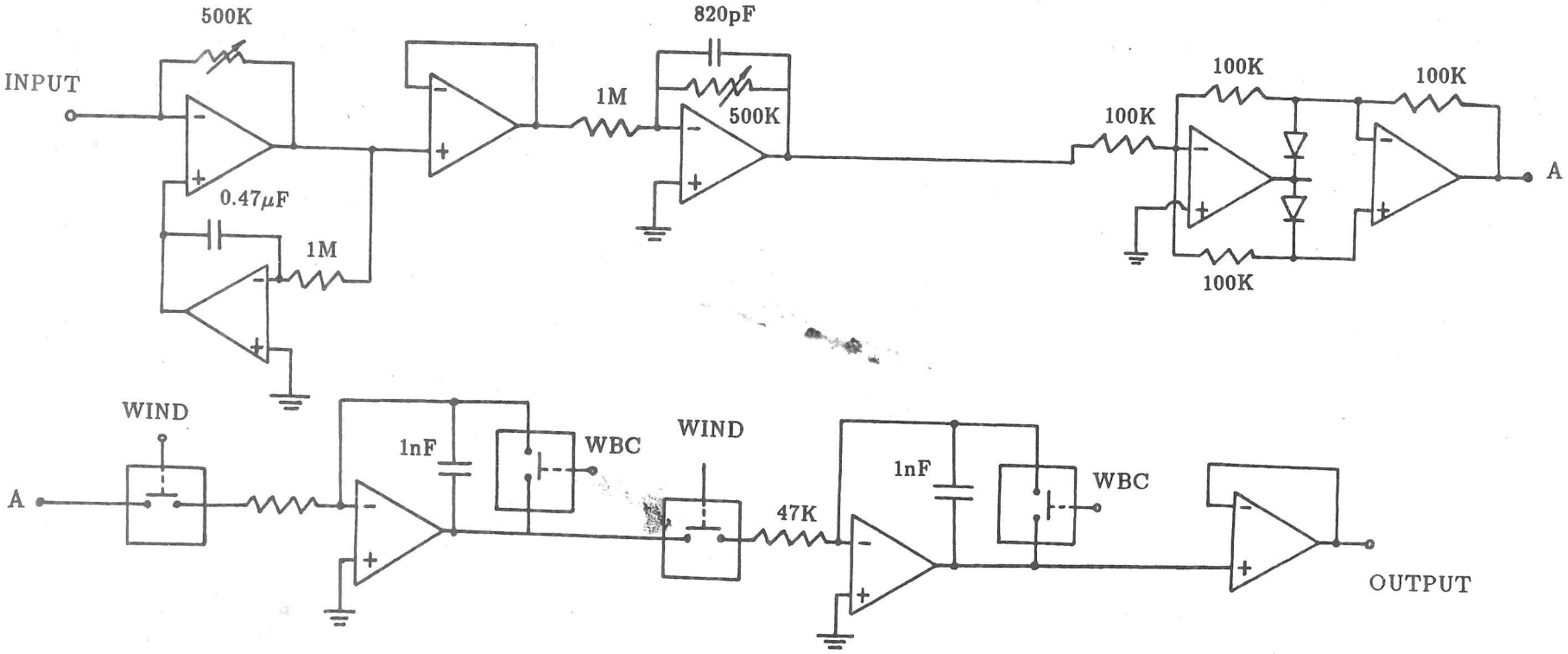

Fig. 2.6 Circuit for smoke signal processing

Chapter Three

Engine modelling

3.1 Introduction

An engine incorporates complex component sub-system including the fuel supply system, manifold, combustion system etc, whereas the engine control system (actuator, sensor, electronics etc) is more precisely defined. The realization of the control system is based upon the modelling of the controlled system. It is necessary to analyze the performance of the system using the model, and then design the controller. In modern control theory, every kind of method for system analysis and design such as Bode diagram, Nyquist criterion or Root Locus method, needs a good understanding of the controlled system. Even for adaptive control which has been developed more recently, the parameters of the transfer function describing the relationship of the input and output can be estimated on-line, but the transfer function is still required to be partly known — the order of the transfer function and time delay have to be specified initially.

Hence, modelling is always the first step in the solution of a control problem. Generally, there are two ways to determine the mathematical model of an engine system:

(1) mathematic-physical analysis based on general physical laws or process dynamics.

(2) experimental analysis based on the information obtained by measurements.

A review of the application of experimental modelling technique to engine control shows that frequency response techniques have been widely used. In 1974, Windett and Flower[F1,F2,F3] applied sample-data theory to frequency response measurements

of a large diesel engine. To eliminate the scatter produced due to the signal processing, a synchroniser was used to produce repeatable measurements and demonstrated by applying it to a variety of simple sampled-data systems.

Chang and Sell[C5] gave another example of the application of this technique to a petrol engine modelling employing an infrared diode laser spectrometer to establish dynamic effects of A/F ratio perturbation about stoichiometry on CO emissions and engine torque. In their work, the input signal was a biased sinusoidal voltage to perturb engine A/F ratio at different frequencies. Two models were derived, one was for A/F effect on torque, another predicted the correlation of engine torque and CO emissions.

Time response techniques were used in [C1] to measure the response of the A/F ratio to the fuel. The input was a step change to the fuel metering system, and the transfer function was found to be first order with a time delay.

Flower et al did more work on engine modelling using P.R.B.S. techniques [F4] to obtain a transfer function between engine speed and fuel rack position. The P.R.B.S. pulse rate and sample time were synchronised with the engine firing. Details of the model however were not discussed.

Engine dynamic modelling using a parameter identification algorithm was described in[M9]. Morris et al used physical principles to obtain a block diagram of the system, and then Landau's hyperstable identification algorithm to determine the parameters of the model. Based upon a sampling interval of one engine revolution, the response of the torque to throttle was described by a fourth-order dynamic model.

The ability to model an engine dynamically suggests that modern control analysis and design techniques can be employed to resolve the engine control problem. However, progress has been impeded by the absence of suitable dynamic models. One of the basic reasons for this is the lack of suitable sensors. This chapter shows how a novel smoke

sensor was used as a basis for establishing the necessary information for modelling. Following this introductory section, section 2 describes the features of different methods used for engine modelling and review some of the results obtained by the author. The problems associated with conventional modelling techniques are discussed in section 3. In section 4 the generation of the input signals, data acquisition and synchronization technique that have been developed for engine modelling are described. Section 5 describes the identification algorithm that is predominantly used in this study. The determination of model order and parameters estimated are described in section 6. Finally, the nonlinearities of the models and simulation results are discussed in section 7.

3.2 Modelling methods used for engine control

The modelling techniques which have been used for engine control are 1) time response method, 2) frequency response method, 3) correlation technique and 4) parameter estimation. In this section, we shall discuss the main features of the application of each method to engine modelling with the experience in the previous work and present work undertaken.

1. Time response methods

The time response method gives the output response to specific types of input in the time domain. With this method the forcing function giving the best insight for transient response studies is the unit step function[S4]. The following are the advantages and disadvantages of time response method:

Advantages:

a) For an engine system, step change of input such as required speed and torque can usually be applied fairly easily.

b) The resulting response very readily gives an idea of the transfer function of engine system. With simple observation we can determine the order of magnitude of the gain, of the dominant time constant, or of the damping ratio and natural frequency of the system.

c) Any pure transport delay involved in the response and indication of non-linearity can be shown with different magnitude of steps.

Disadvantages:

a) The engine speed may not settle, and drifts unacceptably with a step input on the fuel rack.

b) Because engine variables such as speed may change much during the case of the experiment, the model obtained is not necessarily associated with one operating point.

c) It is difficult to predict model order accurately using this approach.

2. Frequency response methods

In this approach, the transfer function of a system in the frequency domain is described in terms of the response to a varying sinusoidally input signal after all initial transients have died away. Provided the system is linear the steady state output, which is the particular integral term of the solution of the governing differential equation, is a sinusoid of the same frequency as the input, but with a shift of phase and a change of amplitude. This method has the advantages:

a) Embodying principles are easily understood.

b) It is convenient to generate the input signals.

c) An indicator (namely a Bode or Nyquist Diagram) is given, which offers a simple and intuitional understanding of the measured system.

and disadvantages:

a) It is time consumed because the steady-state output is a sinusoid of the same frequency as the input when the testing time tends to infinity. Accurate results may only be obtained when the testing time is long enough at each frequency point of the sinusoid input. The frequency response of the system over a specified range has to be measured at each frequency point one after another.

b) It is impractical in some cases because of the limitation imposed by the existence of system noise.

c) The frequency range for the test is limited if the system to be modelled is inherently discrete in nature (e.g. in the case of a car engine one revolution of the engine is a fundamental behavioural quantisation).

Details of the problems associated with the application of this method to engine modelling will be discussed later in section 3.3.

3. Statistical methods

These methods are based on the fact that the cross-correlation function of the input and output in a dynamic system is proportional to the impulse response function when the input signal is white noise[S4]. A random signal which has a white noise spectrum is easy to generate — Pseudo Random Binary Sequence (P.R.B.S.) can be used instead of white noise in system modelling. The features of this method are:

Advantages:

a) The effect of the inherent noise in the system can be largely eliminated and the response characteristics can be determined when the appropriate statistical procedure is used to analyse the signals.

b) P.R.B.S. signals are very useful approximations to periodic white noise and are the input signals most widely used in statistical system testing, which are commonly available in real-time computing environments. The binary nature of the signals

simplifies the cross correlation calculation.

c) The signal intensity of a P.R.B.S. is low, with energy spread over a wide frequency range, hence it is a suitable forcing function for a plant in operation as it causes little disturbance from the operating condition. In addition, it is applicable to the determination of transfer functions on line.

Disadvantages:

a) The method is not as simple to understand as that of other modelling methods.

b) The method is based on the assumption that the noise of the system is uncorrelated with the input. Accurate modelling is difficult to achieve if this assumption breaks down in the real system.

c) The modelling results strongly depend on inherent discrete behaviour (as mentioned above). How this effect influences the modelling results will be discussed in Section 3.3.

4. Parameter estimation

In some cases the parameter values of models may be obtained with the forgoing methods. In other cases, however, it might not be feasible to determine the precise values of the system parameters in this way. In these instances it is sometime possible to deduce the values using parametric identification. This method has following features:

Advantages:

a) Much smaller numbers of experimental data are needed, compared to statistic method or frequency response method. Also, significant simplification in the computation can be achieved by choosing input signals of a special type, e.g. impulse functions, step functions, coloured or white noise, sinusoidal signals, and P.R.B.S.

b) It can be done both on-line or off-line recursively with respect to different

requirement and control algorithms.

c) If the model is expressed in linear discrete form the parameters of the canonical form can be obtained directly because the various criteria are realised by computation, and the inputs and outputs need sampling into discrete results.

Disadvantages:

a) A plausible structure of the transfer function, such as order of the model, and time delay between input and output, has to be postulated before the parameter estimation.

b) The input and output used for identification are sampled signals which cause the error between them and the real signals.

3.3 Application of frequency and statistical methods for engine modelling

The frequency method is widely used for engine modelling. This is because this method is accompanied by the frequency analysis method which is also widely used for system analysis and design. Statistical method has been tried on engine modelling but only in a few examples. In this section, we first discuss the discrete nature of I.C. engines, and then discuss the application of the frequency and statistical methods for engine modelling and indicate the problems of applying these methods for engine modelling with some test results. Lastly, we decide on which modelling technique to use for our control system design.

3.3.1 Discrete nature of the engine

In a diesel engine system, the output of engine speed and movement of the fuel rack are continuous, However, the fuel injector contains a discrete sampling mechanism.

In a typical fuel injection system on a diesel engine, the amount of the fuel injected

is determined mainly by the injection time and pressure. The fuel injection normally starts before top dead center, the timing cam drives the piston of the fuel pump past the fuel inlet so that the injection cylinder is pressurised. The fuel is then continuously injected into the combustion chamber while the fuel pressure is high enough until, for example, the helix in the side of the piston connects the pressurised part of the cylinder with the inlet part. So, the amount of injected fuel for each engine cycle is determined only by the time during the injection stroke when the helix on the piston passes the fuel port. The relative position of the helix and inlet port is varied by the position of the fuel rack which rotates the piston. The injection time is only of the order of 5 percent of each engine cycle, so the injection event can be treated as sampling the movement of the fuel rack. The sample time interval is given

$$T = \frac{120}{n.N}$$

N is engine speed(RPM) and n is the number of cylinders.

3.3.2 Frequency response method

1. The principle of frequency response method

In frequency domain, the transfer function $G(s)$ of a linear system can be shown to be a ratio of two polynomials in s, each of which can be factorized to give

$$G(s) = \frac{Y(s)}{U(s)} = \frac{k(s-z_1)(s-z_2)....(s-z_m)}{(s-p_1)(s-p_2)....(s-p_n)}$$

If a sine wave of unit amplitude and of frequency ω rad/second is taken as the input to system:

$$u(t) = sin\omega t$$

or in frequency domain $$U(s) = \frac{\omega}{s^2+\omega^2}$$

The output $y(t)$ will be[S4]

$$[y(t)]_{t\to\infty} = |G(j\omega)|sin(\omega t + \angle G(j\omega)) \tag{3.1}$$

The magnitude and phase can be obtained as functions of frequency from the transfer function $G(s)$ by replacing s by $j\omega$ and determining the modulus and argument of $G(j\omega)$, which for any particular frequency is generally a complex number.

2. Application of frequency response method for engine modelling

For the samples to be truly representative of the original signals it must be possible to recreate the signals accurately from the samples. It is well known in communication theory that this is possible only when the sampling frequency f_s is at least twice the highest frequency component present in the signals. Otherwise, 'aliasing' will result. In the case of diesel engine the engine output will be a sine wave with a gain and phase lag if the frequency ω is lower than 1/2T. But, when the input frequency to the fuel rack is higher than 1/2T, the movement of the fuel rack will be sampled at too low a rate. The actual process of the fuel supply is cast into another sine wave with frequency ω' which is different from ω, and this makes the output a sine wave of frequency ω' too. This behaviour can be demonstrated easily. Fig. 3.1 and 3.2 show the sine wave inputs (which drive the actuator connected with the fuel rack) and the speed outputs at different frequencies (the engine steady-state speed is about 840RPM, firing frequency is about 7Hz). In Fig. 3.1.a, the input sine wave has the frequency of 1Hz. The sampling (at the time of the injection) thus has a frequency 7 times that of the input sine wave. In Fig. 3.1.b, the frequency of the input sine wave is 2Hz. The frequency of injection is thus a factor of 3.5 times higher than that of the input sine wave. Thus the sine wave outputs of the engine speed have the same frequency as the inputs. In Fig. 3.2, however, the 'aliasing' is very obvious when the input frequency is higher than half of the firing frequency, 6Hz, in Fig. 3.2.a, and 7Hz in Fig.3.2.b. With this problem, the relationship of the input and output will not correspond to equation

(3.1). Hence the modelling of the engine will be misleading at these kinds of frequency points.

To be able to determine the dynamic characteristics of the operating process of an engine with the frequency response method, it is necessary to determine the value of the minimum acceptable frequency of the input sine wave from the engine firing rate. In practice, the Bode diagram starts to become scattered when the frequency of the input sine wave is above 1/4 of the engine firing rate.

3.3.3 Statistical methods

1. Principle of the statistical method

If a linear system, whose transfer function is $G(s)$ in frequency domain, has input $u(t)$ and output $y(t)$, then following representation can be obtained from a fundamental theorem of spectral analysis:

$$\Phi_{yu}(\omega) = G(j\omega)\Phi_{uu}(\omega)$$

where Φ_{yu} is cross-spectrum of the output and input, Φ_{uu} is auto-spectrum of the input, This leads to the following estimate of the frequency response $G(j\omega)$:

$$\hat{G}(j\omega) = \frac{\hat{\Phi}_{yu}(\omega)}{\hat{\Phi}_{uu}(\omega)}$$

By calculating the gain and phase at each frequency point, input $u(t)$ and output $y(t)$ are sampled as $u_1, u_2, \ldots, u_N$ and $y_1, y_2, \ldots, y_N$, the spectrum can then be obtained from these N pairs of sample values by calculating the auto-correlation and cross-correlation functions and using Fourier transforms.

2. Application of the statistical method for engine modelling

When the statistical method is applied to engine modelling, some caution should be taken. As the diesel engine is a discrete system, the continuous input signal for moving the fuel rack is actually sampled by the fuel injection, so the frequency of the input and output samplings, used for calculation of the spectrum, must be taken into account.

The P.R.B.S. signal is widely used in the statistical method due to its approximation of periodic white noise[A5]. Let values of P.R.B.S. sequence for successive interval ΔT be $x_1, x_2, \ldots, x_N$, so that its autocorrelation function is

$$\phi_{xx}(\tau) = \frac{1}{N}\sum_{j=1}^{N} x(j)x(j+\tau)$$

$$= \begin{cases} -\frac{a^2}{N} & \text{if } j \neq 0 \\ a^2 & \text{if } j = 0 \end{cases}$$

This shows that the autocorrelation function of the P.R.B.S. signal is approximate to a δ function when N is large. If the P.R.B.S. sequence is sampled at a frequency f_s ($f_s \neq \frac{1}{\Delta T}$), its random property will be changed, so the P.R.B.S. pulse sequence should have the same frequency as that used to sample the input and output signals.

By way of example, Fig. 3.3 shows the Bode diagram of the transfer function, for speed-to-fuel rack, obtained from a single cylinder (AEC) engine using the statistical method. The basic test point speed was 800RPM. The P.R.B.S. input signal perturbed the fuel rack around a basic position which kept the test speed point. The P.R.B.S. signal was trigged at the same frequency as engine firing. Input and output signals were sampled at the engine firing frequency and calculated on a digital spectrum analyser to give the Bode diagram. As shown in the figure, both the gain and phase become oscillatory when the frequency is higher than 1Hz. The problem here is that the

frequency of P.R.B.S. pulse sequence is the same as the sampling frequency of data acquisition, and the sampling frequency of data acquisition must match the engine firing, hence the system can only be identified at very low frequency when the engine speed is low. This might explain the oscillations in Fig. 3.3.

3.3.4 Experimental modelling activity

Through the review of the modelling techniques used for engine control, the analysis of the problem when the frequency response or statistical methods are used, and consideration of the digital form of the transfer function required in this control system, the method of parameter estimation was chosen as the modelling method for the system design.

With this method, two conflicting requirements must be considered to obtain the production of a suitable model structure and estimation of the parameters within that structure.

1) The model should be as simple as possible. In general, a simple model eases the process of controller design and implementation; this is particularly true if the model can be made linear and the order of the transfer function kept low.

2) The model should be as accurate as possible to provide an adequate representation of the real system. Even though it may be impossible to get a model which exactly represents the actual process, sufficient accuracy is necessary for the controller design methods used and the specified requirements with regards to the control performance.

The modelling work was carried out as follows:

1) Acquisition of the data on the real engine to be controlled.

2) Determining the time delay of the transfer functions from the data acquired and

predetermining the order of the transfer function using initial identification.

3) Derivation of the models with off-line identification of different engine conditions and observation of the nonlinearity of the transfer functions.

3.4 Synchronization technique for dynamic measurement

As mentioned above, the diesel engine is a typical sampler, and the perturbation of the fuel rack in modelling must occur to affect the fuel supply; otherwise, there will be aliasing between the input and output to lead a misunderstanding of the system. In this section it will be shown how this problem was dealt with the synchronization technique, and then data acquisition for off-line identification are described.

3.4.1 Model conventions and notations

In this research, we were considering the implementation of digital control strategies. Therefore, it was appropriate to formulate discrete time models of the system.

The input used in the modelling was a digital signal which was converted through a D/A converter to drive the servo-motor, as described in section 2.4. $u(t)$, the input used for parameter estimation, was the actuation signal to the servo subtracted from a constant input signal which was acting on the servo to maintain the engine speed test point.

The outputs of the controlled system were engine speed and smoke level. Both were processed before A/D conversion. Speed and smoke measurements had the same scale as input measurement. The sampled data for modelling of speed output, $y_1(t)$, and smoke output, $y_2(t)$, were the speed and smoke outputs subtracted from the their initial values respectly. The calibration between engine speed and the digitized value,

DV, of the speed measurement was DV=r·RPM+a. For AEC engine, a was 1832.8 and r was 1.5401.

The diagram of the system for modelling is shown in Fig.3.4 and the layout for data acquisition in Fig.3.5.

3.4.2 Measurement of input and outputs

1. Generation of P.R.B.S. signals

The P.R.B.S. signal was a binary sequence, where switching between one signal level and the other took place in a pseudo random manner, but was discretised in time by allowing switching to take place only at equispaced internals.

The P.R.B.S. signal was generated by a Fortran program. Seven shifters were used in the program to get 127 bits sequence. The amplitude of the signal could be selected by the user before the P.R.B.S. was generated.

2. Data acquisition for off-line identification

Another Fortran program linked with an assembler routine was used to sample and store the data results of the input and outputs into the data files, and to send out the P.R.B.S. analogue signal to the servo motor. The program read the P.R.B.S. data sequence, added it to a basic value(basic voltage to keep the steady-state engine speed), and then the assembler routine moved one of the data sequences from the memory to D/A converter when the trigger arrived. After that, this data was converted into an analogue signal to the servo motor and this signal was held until the next trigger arrived. 300 samples were taken for each program execution.

3. Amplitude of P.R.B.S. and the perturbation of outputs

The amplitude of P.R.B.S. was selected to make small perturbation in the outputs when the sampled data were used for system identification. The final models derived

were in digital form whose discrete time intervals were constants. However, in fact, the real sample frequency for data acquisition was varied because the engine speed was changing due to the perturbation on the fuel rack and the sampling was synchronised with the engine revolution. So the fixed sample frequency in the identified model was actually an average of the real sample frequencies. The more the engine speed was perturbed, the more the sample frequency varied. The accuracy of the model would be unacceptable if the sample frequency in the test changed over a wider range.

The engine speed was sensitive to the small variation of the fuel rack's movement at low frequency, but the smoke signal could not be excited when the amplitude of the P.R.B.S. pulse was smaller than 0.25V. Thus, the amplitude of P.R.B.S. input was chosen to be higher than 0.25V. and with different gains to investigate the non-linearity of the system.

3.4.3 Synchronization of the sampling and engine revolution

A synchronization technique was used to make the samples of data acquisition in the system synchronise with the natural samplers. It required that the samplings to the continuous parts of the system occur at regular intervals of the same variables that govern the natural samplers. In this diesel engine the event of this synchronization is shown in Fig. 3.6:

1) The trigger starting the D/A converter and then sending out the P.R.B.S. pulse has the same frequency as engine firing.

2) The time interval to keep one P.R.B.S. pulse is chosen to be the time for one engine cycle. Each trigger to the P.R.B.S. pulse happens in exhaust process, this keeps the position of the fuel rack unchanged during injection period.

3) The sample frequency to the input and outputs is the same as engine revolution.

4) A/D conversion happens at the time when the piston arrives at TDC.

3.5 System identification algorithm

Recursive Least Square(RLS) method was used to determine the parameters of the models.

1) Model in RLS

The model underlying RLS is

$$y(t+1) = \phi(t)\theta + v(t+1)$$

where

$$\phi(t) = [-y(t), -y(t-1), ..., -y(t-na+1), u(t-nd), u(t-nd-1), ...,$$
$$u(t-nd-nb+1), v(t), v(t-1), ..., v(t-nc+1)]$$

$$\theta = [a_1, a_2, ..., a_{na}, b_0, b_1, ..., b_{nb-1}, c_1, c_2, ..., c_{nc}]'$$

y — the output

u — the input

v — uncorrelated,zero-mean random sequence or white noise

a, b, c — parameters of the model

na, nb, nc — defines the degree of the model

nd — system time delay

This model can be written as

$$A(q^{-1})y(t+1) = B(q^{-1})u(t-nd) + C(q^{-1})v(t+1) \tag{3.2}$$

where

$$A(q^{-1}) = 1 + a_1 q^{-1} + a_2 q^{-2} + ... + a_{na} q^{-na}$$

$$B(q^{-1}) = b_0 + b_1 q^{-1} + b_2 q^{-2} + ... + b_{nb-1} q^{-nb+1}$$

$$C(q^{-1}) = 1 + c_1 q^{-1} + c_2 q^{-2} + ... + c_{nc} q^{-nc}$$

q^{-1}— represents the unit delay operator, $q^{-1}y(t+1) = y(t)$

2) Estimate execution

The parameter estimate $\hat{\theta}(t)$ based on data point at time t is given by

$$\hat{\theta}(t) = \hat{\theta}(t-1) + W(t-1)[y(t) - \hat{y}(t)]$$

where

$$\begin{aligned}\hat{y}(t) =& \phi(t-1)\hat{\theta}(t-1)\\ W(t) =& \frac{\mathbf{P}(t-1)\psi(t-1)}{\psi(t)\mathbf{P}(t-1)\psi'(t) + \lambda(t)}\\ \psi(t) =& \frac{1}{\hat{c}(q^{-1})k(t)}\phi(t)\end{aligned}$$

where $k(t)$ is a contraction factor and $\lambda(t)$ is a forgetting factor.

$$\begin{aligned}k(t+1) =& a_k k(t) + (1 - a_k)\\ \lambda(t+1) =& a_\lambda \lambda(t) + (1 - a_\lambda)\end{aligned}$$

a_λ and a_k control the rates at which $\lambda(t)$ and k(t) reach their final values. $0 \leq a_\lambda \leq 1, 0 \leq a_k \leq 1$

$\mathbf{P}(t)$ is a scaled version of the covariance of the estimate given by

$$\mathbf{P}(t) = \left[\mathbf{P}(t-1) - \frac{\mathbf{P}(t-1)\psi'(t)\psi(t)\mathbf{P}(t-1)}{\lambda(t) + \psi(t)\mathbf{P}(t-1)\psi'(t)}\right]/\lambda(t)$$

3.6 Parameter estimate

1. Pre-determination of the structures of transfer functions

Time delays of the models were determined from the sampled data, which was represented by the number of sample intervals. The time delay in the model of fuel rack-to-speed was one sample interval and in that of fuel rack-to-smoke two sample intervals.

The order of the fuel rack-to-speed model was assumed by referring to a mathematical model of engine[H1] and the experimental results in previous work[Z2]. The

position of the fuel rack is proportional to the fuel per firing, hence fuel per unit time is proportional to that fuel rack position times engine speed. Engine power is approximately proportional to fuel per unit time minus losses. Change of steady state engine speed results from change in fuelling rate, i.e. fuel rack position, and load torque. For an engine on which loading is unchanged, the transfer function between fuel rack and speed is nearly a pure integrator if the engine is not governed[H1]. This is why a diesel engine has a tendency to run away if not governed.

The actuation signal of the controlled engine system was a digital one which was converted through the D/A converter of the computer, processed in a circuit driving the motor before it moved the fuel rack. To account for these additional components, higher orders of the transfer function of speed-to-fuel rack were investigated.

No previous work has been found on the experimental determination of fuel rack-to smoke model. In the work of Chang and Jeffery[C5], the model of fuel rack-to-CO emissions was derived as a second order one. Since the relative proportions of particulates, unburnt HC and CO might be conceived to be roughly proportional to each other when the engine condition is kept unchanged, the transfer function of fuel rack-to-smoke was assumed to be second order.

2. Investigation of the order of the transfer function

The range of the order of transfer function for the model was investigated and accuracy of the models was utilised to finally determine the order of the model. With the same algorithm for identification, the transfer function of speed-to-fuel rack was investigated from first order to third order and the number of zeroes from 0 to $na-1$. The transfer function of smoke-to-fuel rack was investigated in the same range. The coefficients produced for the various models are given in Table 3.1 and 3.2 respectly for speed and smoke models. In Table 3.1, the data were taken at engine steady-state speed 800RPM and torque 30 Nm, and Table 3.2, speed 900RPM and torque 45 Nm.

The simplest speed model which gives a near minimum square error is that for na=2, nb=0 and nd=1. A near minimum error of the smoke model is obtained for the simple choice na=2, nb=0 and nd=2.

Similar results about the order of the transfer function were obtained at other speed-torque points, here only the final models used for system analysis and design are given in Table 3.3 and 3.4.

3. Convergence of the estimated parameters

Parameters of the model were estimated with 50 — 100 sample points at each engine test condition. The initialization of the parameters was zero. Convergence of the parameter estimate is shown in Fig. 3.7 and 3.8. In Fig. 3.7 are the results of speed-to-fuel rack model and in Fig. 3.8 the smoke-to-fuel rack. There are some fluctuations in the first 4 — 20 iterations for speed models, as shown in Fig. 3.7, after which the values of the parameters settle down to the steady-state ones. The identification processes for the smoke model have more fluctuations, as shown in Fig. 3.8, and the values of the parameters are not very stable after 20 iterations.

4. Comparison of real and predicted results

Comparison of $y(t)$, the real output, and $\hat{y}(t)$, the predicted output, are shown in Fig. 3.9–11. In Fig. 3.9 is the predicted speed output compared with the real speed output at engine condition speed=800RPM and torque = 30Nm. The model for prediction is second order with one infinite zero. The two traces are in good agreement. Even in the identification with first order transfer function for speed model, the predicted and real speed outputs are still in good agreement, as shown in Fig. 3.10.

Fig. 3.11 shows the comparison of smoke outputs. The model of smoke-to-fuel rack is second order with one infinite zero. The two outputs agree well although difference between them looks bigger than that between real and predicted speed outputs.

Table 3.1 Coefficients for various orders of fuel rack-to-speed model

na	nb	nd	a_1	a_2	a_3	b_0	b_1	b_2	V
1	0	1	-0.9318			0.0296			1830.2
2	0	1	-1.5375	0.5627		0.0145			1104.3
2	1	1	-1.4198	0.4621		0.0136	0.0067		1071.9
3	0	1	-1.6712	0.8033	-0.1009	0.0131			1472.6
3	1	1	-1.4159	0.4888	-0.0305	0.0131	0.0076		1122.2
3	2	1	-1.4328	0.4983	-0.0249	0.0127	0.0080	-0.0012	1168.7

V — the sum of the squared errors between real and simulated results over N samples

$N = 100$ in Table 3.1, $N = 40$ in Table 3.2

Table 3.2 Coefficients for various orders of fuel rack-to-smoke model

na	nb	nd	a_1	a_2	a_3	b_0	b_1	b_2	V
1	0	2	-0.8798			0.0476			372.297
2	0	2	-0.5719	-0.2883		0.0616			226.351
2	1	2	-0.4595	-0.3861		0.0653	0.0036		223.151
3	0	2	-0.6330	-0.1793	-0.0524	0.0603			224.915
3	1	2	-0.3700	-0.1668	-0.2788	0.0674	0.0203		215.791
3	2	2	-0.2769	0.1794	-0.6517	0.0708	0.0318	0.0173	223.244

Table 3.3 Parameters of fuel rack-to-speed model at different engine conditions

Speed (RPM)	Torque (Nm)	Gain k_1	Pole 1 p_{11}	Pole 2 p_{12}	Time delay $nd1$ (sample interval)
800	30	0.0145	0.9368	0.6006	1
800	60	0.0094	0.9447	0.5369	1
700	30	0.0140	0.9613	0.5741	1
700	72	0.0075	0.9775	0.4801	1
900	30	0.0180	0.9351	0.3583	1
900	60	0.0101	0.9556	0.3807	1

Table 3.4 Parameters of fuel rack-to-smoke model at different engine Conditions

Speed (RPM)	Torque (Nm)	Gain k_2	Pole 1 p_{21}	Pole 2 p_{22}	Time delay $nd2$ (sample interval)
800	30	0.0099	0.7767	0.1197	2
800	60	0.0335	0.9506	0.3536	2
900	45	0.0616	0.8943	-0.3224	2
900	60	0.0322	0.9448	0.2132	2

3.7 Discussions on the final models

The engine speed response to the fuel rack movement was tested at different speed-

torque points. The results in Table 3.3 show that in the speed model there is always a slow pole which is bigger than 0.9 and less than 1 in the Z-domain. A tendency can be found that the slow pole in the transfer function goes towards the position which is more unstable when the speed is lower. This agrees with the results of engine speed modelling in the previous work[H1,Z2] and also the speed-torque characteristics of the engine.

The poles in the smoke model are more stable than those of the speed model. The steady-state gain of the transfer function increases very quickly with the increase of engine torque. But, the smoke model is more difficult to be identified due mainly to its nonlinearity. Three different sizes of the P.R.B.S. input were adopted to measure the response of the smoke model at the same speed-torque test point. The test data shown in Fig. 3.12 were estimated to investigate the nonlinear gain of the transfer function. The amplitudes of the P.R.B.S. input pulses, as shown in the figure, were 51(0.5V.), 102(1.0V.) and 204(2.0V.). Identified with these three inputs, the steady-state gains were 0.0232, 0.3239 and 1.2301 respectively when the transfer function was second order with a time delay of two sample intervals. The nonlinearity of the smoke response to the fuel rack might result from the engine combustion process and derivation of the sensor's output from real smoke level. From the control standpoint, the main parameter to be controlled is engine speed and the smoke is to be detected in the transients, so the accuracy requirements to the speed model and smoke model are different.

The time delay of either speed response to fuel rack or smoke is less than one engine cycle from the view of engine operation. In the models shown in Table 3.3 and 3.4, the time delay of the speed model is one sample time interval and smoke model two sample time intervals. In fact, the smoke response does not take the time delay twice of that speed response does. This is caused by the sample process. During the period one P.R.B.S. pulse takes, the first sample starts at the TDC after compression

stroke, the second one happens at the TDC after expansion stroke, at this moment the speed signal affected by the alteration of the fuel supply is ready to be output but the smoke signal is being processed. So the smoke signal can only be sensed one sample interval later than the speed signal.

Simulation was carried out in an open loop. The P.R.B.S. signal used for modelling was still taken as the input signal in simulation, and the simulated outputs were compared with the actual outputs. Graphical illustration of the accuracy of the models is given in Fig. 3.13–16 which show that the agreement between the measured and calculated results is quite acceptable and also show that the model of the fuel rack-to-speed(Fig. 3.12 and 3.13) is more accurate than that of fuel rack-to-smoke(Fig. 3.14 and 3.15).

3.8 Conclusions

The work in this Chapter was undertaken to utilize the modelling techniques with the concern about the discrete nature of the diesel engine.

Two models, speed-to-fuel rack and smoke-to-fuel rack which are necessary to controller design, were obtained with the synchronization technique for data acquisition and Recursive Least Square method for system identification. The comparisons of the test and simulated results show the acceptable accuracy of the derived models.

The engine speed model can be linearised as a second order transfer function in Z domain with a time delay of one sample interval, i.e. one engine revolution.

The nonlinearity of smoke-to-fuel rack model was investigated in a preliminary way, and the model was approximated as a second order transfer function with a time delay of two sample intervals when the amplitude of the input signals was limited in some range. It must be emphasised that more accurate modelling of the particulate emissions is extremely difficult since it is highly nonlinear.

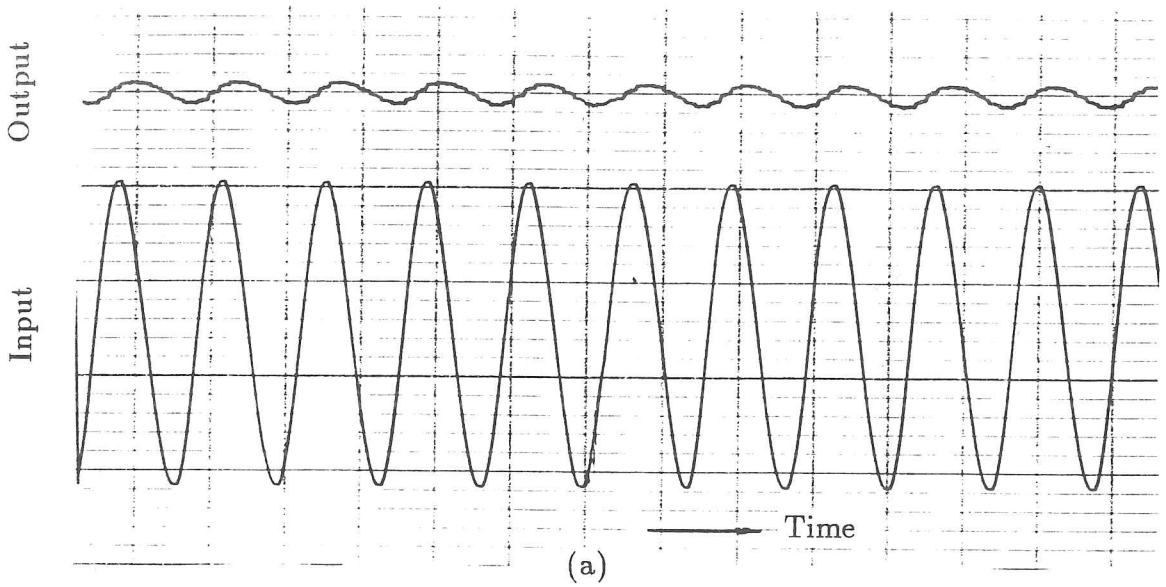

(a)

frequency of input sinewave = 1Hz, test engine speed point: 840RPM

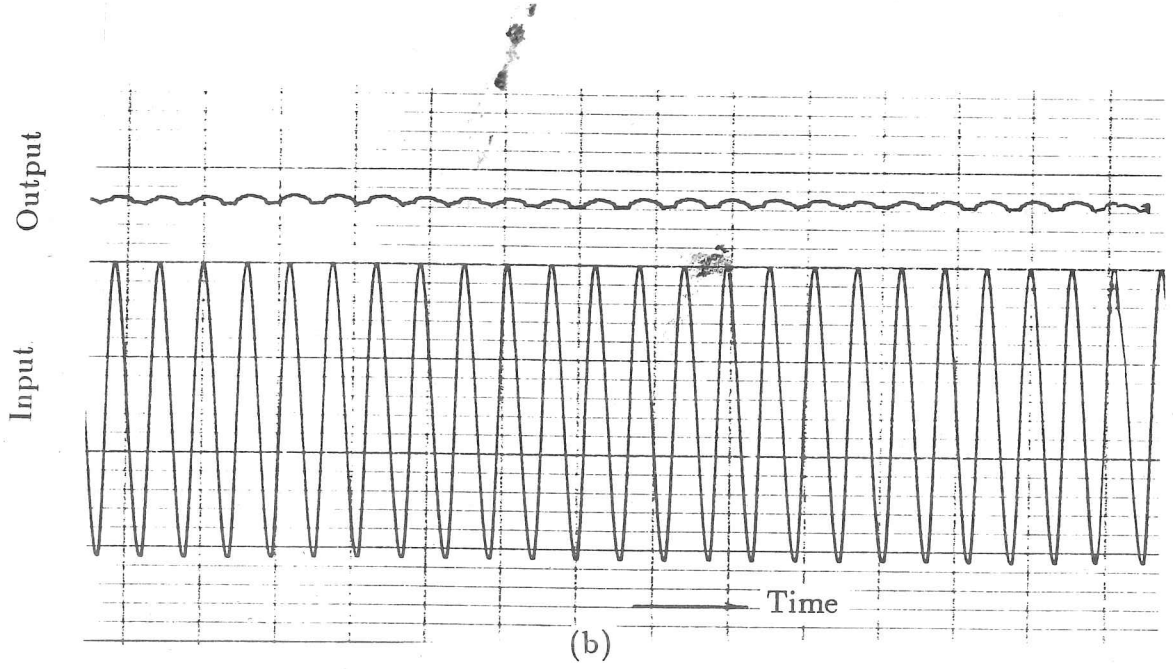

(b)

frequency of input sinewave = 2Hz, test engine speed point: 840RPM

Fig. 3.1 Engine speed response to sinusoid input of fuel rack

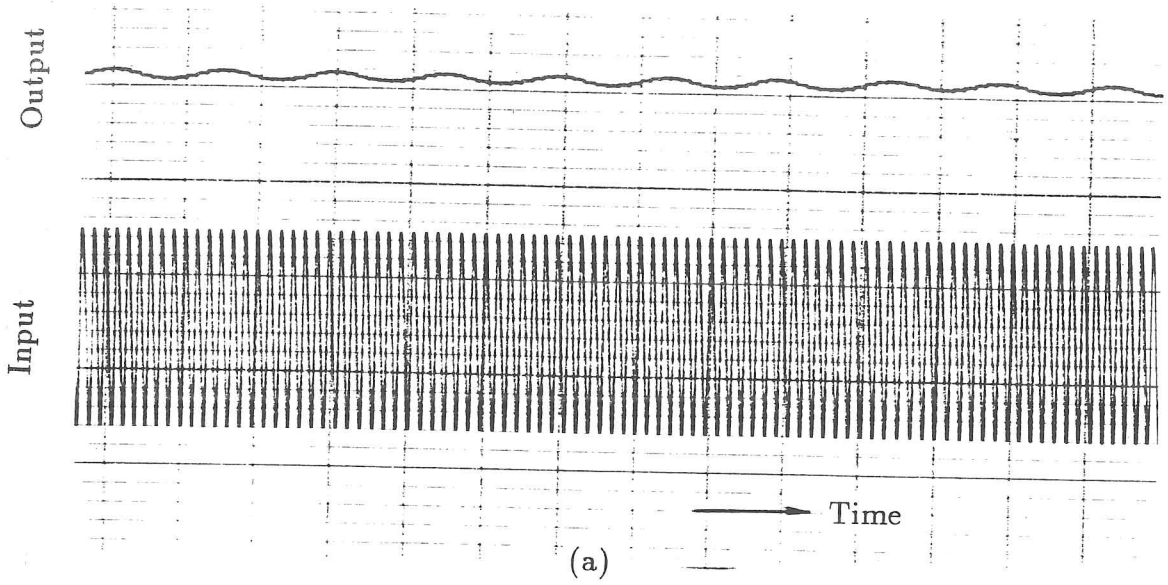

frequency of input sinewave = 6Hz, test engine speed point: 850RPM

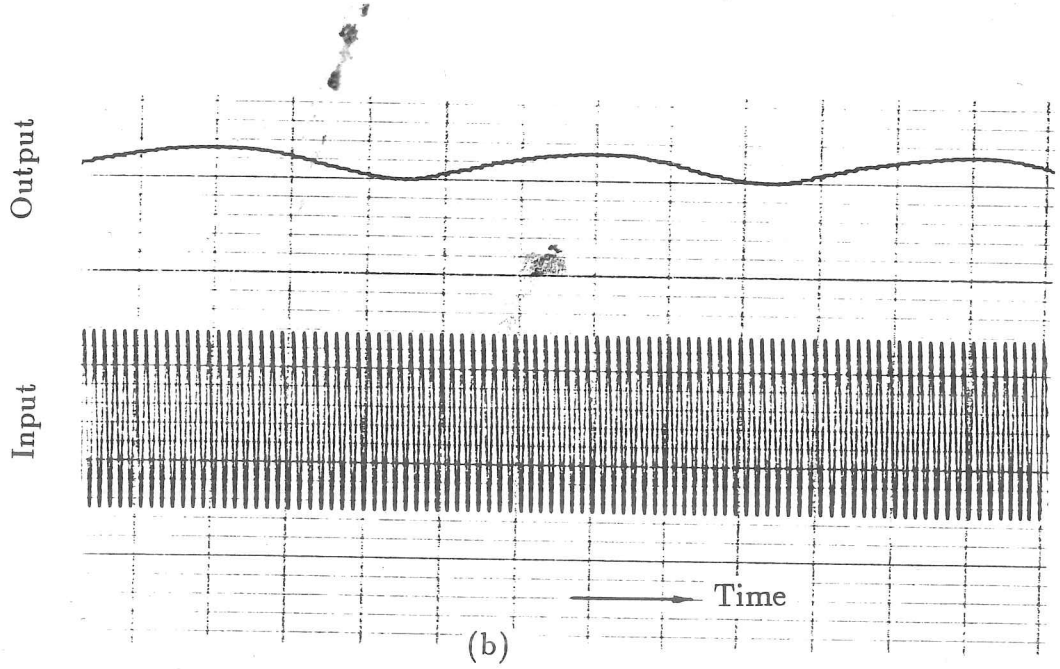

frequency of input sinewave = 7Hz, test engine speed point: 815RPM

Fig. 3.2 Engine speed response to sinusoid input of fuel rack

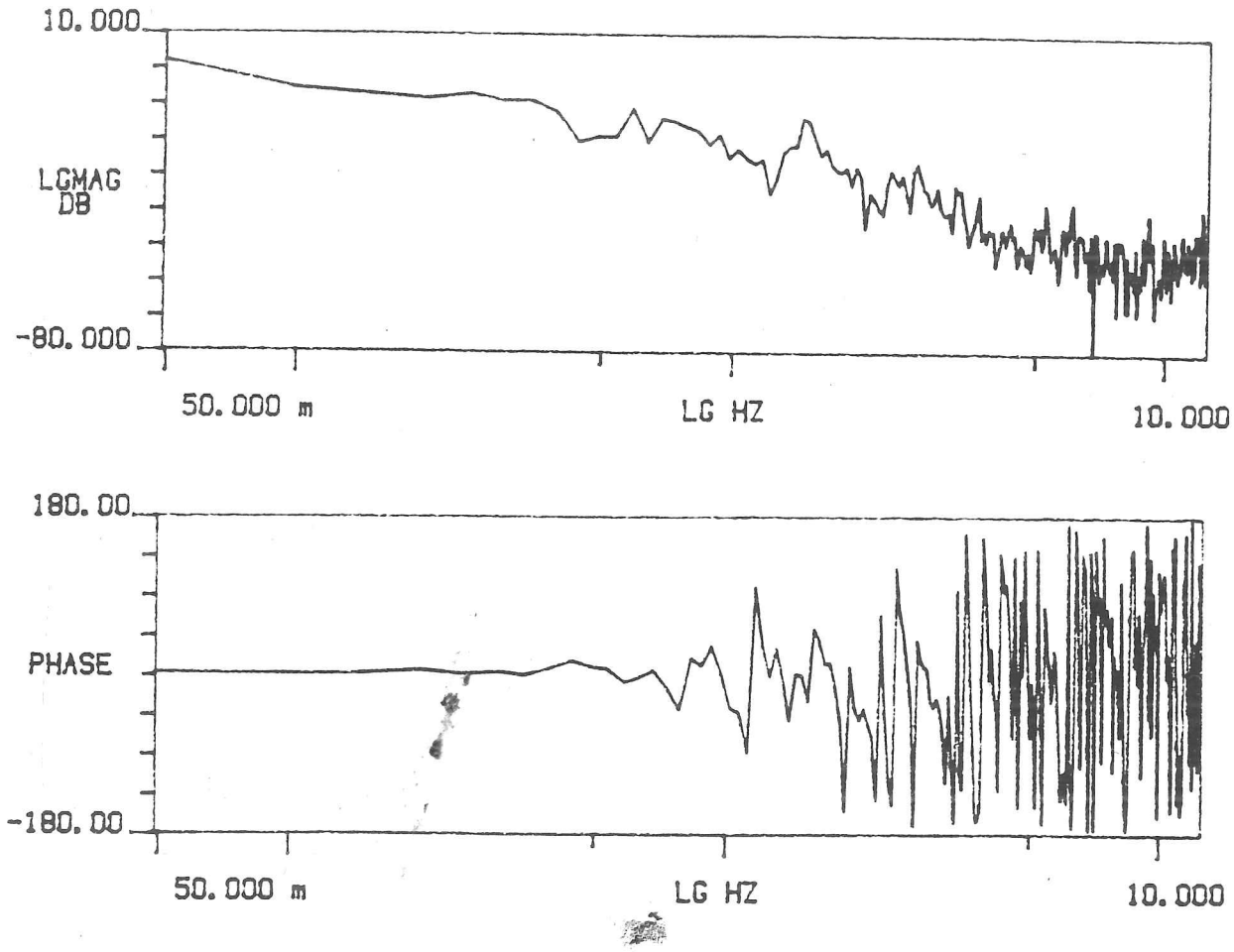

Fig. 3.3 Bode diagram of the transfer function of speed-to-fuel rack with P.R.B.S. technique (test point: speed = 800RPM, torque = 30Nm)

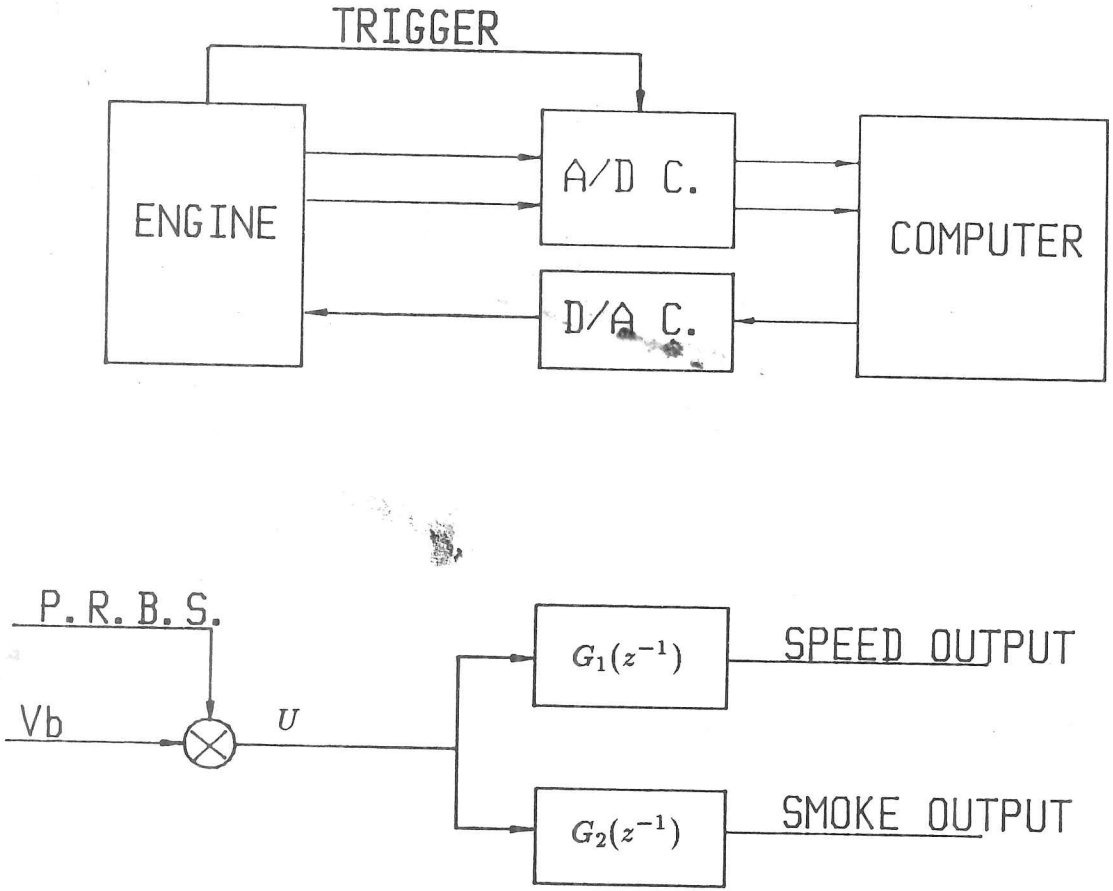

Fig. 3.4 Diagram of the modelling system

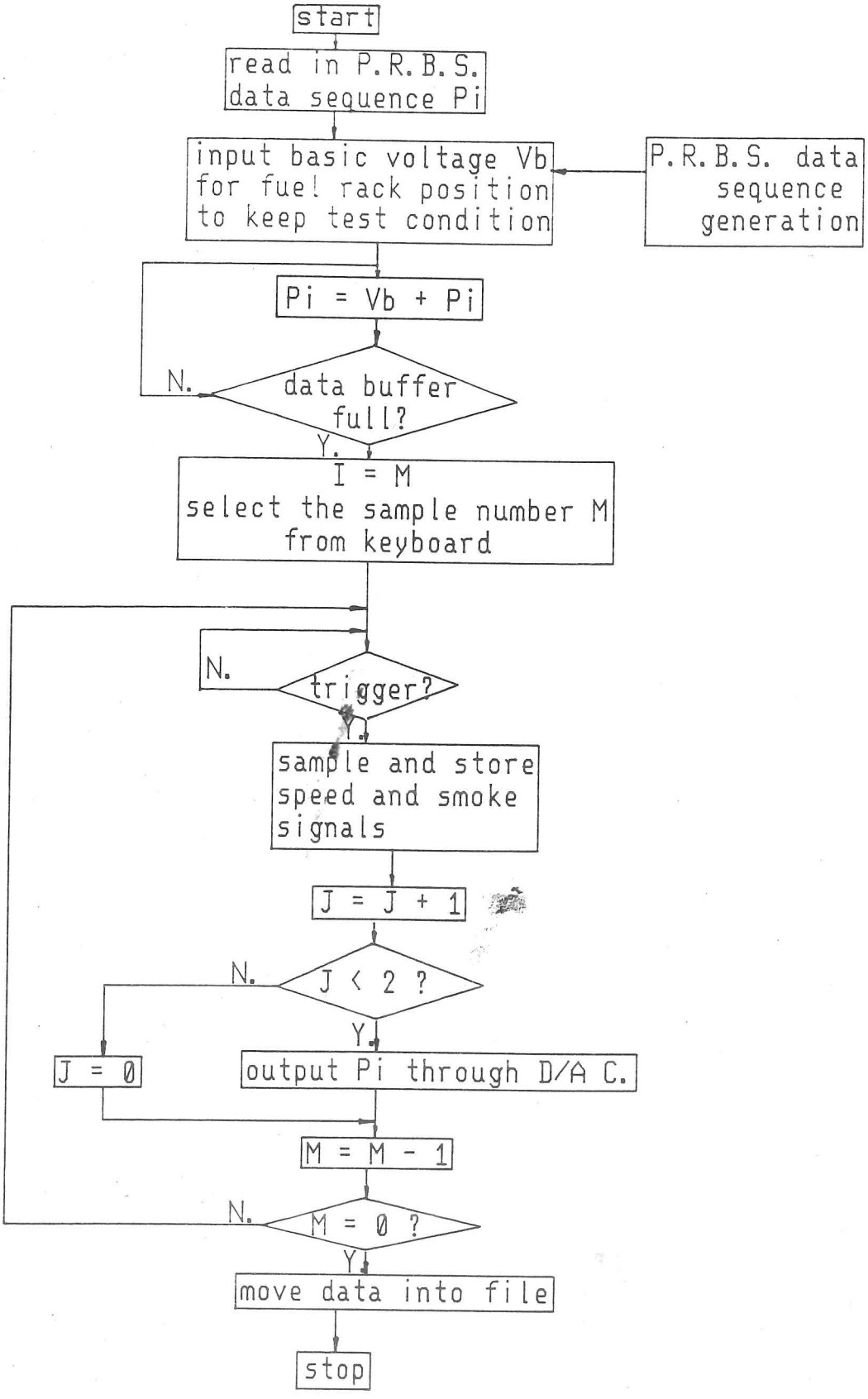

Fig. 3.5 Flow chart of data acquisition

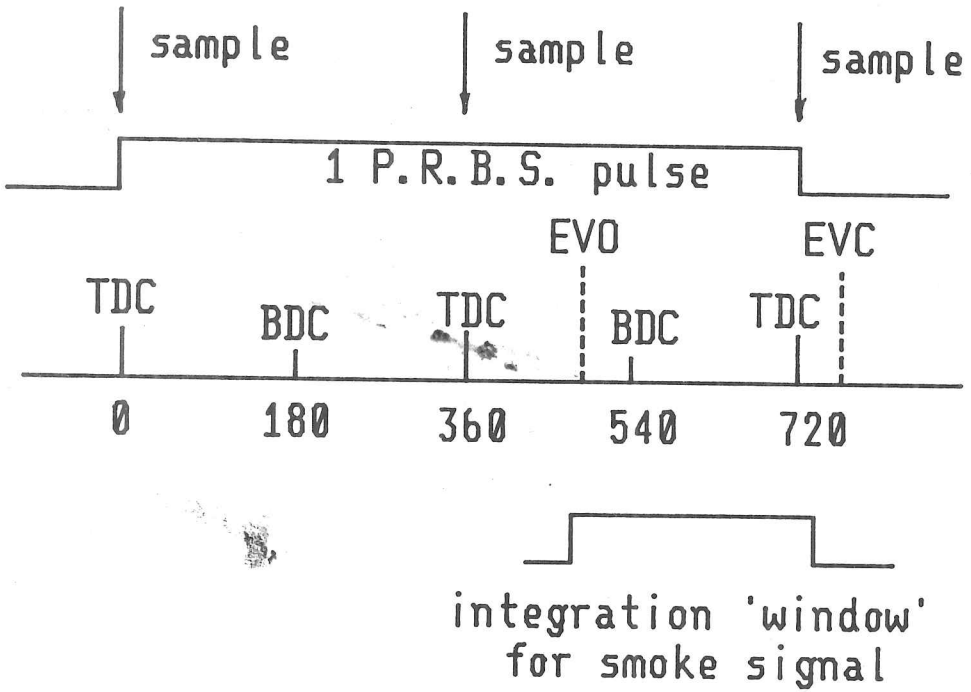

Fig. 3.6 The event which occurs with synchronization technique

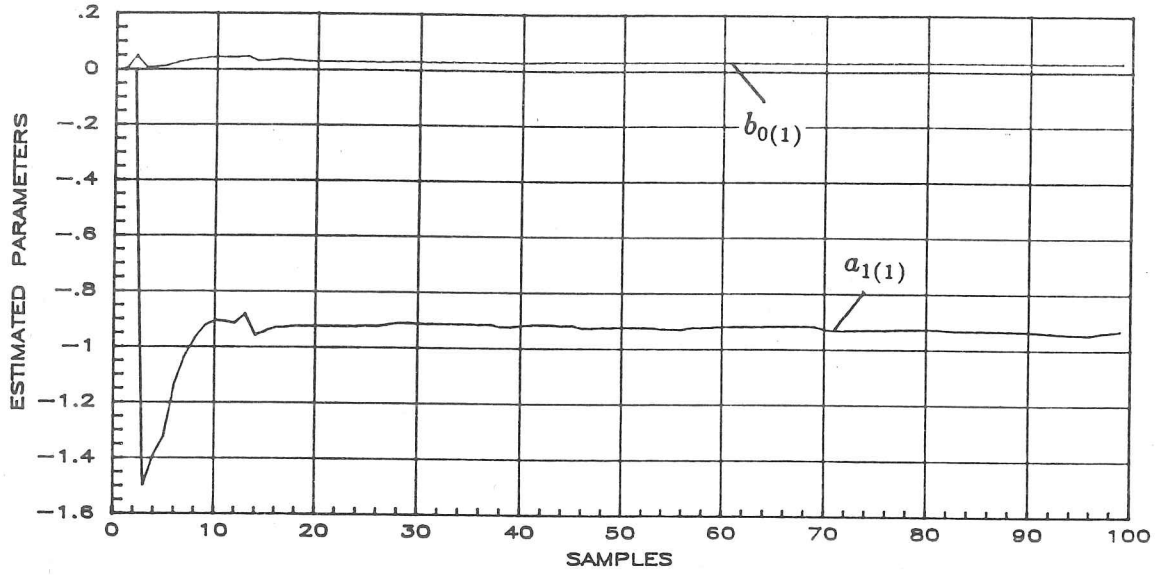

Fig. 3.7.a Convergency of the parameter estimates (speed model, first order)

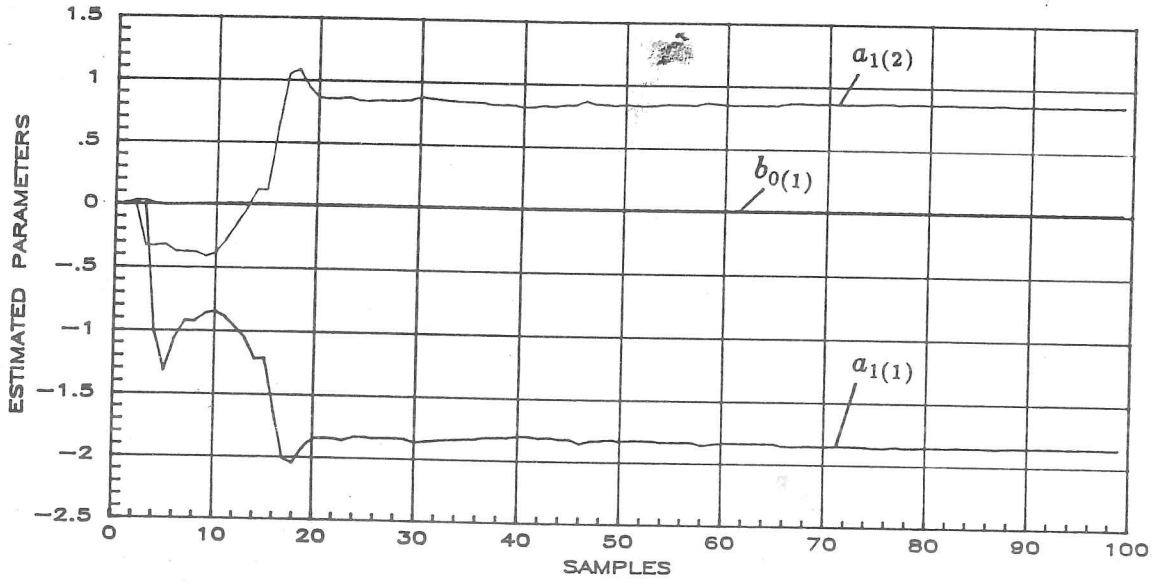

Fig. 3.7.b Convergency of the parameter estimates (speed model, second order)

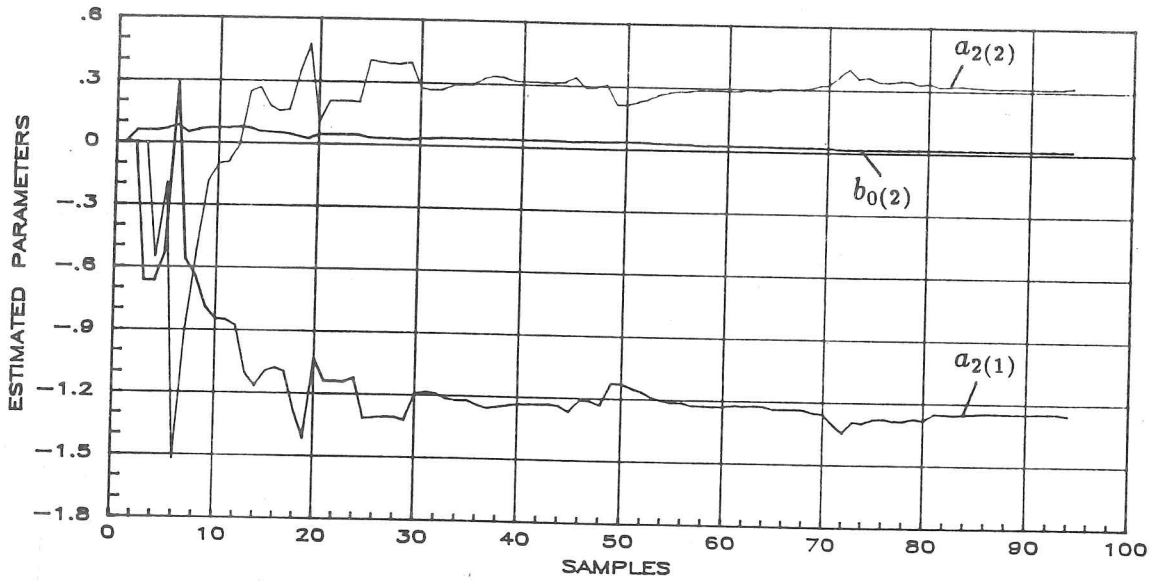

Fig. 3.8.a Convergency of the parameter estimates (smoke model, second order)

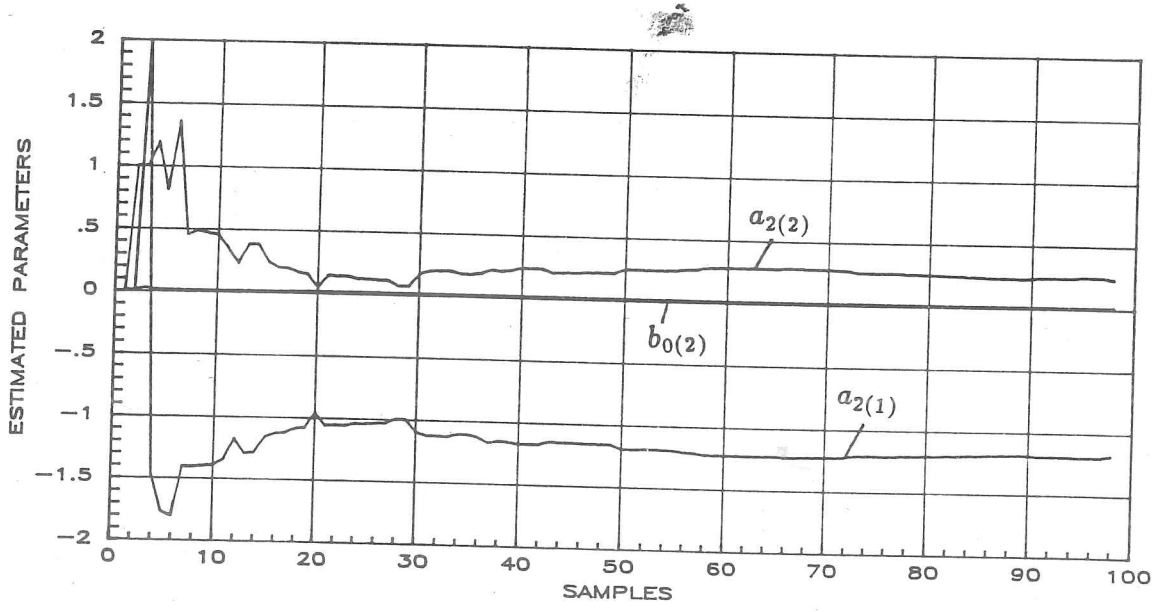

Fig. 3.8.b Convergency of the parameter estimates (smoke model, second order)

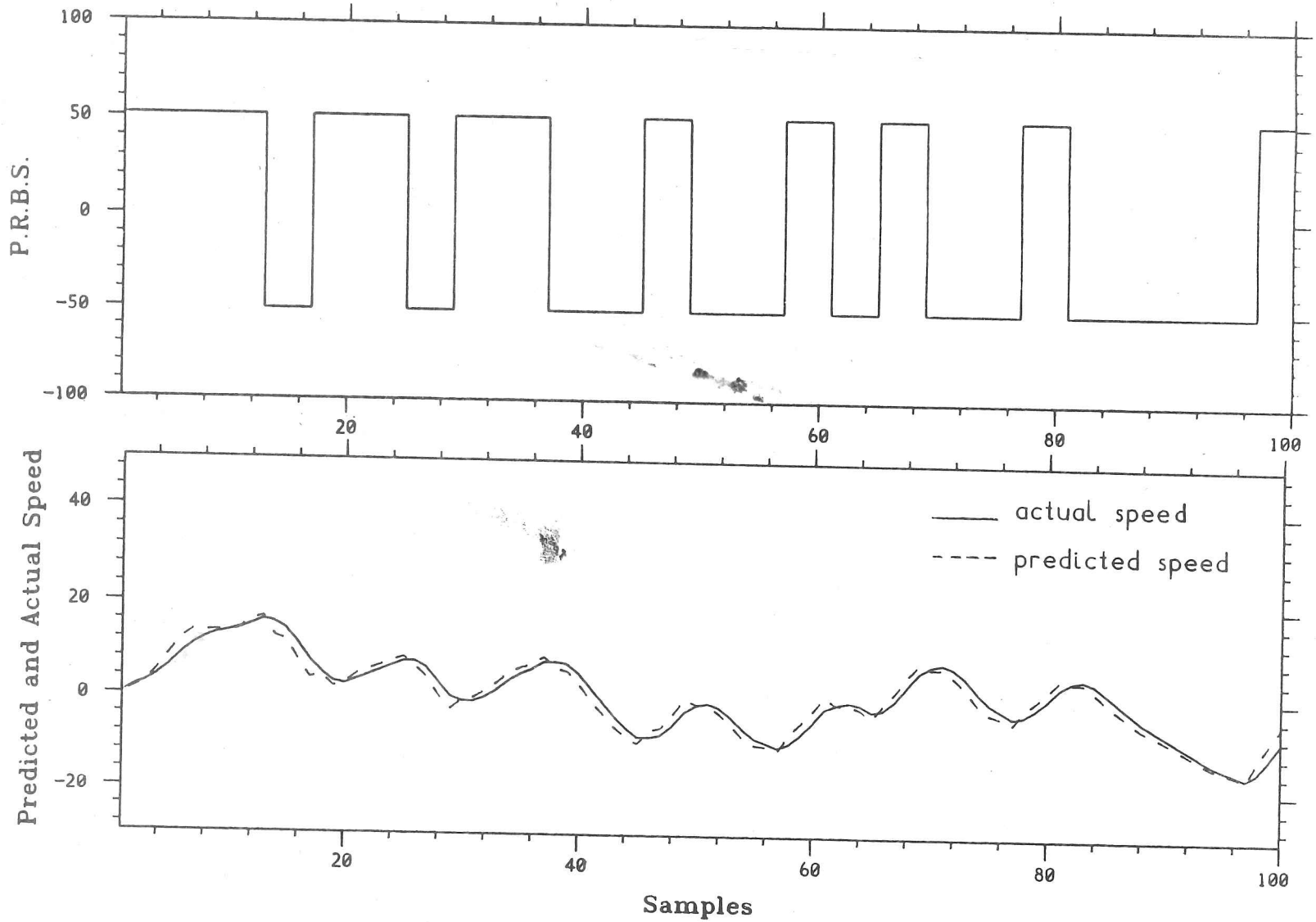

Fig. 3.9 Input signal and comparison of actual and predicted speed outputs (second order transfer function)

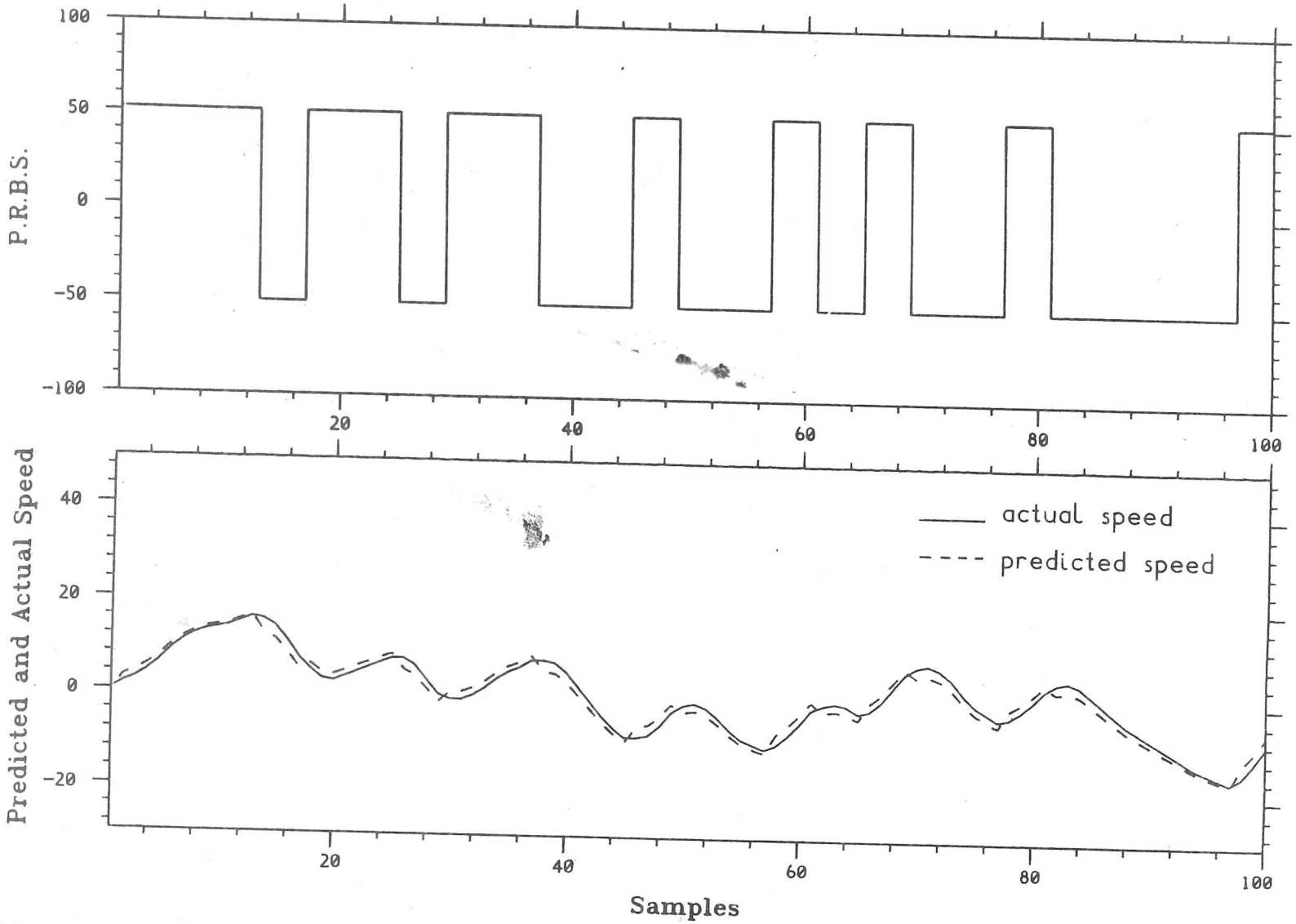

Fig. 3.10 Input signal and comparison of actual and predicted speed outputs (first order transfer function)

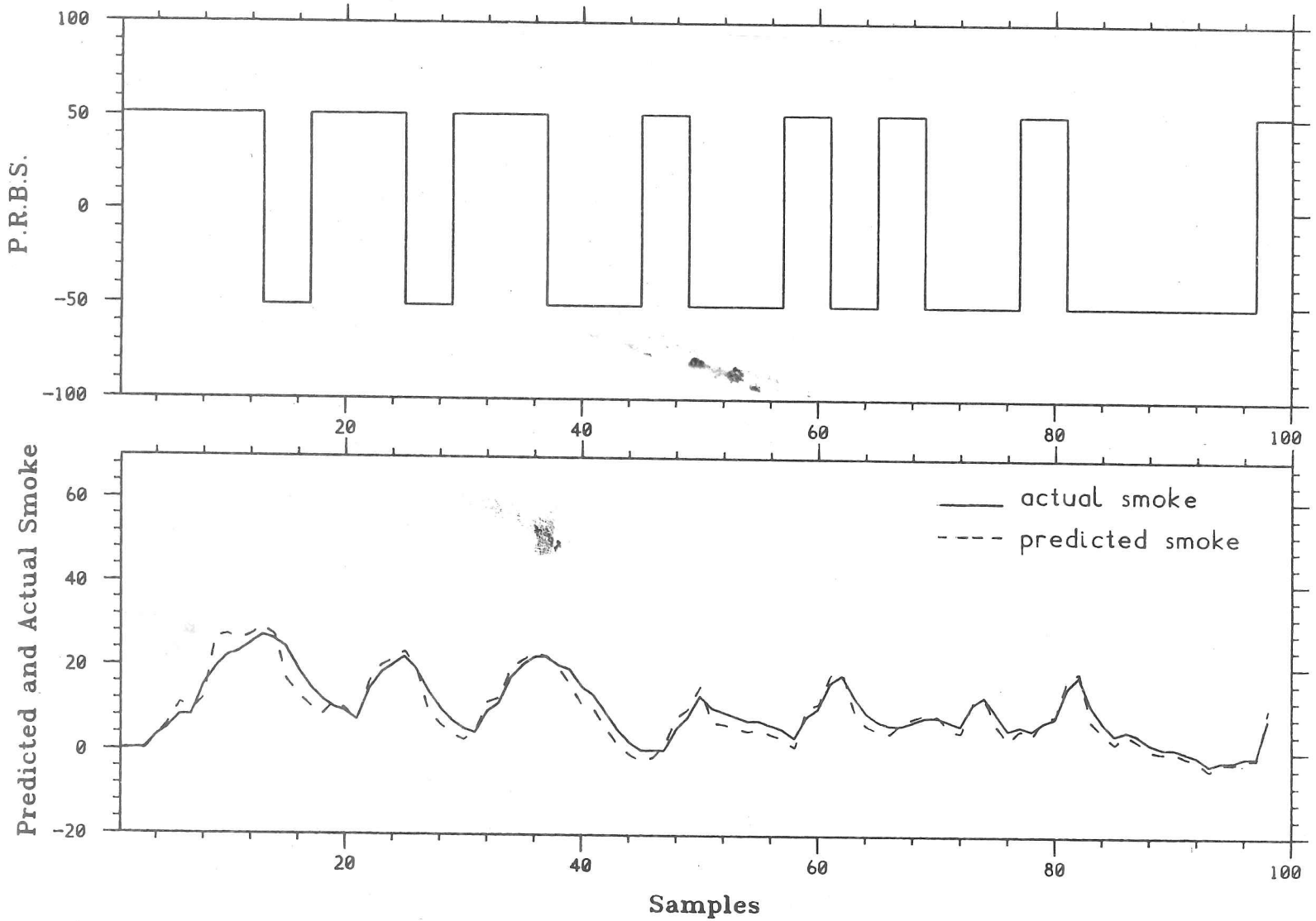

Fig. 3.11 Input signal and comparison of actual and predicted smoke outputs (second order transfer function)

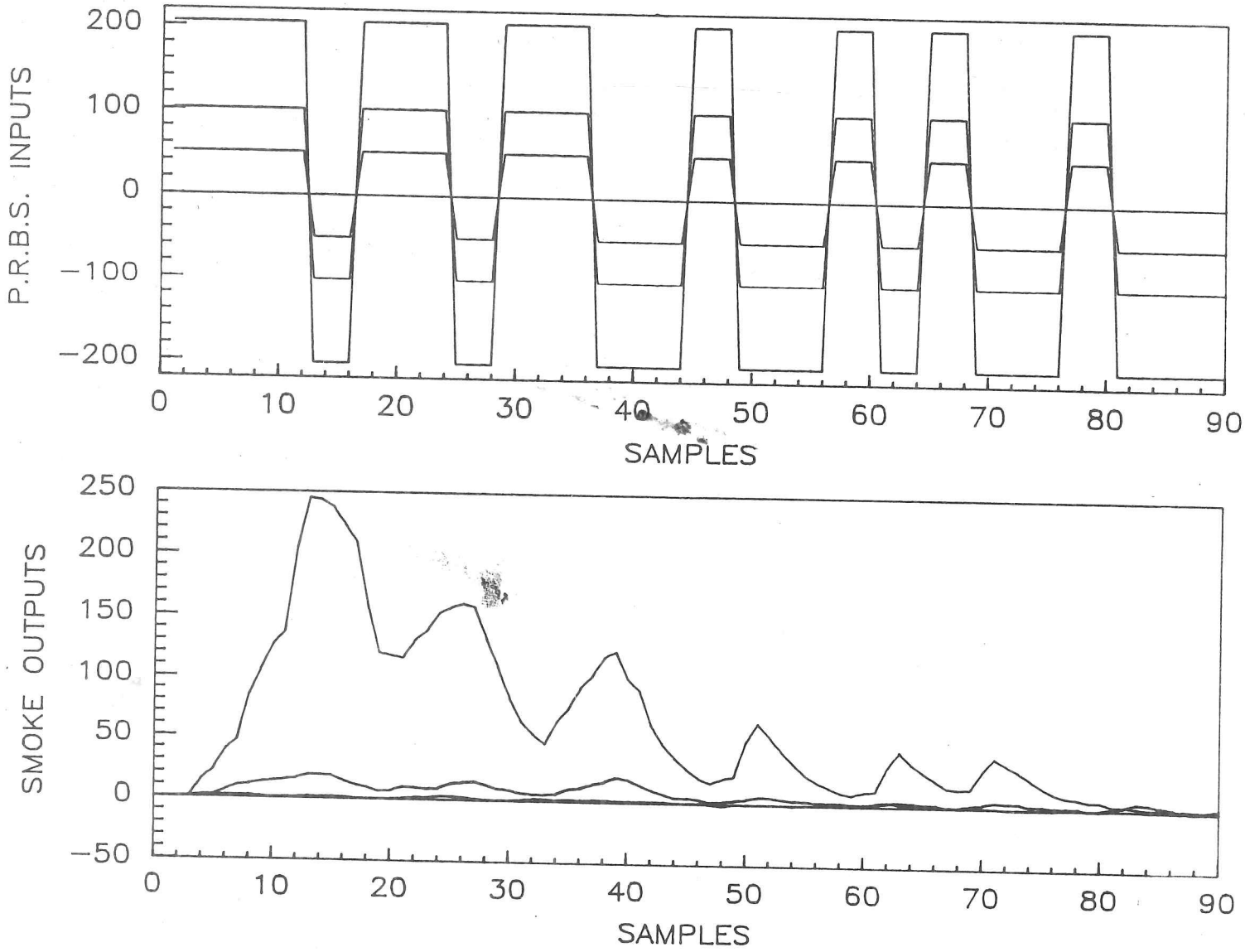

Fig. 3.12 Experimental results for investigating the nonlinearity of the smoke model

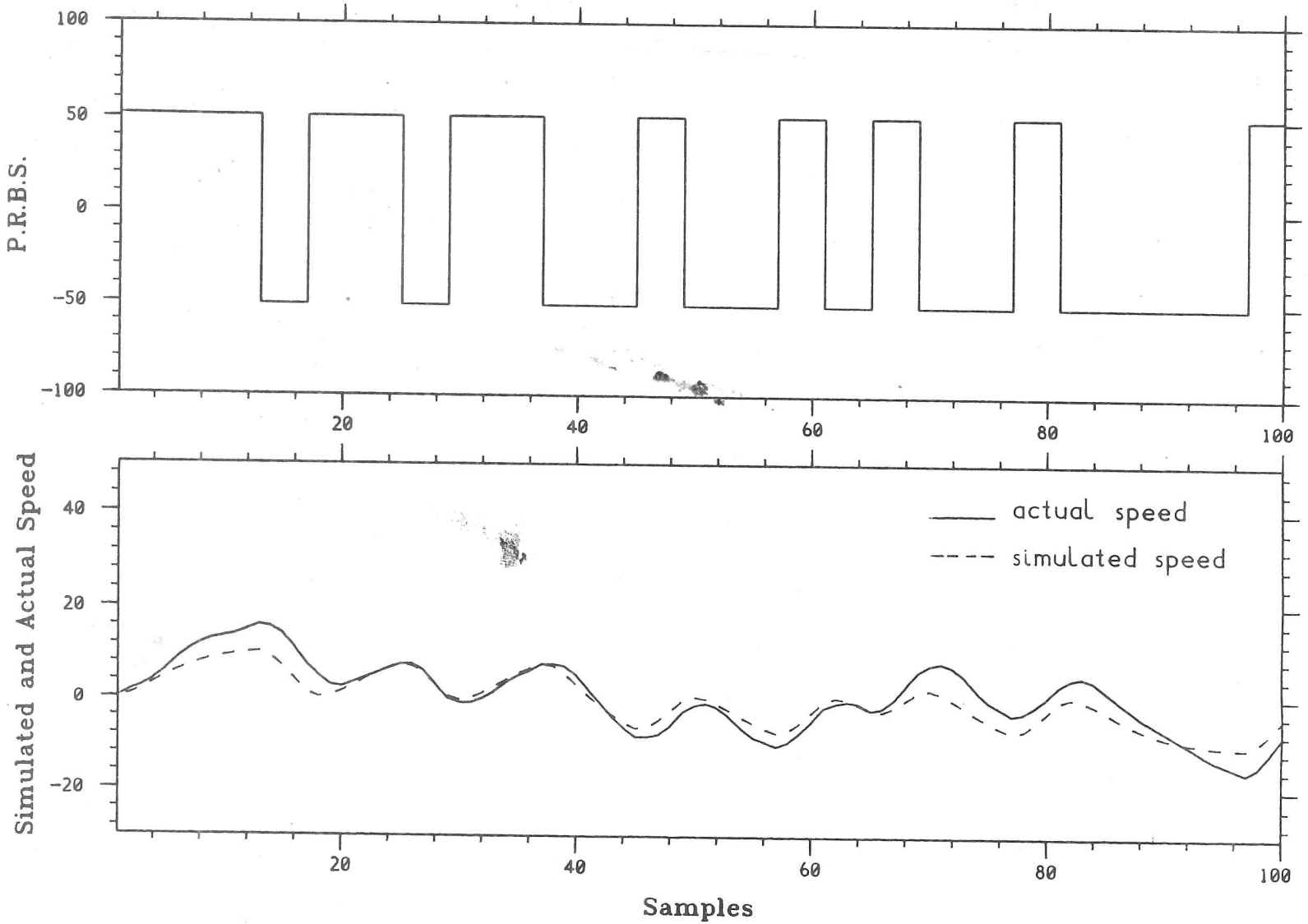

Fig. 3.13 Comparison of actual and simulated speed outputs (speed = 800RPM, torque = 30Nm)

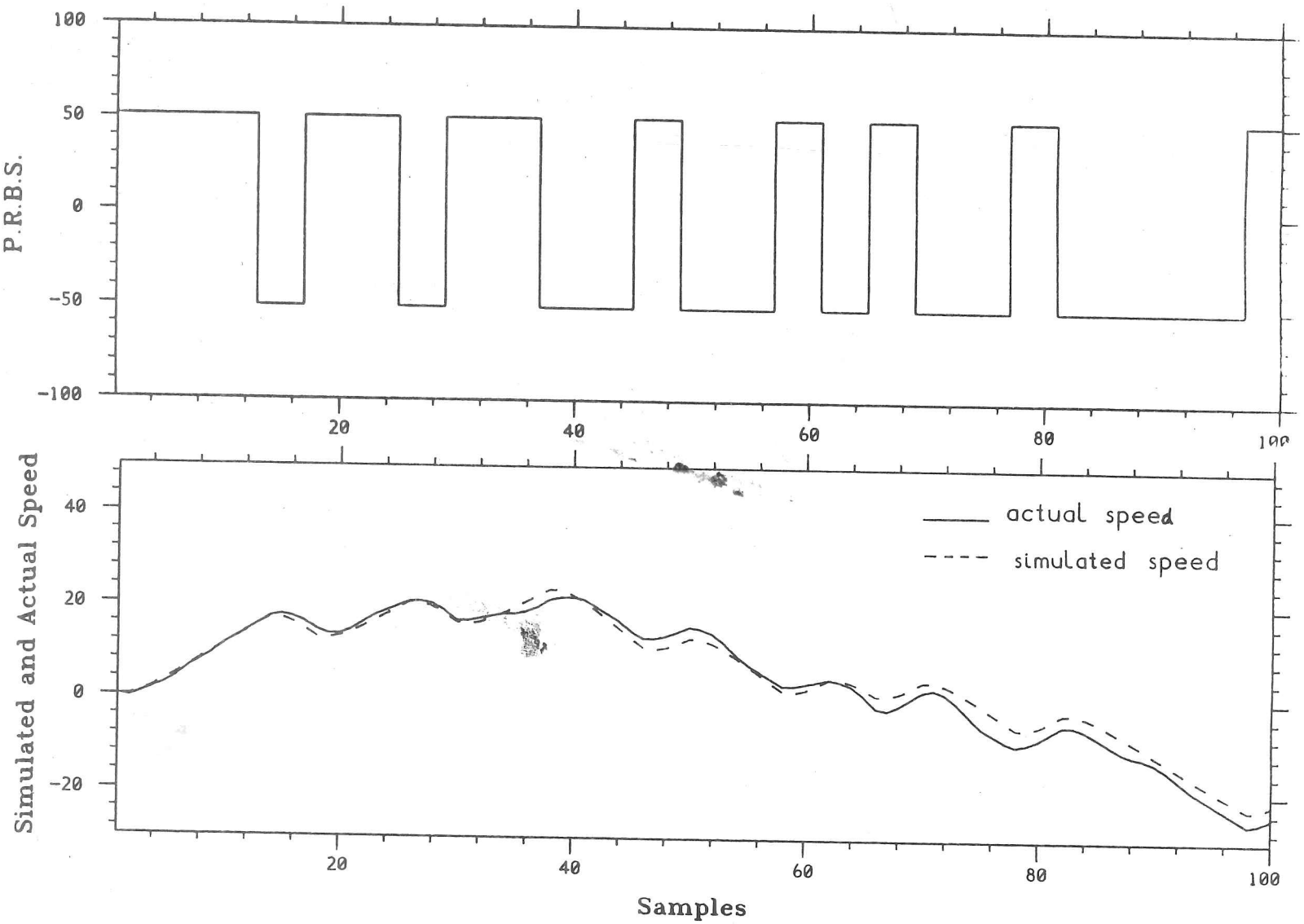

Fig. 3.14 Comparison of actual and simulated speed outputs (speed = 900RPM, torque = 30Nm)

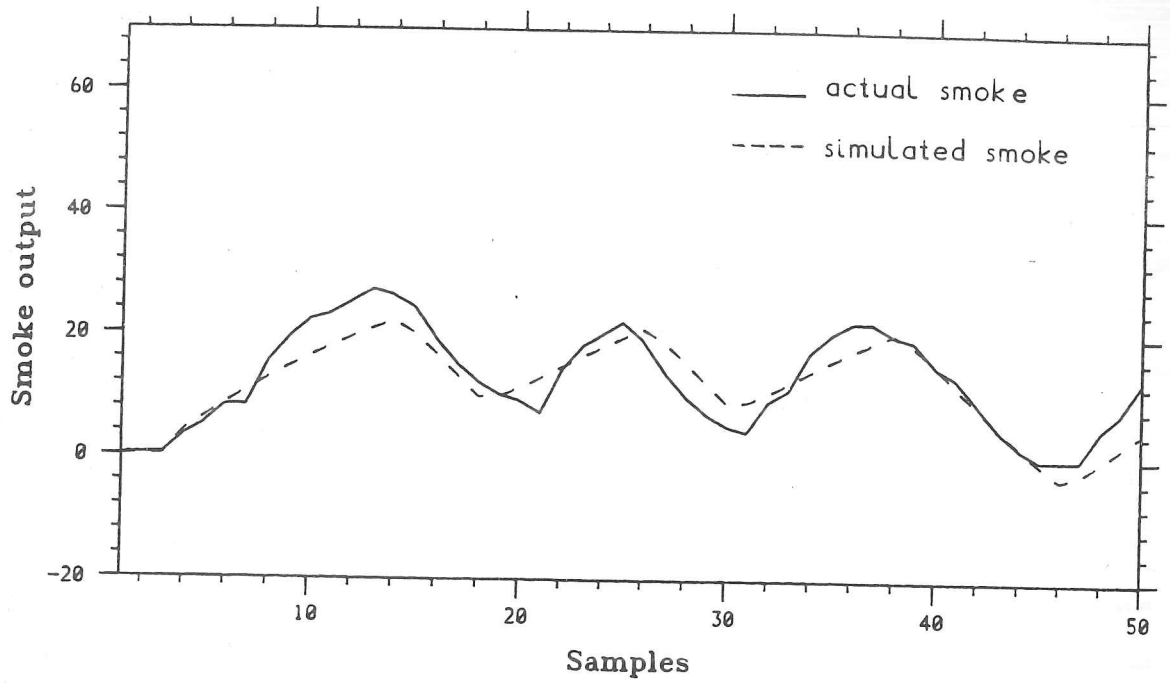

Fig. 3.15 Comparison of actual and simulated smoke outputs

(speed = 800RPM, torque = 60Nm)

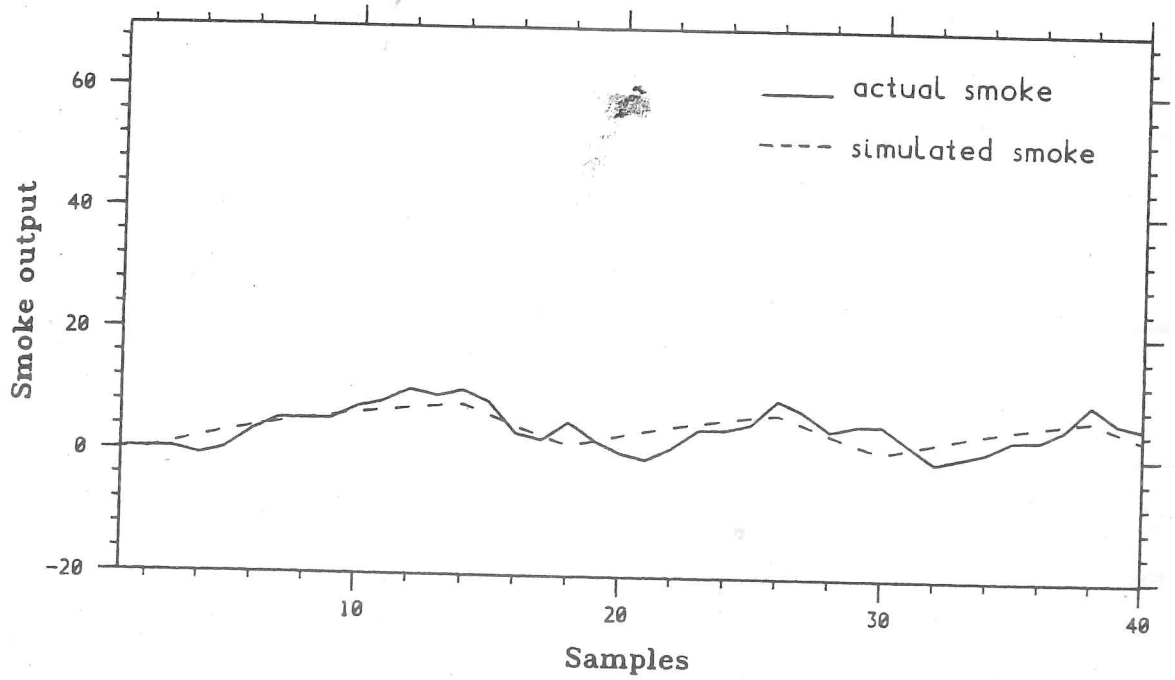

Fig. 3.16 Comparison of actual and simulated smoke outputs

(speed = 800RPM, torque = 30Nm)

Chapter Four

Control System Design

4.1 Introduction

Feedback control is generally deemed to be a better way than 'open-loop' control.This technique involves measuring the output variables at time t and, after measurement, comparing them with what is required at time t and calling the difference between the desired value and the actual one, the 'error'. Using the errors in each of the variables the whole system acts to drive the errors to zero.

In a single-input single-output (SISO) engine speed feedback control loop(Fig. 4.1.a), the controller always works to reduce the error between speed requirement and actual engine speed, so only the speed error is used to control the fuel quantity injected. Normally the smoke is entirely set by a limit on the maximum fuel that can be injected. Such a system cannot cope with the smoke limit because the fuel rack position demanded by the controller will move with a very big step due to the initially large speed error, and the subsequent, over-fueling will cause a high smoke level which normally appears as a 'smoke puff' during blowing down. Fig. 4.1.b shows this 'smoke puff' which is the output of the smoke sensor during acceleration. Although more sophisticated controllers, using the boost pressure to limit the maximum fuel flow are often implemented, these are still difficult to optimize in the sense of allowing truly smoke-limited power during acceleration. This is especially true if the smoke limit itself may be desired as a variable.

For the reason given above, it appears that there is a useful role for an effective real time smoke sensor as part of a control system. Initial work on smoke sensor done

by Collings et al[C10] was the starting point in realizing this control system.

With the objective of smoke limited operation, the engine control system we dealt with had two inputs, required engine speed and smoke, and outputs, transient engine speed and smoke. Normally, the design of a multivariable control system is based on the linear models of the controlled plant. As was found in the results of the engine modelling, the smoke model was nonlinear and could only be linearised locally. This was incentive to design the engine control system with the method different from the usual ones. Two designs of the engine control system will be described in this Chapter. They were based on a combination of the conventional controller design and optimisation for an appropriate interpretation of the overall performance specification. Following the system analysis, the conventional method of the PI controller design was used to initially set the controllers, and then objective functions were chosen for optimization of the closed-loop behaviours together with the selection of the controller's coefficients.

This chapter is organized as follows: In section 2 is the analysis of the engine system to be controlled. Section 4.3 describes two control strategies and section 4.4 considers the problem of optimal performance. Section 4.5 describes the controller design details, whilst in section 4.6 the two control system designs are compared by analysis of the system stability and sensitivity. Section 4.7 then describes the implementation of one control strategy on computer. Finally in section 4.8 we present an evaluation of control performance with experimental results.

4.2 Analysis of the engine system

The engine control system we were considering was not a SISO system and had nonlinear models, so the conventional control approaches were extended to design the proper controllers and satisfy the control requirements. However, observing the performance and analysing the characteristics of a proposed feedback loop was necessary

in order to find control problems and to design efficiently. Classical control approaches were widely used for doing these in terms of directly measured transmission characteristics. Hence Bode diagram and time response methods were used for preliminary analysis of the engine system and the results of this analysis were referred to in the control system design.

The analysis and design of the engine control system were carried out with the models at an engine condition of 800RPM speed and 30Nm torque which were taken from the modelling work described in Chapter 3. The transfer functions of speed-to-fuel rack and smoke-to-fuel rack taken from that chapter are:

$$\begin{pmatrix} y_1(t) \\ y_2(t) \end{pmatrix} = \begin{pmatrix} 1.5375 & 0 \\ 0 & 1.0672 \end{pmatrix} \begin{pmatrix} y_1(t-1) \\ y_2(t-1) \end{pmatrix} + \begin{pmatrix} -0.5627 & 0 \\ 0 & -0.2084 \end{pmatrix} \begin{pmatrix} y_1(t-2) \\ y_2(t-2) \end{pmatrix} + \begin{pmatrix} 0.0145 \\ 0 \end{pmatrix} u(t-nd1) + \begin{pmatrix} 0 \\ 0.0451 \end{pmatrix} u(t-nd2)$$

As defined before, y_1 is the engine speed output, y_2 is the engine smoke output and u is the actuation which acts on the fuel rack.

Fig. 4.2 is the time response of the engine speed to unit step input. The slower pole of the two poles, 0.6006 and 0.9369, in the model of speed-to-fuel rack causes the slow response. As shown in the figure, the rise time is 2.55 seconds and settling time is 4.2 seconds at the point that the error becomes smaller than 3 percent of the steady-state speed value. The steady-state error is about 40 percent of the step input.

In Fig. 4.3 are the Bode plots of engine speed and engine smoke to fuel rack in open loop. For the model of speed-to-fuel rack, the gain margin is 33dB and the phase margin ∞ . The model of smoke-to-fuel rack has a gain margin of 25.8dB and a phase margin of ∞. Two poles of the smoke model in open loop are 0.8099 and 0.2573.

4.3 Control Strategies

Two engine control strategies were constructed in terms of the control objective.

1. Cascade control loop – system 1

Fig. 4.4 is a block diagram representation of the component in system 1. Several simplifications have been made in this diagram to facilitate the discussion of the general concepts involved in the control strategy.

The block labelled 'engine' includes the fuel delivery system, its outputs have been shown as the crankshaft speed and the smoke signals. The 'actuator' includes a servo motor and a circuit to drive it. The sample frequencies of T_s is limited by the execution time in the control program. T_c is the time interval to hold the command signals from D/A converter to the servo motor. T_s is equal to T_c, but T_c and T_s are not uniform in time as indicated in the diagram.

The corresponding control diagram is shown in Fig. 4.5, $R_1(z^{-1})$ is the speed requirement, and $R_2(z^{-1})$ the smoke requirement. Two feedback outputs are $Y_1(z^{-1})$, the actual speed, and $Y_2(z^{-1})$, the actual smoke. $C_1(z^{-1})$ and $C_2(z^{-1})$ are the controllers to process the speed and/or smoke error signals. The speed requirement, $R_1(z^{-1})$, is a step input with positive amplitude. The smoke requirement, $R_2(z^{-1})$, is the smoke level at steady-state engine condition. It can be treated as a step input with zero amplitude.

For the control strategy of this system, the feedback smoke signal is first compared with the allowable smoke level in order to calculate the smoke error. The smoke error passes through a gate which assigns a zero to it if the actual smoke level is less than the allowable one; otherwise, the error remains unchanged. The output of controller 2 is added to speed error, the new error value $e(t)$ is then processed in controller 1.

As the smoke requirement, $R_2(z^{-1})$, is zero, the transfer functions between outputs and inputs are:

$$\begin{pmatrix} Y_1(z^{-1}) \\ \\ Y_2(z^{-1}) \end{pmatrix} = \begin{pmatrix} G_1(z^{-1}) \\ \\ G_2(z^{-1}) \end{pmatrix} R_1(z^{-1}) \tag{4.1}$$

where

$$G_1(z^{-1}) = \frac{C_1(z^{-1})G_1(z^{-1})}{1 + C_1(z^{-1})G_1(z^{-1}) + C_1(z^{-1})C_2(z^{-1})G_2(z^{-1})} \tag{4.2}$$

$$G_2(z^{-1}) = \frac{C_1(z^{-1})G_2(z^{-1})}{1 + C_1(z^{-1})G_1(z^{-1}) + C_1(z^{-1})C_2(z^{-1})G_2(z^{-1})} \tag{4.3}$$

The characteristic equations of these two transfer functions are the same. This means that the stability of the two pairs of inputs and outputs correspond.

2. Parallel control loop – system 2

Fig. 4.6 is the control diagram of system 2. In this system, the actual speed is compared with the required one while the actual smoke is compared with the requirement in a parallel way. Two error signals are processed in their respective controllers, then combined to give the command to the fuel rack.

The transfer functions of this system can be represented by (4.1), but the elements, $G_1(z^{-1})$ and $G_2(z^{-1})$, are different:

$$G_1(z^{-1}) = \frac{C_1(z^{-1})G_1(z^{-1})}{1 + C_1(z^{-1})G_1(z^{-1}) + C_2(z^{-1})G_2(z^{-1})} \tag{4.4}$$

$$G_2(z^{-1}) = \frac{C_1(z^{-1})G_2(z^{-1})}{1 + C_1(z^{-1})G_1(z^{-1}) + C_2(z^{-1})G_2(z^{-1})} \tag{4.5}$$

Two transfer functions have the same characteristic equations, but the two controllers, one for smoke error processing and another for speed, work independently. This is different from system 1 in which the two controllers affect each other.

4.4 Optimisation of the engine performance

The ability to adjust the transient performance is a distinct advantage in feedback control systems. Definition and measurement of the best system performance must be given first in order to analyse and design control systems. As control systems are inherently dynamic systems, the performance is usually specified in terms of both the time response for a specific input signal and the resulting steady-state error.

1. Input signals

For a system which is stable, the response to a specific input signal will provide several measurements of the performance. The standard test input signals commonly used are (1) the step input (2) the ramp input and (3) the parabolic input. In this engine control system, engine speed and smoke were controlled in transients caused by an engine demand change. The speed requirement is a step signal for engine acceleration. Thus the measurement of the system was the response to the step signals.

2. Performance index

There are certain gross system properties which are indicative of acceptable system performance. These performance specifications are generally categorised as either time domain or frequency domain specifications. In the time domain, typical specifications are rise time T_r, percent overshoot P, settling time T_{st} for the transient response of the system to a step input.

During the process of engine acceleration, the speed is always expected to rise up

to the target as soon as possible, i.e. with a short rise time but additional constraints on overshoot and settling time. Thus rise time, settling time and overshoot of the engine speed were taken as three of the performance indices. Also, smoke error was one index which must be considered due to our control objective.

3. Steady-state error

The steady-state error of engine speed was chosen to be less than 5 percent of the step of the input speed. The steady-state error of engine smoke was not taken as a consideration since the smoke level was only required to be lower than the requirement.

4. Optimal criterion

A performance index is a quantitative measure of the performance of a system and is chosen so that emphasis is given to the important system specifications. Modern control theory assumes that the systems engineer can specify quantitatively the required system performance[D5].

With the specified objective functions involving the performance indices, the controllers were designed to minimize an objective function (which was denoted by the symbol J). As a result, any objective function to be minimized should involve penalties or weightings for both excessive deviation from equilibrium and excessive control efforts.

In the control system under study, speed performance was controlled and the error of smoke was only effective when it was bigger than zero even though the actual smoke output was always detected. Remembering that the objective of this control system was to reduce or remove the 'smoke puff', the criterion was defined as

$$\min J = \sum_{i=1}^{N} q_i \cdot X_i$$

where q_i is penalty, X_i includes T_r(rise time of engine speed), T_{st}(settling time of engine speed), P(percent overshoot of engine speed) and E_{sm}, the sum of the smoke errors

over 100 samples. The choice of the penalties was quite arbitrary and at the discretion of the system designer in terms of the control objective.

4.5 Controller design

4.5.1 Computational simulation of the designed system

Simulation study was made on the models of the real engine systems in order to

(a) select the weights in the objective functions through observing the engine process,

(b) determine a set of coefficients for the controllers essential for optimizing the performance,

(c) compare different control strategies in terms of the engine performance during transients and required measurement of the control system.

The inputs of the simulated process were the requirements of engine speed and smoke, and the outputs were the responses of the engine speed and smoke to the fuel rack. With the calibration between the output of the speed sensor(voltage) and the numerical results after A/D converter in the computer, the numerical representation of a step signal corresponding to an engine speed change was obtained.

The models of fuel rack-to-speed and fuel rack-to-smoke were those described in Chapter 3. They were the identified results under engine condition with 800RPM (engine speed) and 30Nm (engine torque). The model of fuel rack-to-speed used for simulation was

$$y_1(t+1) = a_{1(1)}y_1(t) + a_{2(1)}y_1(t-1) + b_{0(1)}u(t-nd1)$$

For reducing the effect of the nonlinearity of the smoke model, the smoke level was

calculated using two groups of parameters of the transfer function:

$$y_2(t+1) = \begin{cases} a_{1(2)}y_2(t) + a_{2(2)}y_2(t-1) + b_{0(2)}u(t-nd2) & \text{when } u \leq u_m \\ a'_{1(2)}y_2(t) + a'_{2(2)}y_2(t-1) + b'_{0(2)}u(t-nd2) & \text{when } u > u_m \end{cases}$$

Two groups of parameters were obtained by modelling with different sizes of the inputs.

The language used for simulation was Fortran which was also used in the main program for the implementation of the control algorithm on real engine. Thus the simulation of the controllers gave a very close approximation to those in real engine control system.

4.5.2 PI controller for speed loop

The engine control system under study had one controllable actuation input and two outputs. One of the outputs, the engine speed, was mainly controlled to meet the desired performance. Design was started with the consideration of the speed loop at first, then the smoke control based on the initially optimized speed loop was designed.

The well known PID (proportional-integral-derivative) controller is deservedly popular in many control systems. It gives satisfactory performance for a wide class of processes, and it is easy to implement using analogue or digital hardware. The combination of P and I controllers which are used most generally gives a stable closed loop provided that k_p, proportional gain, k_i, integral gain, and integral time are appropriately chosen.

The controller 1 in Fig. 4.3 was chosen as a PI controller designed with the model of fuel rack-to-speed. The model of fuel rack-to-speed was second order as described in Chapter 3,

$$G_1(z^{-1}) = \frac{b_{0(1)}}{1 + a_{1(1)}z^{-1} + a_{2(1)}z^{-2}} z^{-m}$$

$$= \frac{b_{0(1)}z^2}{(z-p_{1(1)})(z-p_{2(1)})}z^{-m}$$

m is the sample steps which time delay takes, $m = 1$ when engine speed is 700–1000RPM.

The principle of the design can be described as follows,

The transfer function of controller 1 is,

$$C_1(z^{-1}) = k_{p1} + k_{i1}\frac{z}{z-1}$$

$$= (k_{p1} + k_{i1})\frac{z + \frac{k_{p1}}{k_{p1}+k_{i1}}}{z-1}$$

Let $k_{p1} + k_{i1} = k_0$, $\frac{k_{p1}}{k_{p1}+k_{i1}} = f_0$, then

$$C_1(z^{-1}) = k_0 \cdot \frac{z-f_0}{z-1}$$

Let f_0 be a zero to cancel the slow pole $p_{1(1)}$, so

$$f_0 = p_{1(1)} = \frac{k_{p1}}{k_{p1}+k_{i1}}$$

The transfer function of the closed loop is,

$$G_1'(z^{-1}) = \frac{k_0 b_{0(1)}z}{(z-1)(z-p_{2(1)}) + k_0 b_{0(1)}z}$$

The characteristic equation is,

$$(z-1)(z-p_{2(1)}) + k_0 b_{0(1)}z = 0$$

$$z^2 - (1 + p_{2(1)} - k_0 b_{0(1)})z + p_{2(1)} = 0$$

k_0 can be determined from desired characteristic equation, then k_{p1} and k_{i1} can be found by resolving the following equations,

$$\begin{cases} \dfrac{k_{p1}}{k_{p1}+k_{i1}} = f_0 \\ \\ k_{p1}+k_{i1} = k_0 \end{cases}$$

The selection of the gains in controller 1, k_{p1} and k_{i1}, were based on three performance indices, rise time T_r, settling time T_{st}, and percent overshoot P. The rise time is the time required for the system to move from 10 to 90 percent of the steady-state value (before the first overshoot). The settling time is defined as the time when the speed error settles to be 5 percent of the step input; and the percent overshoot is defined as

$$P = \frac{M_{pt}-1}{1}/100$$

$$M_{pt} = \frac{\text{peak speed value}}{\text{required speed}}$$

So the optimal criterion for the design of speed loop was to minimize

$$J_1 = q_{1(1)} \cdot P + q_{2(1)} \cdot T_r + q_{3(1)} \cdot T_{st}$$

Fig. 4.7 shows the result of J_1 against the variation of k_0 which determines two gains in controller 1. Since the best performance of controller 1 in the speed loop in terms of speed control might not result in the best results for a combined speed and smoke control system, three groups of the gains of the controller 1 were selected for the design of the whole system. In Table 4.1 are the selected coefficients of controller

1 based on the model at engine speed 800RPM and torque 30 Nm.

Table 4.1 Selection of the coefficients in controller 1

No.	k_{p1}	k_{i1}	percent overshoot	rise time (seconds)	settling time (seconds)
1	3.75	0.60	0.0	1.01	1.50
2	4.68	0.54	0.0092	0.74	1.40
3	5.62	0.40	0.0221	0.60	1.60

Fig. 4.8 are the simulation results of the engine speed and smoke outputs with the controller in No. 3 of Table 4.1. The speed outputs with controller 1 in No. 1 – 3 of Table 4.1 are shown in Fig. 4.9. These results were obtained from the processes with only speed control.

4.5.3 Design of combined speed and smoke control system

The design of the speed loop was to select the gains of the controller 1 with the emphasis put on cancelling the slow pole in the transfer function of fuel rack-to-speed, and then meet the performance specifications. Instead of this method, the coefficients of the controller 2 for smoke error processing and the controllers of the combined speed and smoke control system were determined by minimizing the objective function J_2. Based on the optimization of engine speed performance, the requirement of the engine smoke output was adopted as one of the three performance indices. The other two indices were percent overshoot and settling time of the engine speed. The objective function was

$$\min\ J_2 = q_{1(2)} \cdot P + q_{2(2)} \cdot T_{st} + q_{3(2)} \cdot E_{sm}$$

Controller 2 was a proportional controller which was chosen in terms of the simple algorithm and control purpose. Still based on the models at engine condition of 800RPM and torque 30Nm, simulations were carried out with both controllers for processing speed and smoke signals. For the three selected PI controllers designed in 4.4.2, the gain of the controller 2 was varied to find the k_{p2} with which the objective function J_2 was minimum. Fig. 4.10.a shows the optimization results of system 1, and Fig. 4.10.b those of system 2. In these figures, k_0 varies from 4.0 to 6.0 with a 0.2 step, and k_{p2} varies from 0.1 to 2.0 with a 0.2 step.

As shown in the figures, the optimal values of k_{p2} are obvious with different coefficients of controller 1. To system 1, value of k_{p2} with minimum J_2 is 0.4 when PI controller has proportional gain of 3.75 and integral gain of 0.25. The optimal value of k_{p2} of system 2 is 1.2 with controller 1 in which k_{p1} is 3.75 and k_{i1} is 0.25.

Basically, the speed control loop works to reduce the speed error through moving the fuel rack forward at first in acceleration, and smoke control means detecting the high smoke level with impeding the quick movement of the fuel rack. This is done in different way with control strategy 1 and 2.In system 1, the speed error between actual and required speed outputs to cause quick moving of the fuel rack is reduced by adding smoke error before PI controller (controller 1). But in system 2, the command signal to move the fuel rack is reduced directly by the processed smoke error signal. In fact, controller 2 in system 1 acts as a scaling factor rather than a proportional controller to make the smoke error match the speed one. Fig. 4.11 shows the simulation results of speed and smoke outputs with strategy 1 when speed requirement is 100RPM (numerical representation 154.01). In Fig. 4.12 are the results with control strategy 2.

4.6 Comparison of two control strategies

The transfer functions of the controllers which are developed and the controlled en-

gine have certain characteristics that permit transient and steady-state analysis of this control system. Three factors of prime importance in feedback-controlled systems are stability, steady-state error and parameter sensitivity. In this section we will compare the two control system designed with different strategies in these three aspects.

4.6.1 Steady-state error

It is found that the steady-state error of system 2 is zero, but that of system 1 depends on the coefficients of the controllers and the engine models [Appendix A].

4.6.2 Stability

In contrast to single-input and single-output control systems, an interesting and important feature in multivariable feedback systems, is that each input/output combination will have a different stability margin.In this sense, analysis moves from studying a single Bode magnitude and phase plot to studying, for each pair of output-to-input, a set of Bode plots. However, as described in section 4.2, the transfer functions of the engine control system have the same characteristic equations. This makes the stability analysis of this system as simple as that of a SISO system.

The characteristic equation in system 1 is

$$1 + C_1(z^{-1})G_1(z^{-1}) + C_1(z^{-1})C_2(z^{-1})G_2(z^{-1}) = 0$$

The characteristic equation in system 2 is

$$1 + C_1(z^{-1})G_1(z^{-1}) + C_2(z^{-1})G_2(z^{-1}) = 0$$

Fig. 4.13.a and 4.13.b are the Bode diagrams of system 1 and system 2. The controller 1 in both of the systems have the proportional gain $k_{p1} = 3.75$ and integral gain $k_{i1} = 0.25$. The proportional gain k_{p2} of controller 2 is 0.4 in system 1 and 1.2 in

system 2. To system 1(Fig. 4.13.a), the gain margin is 10.6dB and the phase margin 66.2^0. In system 2(Fig. 4.13.b), the gain margin is 15.1dB and phase margin 76.7^0.

Both systems are satisfied with the essential requirement to the stability, gain margin of 5 dB and phase margin of 45^0[F5].

4.6.3 Sensitivity to the variation of the controllers' parameters

The principle concern with parameter sensitivity is that the dynamic response and especially the stability of the system will be altered when the parameters are varied. It is well known that using negative feedback control can reduce the effect of parameter variations of the controlled system. The effect of parameter variations can be described by a measure of sensitivity of the system performance to specific parameter changes, the root sensitivity means how the parameter change has its effect on the characteristic roots[D5].

The root sensitivity can be defined as

$$S_k^{p_i} = \frac{\partial p_i}{\partial ln\alpha_m} = \frac{\partial p_i}{\partial \alpha_m / \alpha_m} \tag{4.6}$$

where p_i equals the ith root of the system and α_m is the parameter of interest.

The change in p_i due to the change of α_m is given by

$$\delta p_i = \frac{p_i^{n-m}}{\prod_{i \neq j}(p_i - p_j)} \cdot \delta \alpha_m \tag{4.7}$$

where n is the order of the characteristic equation, m is the index number of the parameter considered. If the magnitude of p_i is less than one, the larger the power of p_m^{n-m}, the smaller the variation. Here can be concluded that the most sensitive parameter is α_n, the constant term in the characteristic equation, when p_i is less than one.

The characteristic equation of system 1 is

$$[(z-1)(z^2+a_{1(1)}z+a_{2(1)})+k_0b_{0(1)}z(z-f_0)](z^2+a_{1(2)}z+a_{2(2)})$$
$$+k_{p2}k_0b_{0(2)}(z-f_0)(z^2+a_{1(1)}z+a_{2(1)})=0 \qquad (4.8)$$

The characteristic equation of system 2 is

$$[(z-1)(z^2+a_{1(1)}z+a_{2(1)})+k_0b_{0(1)}z(z-f_0)](z^2+a_{1(2)}z+a_{2(2)})$$
$$+k_{p2}b_{0(2)}(z-1)(z^2+a_{1(1)}z+a_{2(1)})=0 \qquad (4.9)$$

We can see these two equations are similar except the terms including k_{p2}. The variation of k_{p2} affects the coefficients of the terms: z^3, z^2, z and z^0. But when the variations of k_{p2} in two cases are same, the coefficients with k_{p2} in (4.9) is amplified more than that in equation (4.10) when k_0 is bigger than 1. This must cause the different results of the denominator in (4.8) of two systems. So the roots of the two systems behave differently to the variation of k_{p2}.

How the systems sense to the variation of k_{p2} with different control strategies can be analysed and displayed using Root Locus diagram. The tendencies of the roots' variation of the characteristic equation are observed rather than finding the locus.

Fig. 4.14.a and 4.14.b are the Root Loci of two system with the engine condition: speed=800RPM and torque=30Nm. The gain of controller 2, k_{p2}, varies from 0.5 to 10. in Fig. 4.14.a and from 1 to 25 in Fig. 4.14.b. Comparing the results of two systems, we can find that the roots' positions of the characteristic equations of two systems are similar when k_{p2} is small, 1 or 2. But the roots of system 1 go towards unstability more quickly, system 1 becomes unstable when k_{p2} is 4.2 and system 2 when k_{p2} is 7. k_{p2} in system 1 acts as a scaling factor between speed error and smoke error. The processing of smoke error depends on not only controller 2 but also controller 1. When the proportional gain in controller 1 is bigger than 1, the smoke error is amplified by a gain which is k_{p1} times of k_{p2}.

4.7 Implementation of the controller strategies

4.7.1 Language of the control programs

For a control system, the software, including microcomputer programs, should be maintainable. That is, in the event of hardware changes or revised specifications, it should be possible to easily and successfully adapt existing programs to meet the new operating environment. With all but the most trivial programs, a high level programming language must be used in order to ensure a maintainable program.

Programs written in a high level language, even a compiled high level language, can never be as efficient as a well written assembly language program due to restrictions imposed on program structure. In some control systems, assembly language must be used if the system specially has a requirement of high sample frequency. However from the experience of the engine control system, good performance of the control system can be obtained with a sample frequency equal to or less than 10Hz which depends on the engine revolutions. The high level language used in the PDP11/23 — Fortran IV is a compiled language and in execution more efficient than interpreted high level languages.

Taking account of the requirement of the sample frequency which was low in engine digital control and the conveniency of program adaptation, high level language, Fortran IV, was chosen for the main program, and assembly language was used for I/O routines.

4.7.2 Construction of the control program

The control strategy was implemented on the computer PDP/11-23. Software is composed of four parts:

1) Initilization

2) Data acquisition, data processing

3) Controlling tasks

4) Parameter display, adaptation and data storing

The main program was written with Fortran language. It has several assembly language routines and Fortran language routines. The assembler language routines are as follows:

1) Analogue-to-digital conversion

2) Digital-to-Analogue conversion

3) Counter of sampling time

4) Memory storage

The Fortran routines are for keyboard controlled actions:

1) Interruption

2) Display and adaptation of some parameters

3) Create the data files for storage

The main program monitors desired quantities, performs as a controller, holds the results in memory, and stores the data necessary.

4.7.3 Sampling frequency

The selection of the sampling frequency is usually limited by the speed of the computer and physical consideration of the system. The limitation on the rate at which

sampling can be done is that the sampled signal must be processed by the computer before the computer can drive the D/A converter with the new control command. An algorithm to provide the control signal takes time to execute and hence limits the rate at which control effort update can occur.

In the engine control system we were studying , the minimum time between the firings was $171ms$ at 700 RPM and $133ms$ at 900RPM. The control program could not be easily made to sample faster than $100ms$. The controller in z transform was designed with the transfer functions in which the sample time interval was constant and dependent of engine revolutions, Hence, the convenient way to make the controller work effectively was to select the sampling frequency as the same as that in the designed controller or derived transfer functions if this frequency was realisable. Referred to the previous work on engine digital control, the experience suggested that $125ms$ (8Hz) be a reasonable value for sampling interval in this engine control system.

The sampling frequency was controlled and adapted by a 'line clock' in the computer.

4.8 Experimental results

The control systems designed above were tested to demonstrate that the speed and smoke control system was capable of reducing the smoke 'puff' at transients while the speed requirement was met. Based on the comparison of the two control strategies with analysis of stability, steady-state error and sensitivity, control strategy 2 showed better performance than strategy 1. This section will describe the set up of the experiment and display the results of an experimental study to evaluate the operation of control strategy 2.

1. Initial condition of the experiments

The computer was not equipped to start the diesel engine. This had to be done manually. Control of running engine was taken initially by a hand-over procedure as follows:

1) set up the position of fuel rack with ODT(Octal Debugging Technique) to access engine speed 800 – 900RPM at medium load when the engine ran. The initial load was set to be about 33Nm. Experience showed that a medium initial speed demand was usually best, as a high initial speed could often lead to the engine overspeeding in the first few seconds of the run before controller operation,

2) set the engine load and the control program ready to run, the initial engine speed required was given in the control program,

3) start the engine manually,

4) run the control program, and allow the engine to warm up.

2. Test conditions

Four speeds and three load settings were chosen to span the operating range. 700, 800,900 and 1000RPM were chosen as the speed test points. For each test cycle, the engine was run at steady-state condition at first, and one of the load points was set initially. After the required speed was input from the keyboard by the operator, the engine was accelerated by the control program from one speed point to another. The engine ran at a new speed-load condition until next engine speed was required. The speed output and the smoke output during the acceleration were sampled, converted and stored into the data files.

3. Results and discussion

Fig. 4.15 — 19 show the experimental results of control system 2. In Table 4.2 are the corresponding engine test conditions of the figures. 'Speed' shows the step between the initial and final required engine speed. 'Torque' means the initial load in each

acceleration process. The limited smoke levels in the experiments were determined as the levels at steady-state engine condition.

Table 4.2 Engine test points

Fig.	Speed(RPM)	Torque(Nm)	k_{p1}	k_{i1}	k_{p2}
4.15	700-900	40	3.75	0.25	1.20
4.16	700-900	30	3.75	0.25	1.20
4.17	700-900	30	2.82	0.18	1.20
4.18	800-900	60	1.80	0.20	1.00
4.19	800-1000	30	3.75	0.25	1.20

In Fig. 4.15, the smoke 'puff' (trace 1) was produced by the control program which simulated the usual engine acceleration process without smoke detection. Trace 2 is a result of strategy 2 when the requirement of engine speed was the same as that of trace 1 but with smoke feedback control. The loop of smoke feedback in Fig. 4.3 acted so as to impede forward the movement of the fuel rack as the smoke level exceeded that limited. So the difference between the two traces was caused by different $u(t)$ signal sequences, one was produced by only the speed error, another by both the speed and smoke errors.

In Fig. 4.16 and 4.17 are two traces of engine speed and smoke outputs. They show that the smoke 'puff' is reduced with the control effects while the required speed steps are met at light load conditions.

The results shown above demonstrate that the smoke exhausts during engine transients could be reduced with the developed control system. The experimental results

with these non-adaptive controllers were satisfied when engine acceleration spanned the range of 700–900RPM with light torque below 40Nm.

However these controllers with fixed coefficients were not able to keep working well a) with heavy load or b) when the final engine speed was 1000RPM with light load. Fig. 4.18 shows the results when the engine speed was increased from 800 to 900RPM with engine load set on 60Nm. As shown in the figure, the smoke is hardly reduced and oscillation happens when the engine speed should settle down. Fig. 4.19 are the results of an acceleration process in which the engine speed increased from 800 to 1000RPM. The speed trace does not properly settle to 1000RPM even though the oscillation has a small amplitude and low frequency. The problems shown in these two figures were caused by the nonlinearity of the smoke model and the variation of the parameters in speed models with the change of engine conditions.

In the case of a) as mentioned above, the smoke model in the condition with heavy load might become more nonlinear than that with light load, and it is very difficult to design the proper controllers with fixed coefficients to detect the high smoke level. In the case b), the slow pole in the fuel rack-to-speed model, $p_{1(1)}$, moves towards the center of the unit circle in z-plane when the engine speed is increasing. This means that the value of $p_{1(1)}$ becomes smaller, and it cannot be cancelled by the numerator of the controller 1 because the zero in the controller is determined with the consideration of replacing the slow pole in the speed model at engine speed 800RPM and torque 30Nm. Hence $\frac{z-f_0}{z-p_{1(1)}}$ is not equal to 1 in this case but acts as a phase lead component in the control system. Phase-lead generally increases the bandwidth as a high pass filter and so introduces undesirable effects resulting from noise transmission through the system.

4. Comparison of the simulated and test results

With the models derived, simulated results in the open loops were compared with the test data, as described in Chapter 3. The comparisons presented there showed the

acceptability of the models. Hence these models were used further in control system analysis and design. With the consideration of the effect of the controllers and feedback loop, here it is necessary to compare the simulation results of the control processes in the controller design and the experimental results in the real engine control system.

Fig. 4.20 is a comparison of the test and simulated results when engine speed was increasing from 700 to 800RPM and initial torque of the control process was 30Nm. In Fig. 4.21, the compared results were obtained from the process in which the engine was required to accelerate from 700 to 900RPM and initial torque was 24Nm. As shown in the figures, the errors between the simulated and test results look larger than those in Chapter 3. This is because the controlled engine outputs were fed back and the errors between the requirements and real outputs were processed (amplified and integrated in the controller), so that the simulated and real outputs became more different. With attention to the speed traces, the error between the real and simulated results are bigger in transients than when speed is settled down. This is due partly to the accuracy of the speed model and partly the difference of the smoke emission processes between the real test and simulation. However the compared traces show good agreement.

4.9 Conclusions

The feedback control of the engine smoke was realized using a new smoke sensor. The control system detected the smoke during engine transients. The non-adaptive controllers in this control system were designed with a method which combined the conventional PI controller design and the observation of the optimal engine performance. This design method was used to solve the problems caused by the nonlinearity of the engine models. Experimental results at light-load engine conditions demonstrated that this engine control system effectively reduced the smoke 'puff' when it controlled the engine acceleration to meet the target engine speed.

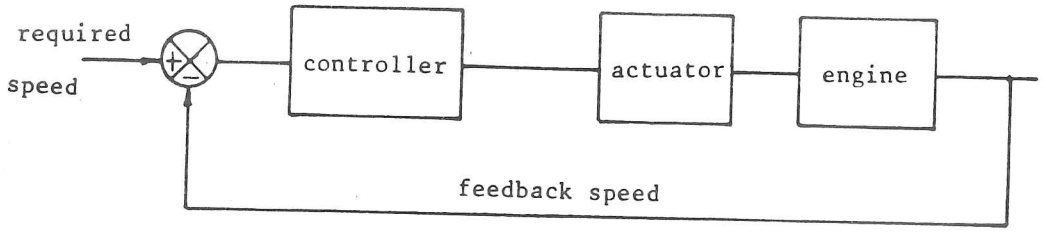

a. Diagram of the control loop

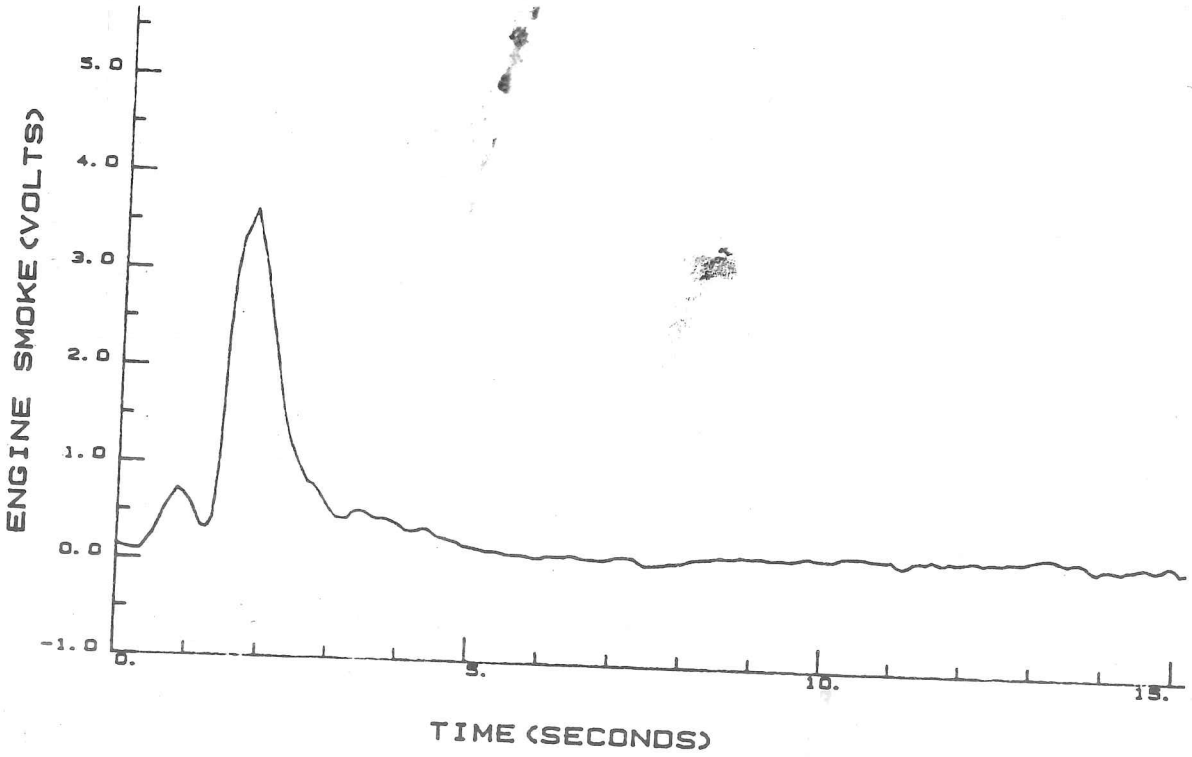

b. Smoke 'puff'

Fig. 4.1 Single-input single-output engine speed feedback control

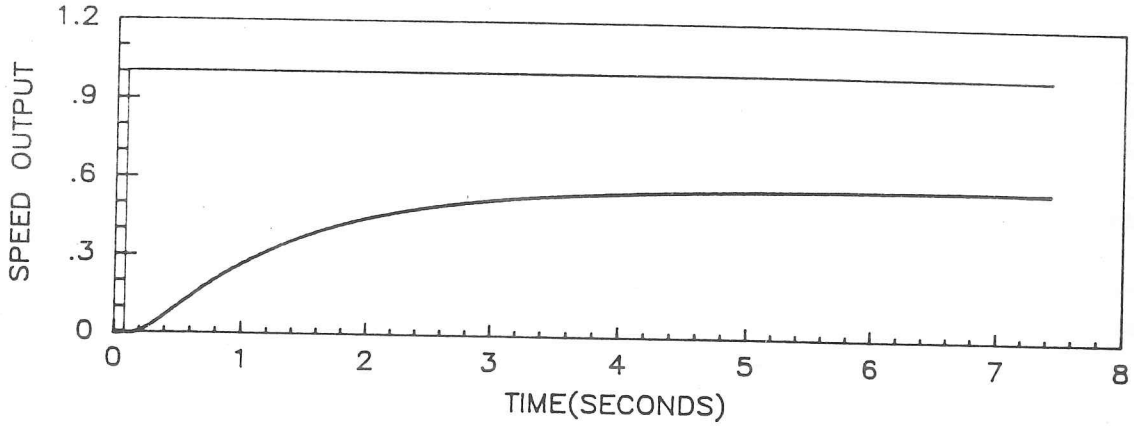

Fig. 4.2 Time response of speed to an unit step input on AEC engine

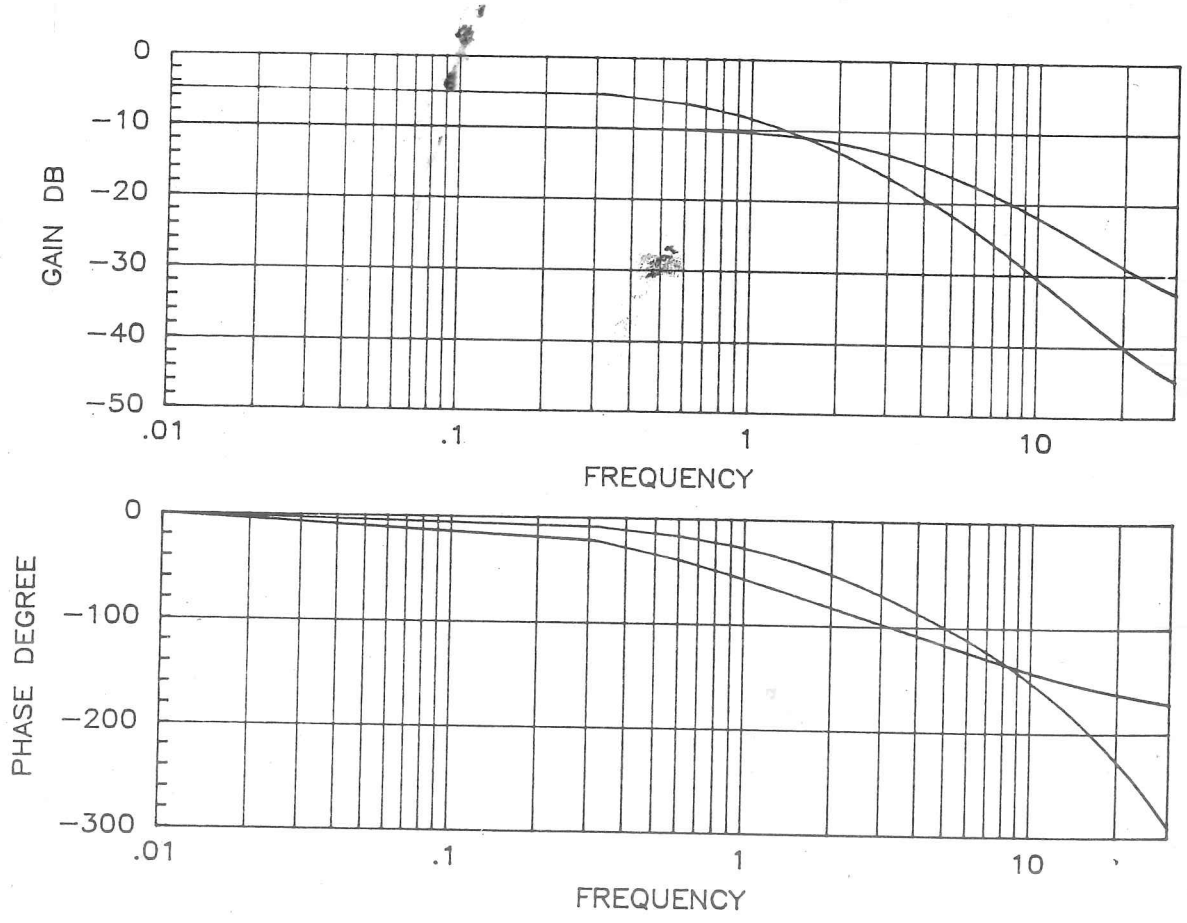

Fig. 4.3 Bode diagram of engine system in open loops

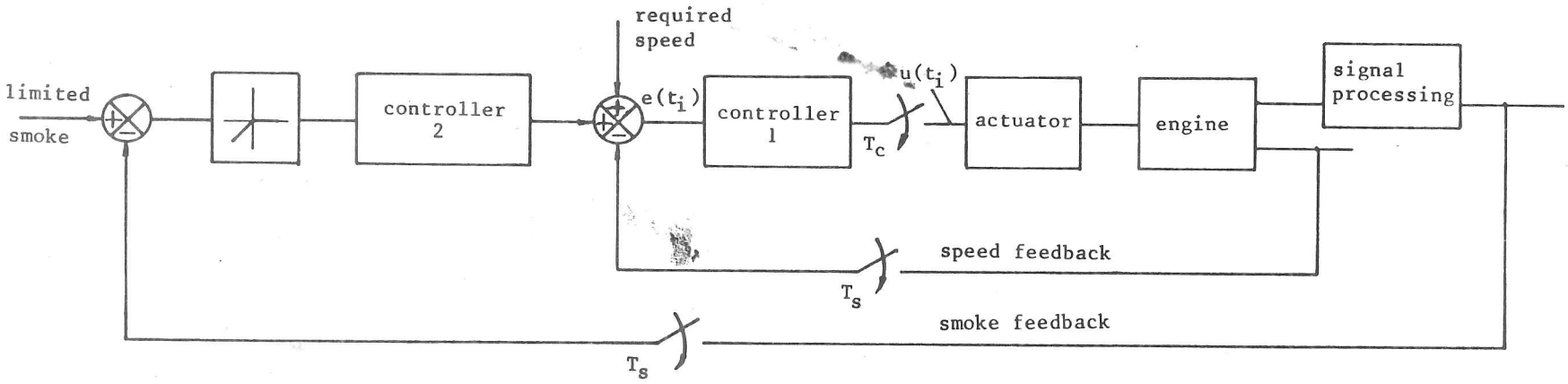

Fig. 4.4 Block diagram of engine control system

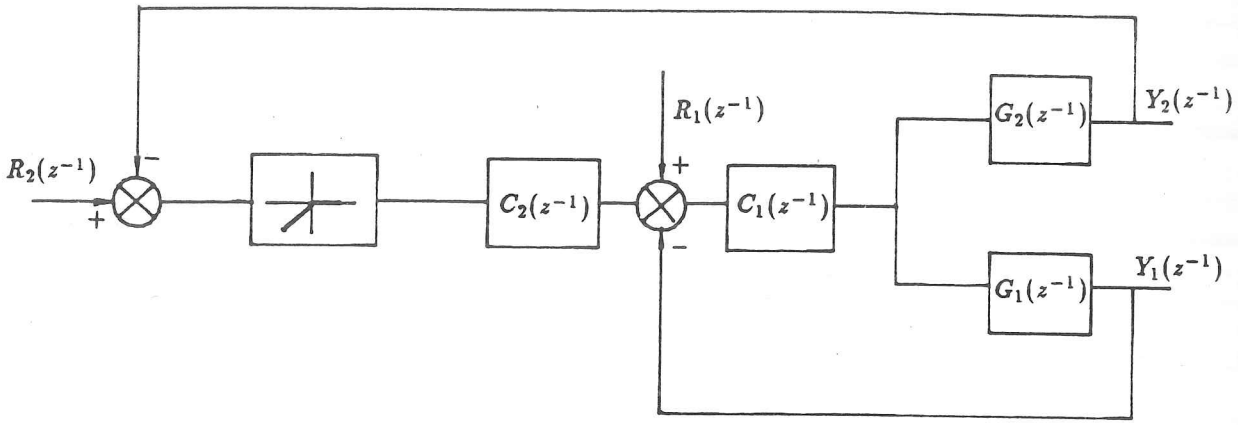

Fig. 4.5 Block diagram of control strategy 1

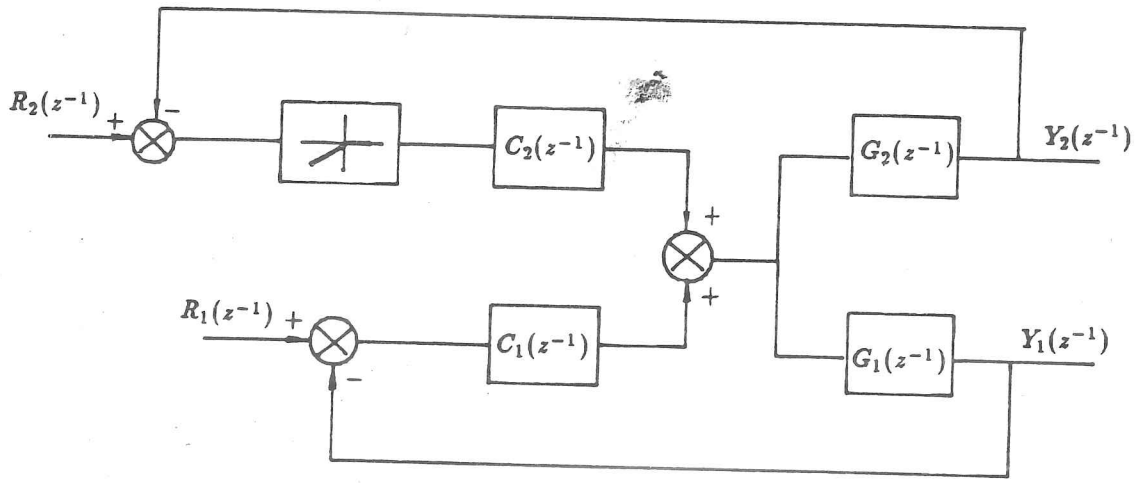

Fig. 4.6 Block diagram of control strategy 2

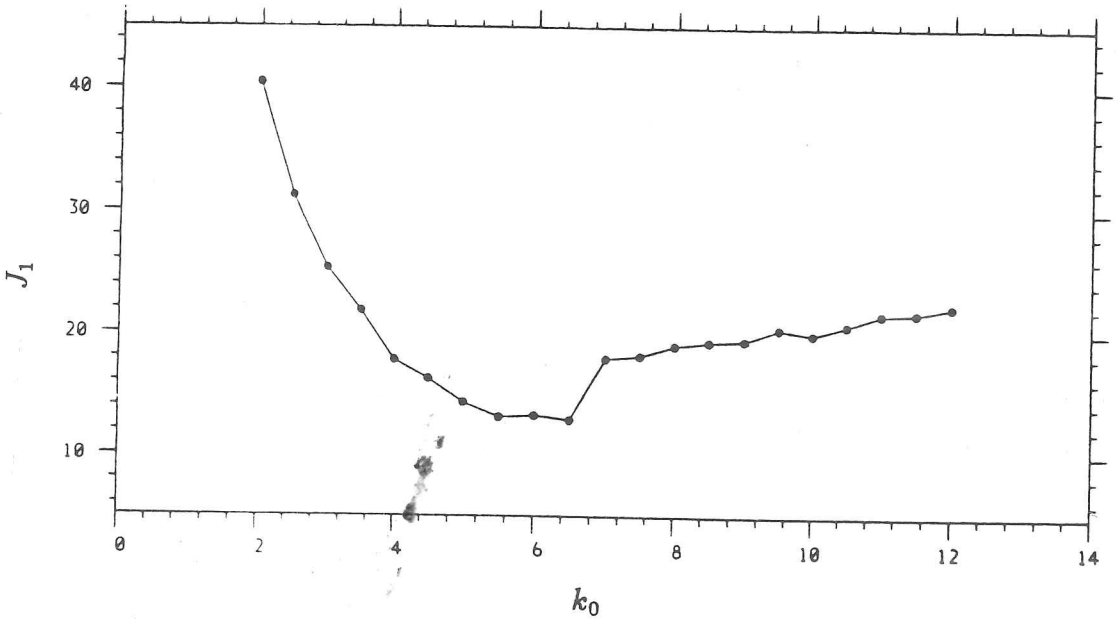

Fig. 4.7 Result of J_1 against the variation of k_0

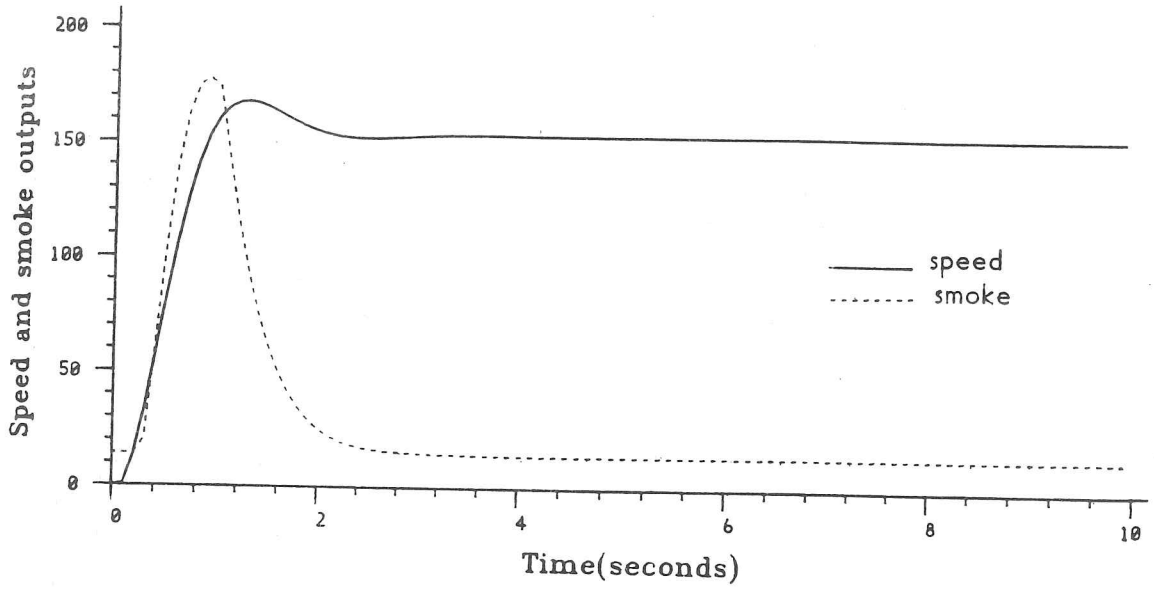

Fig. 4.8 Simulation results of engine speed and smoke outputs

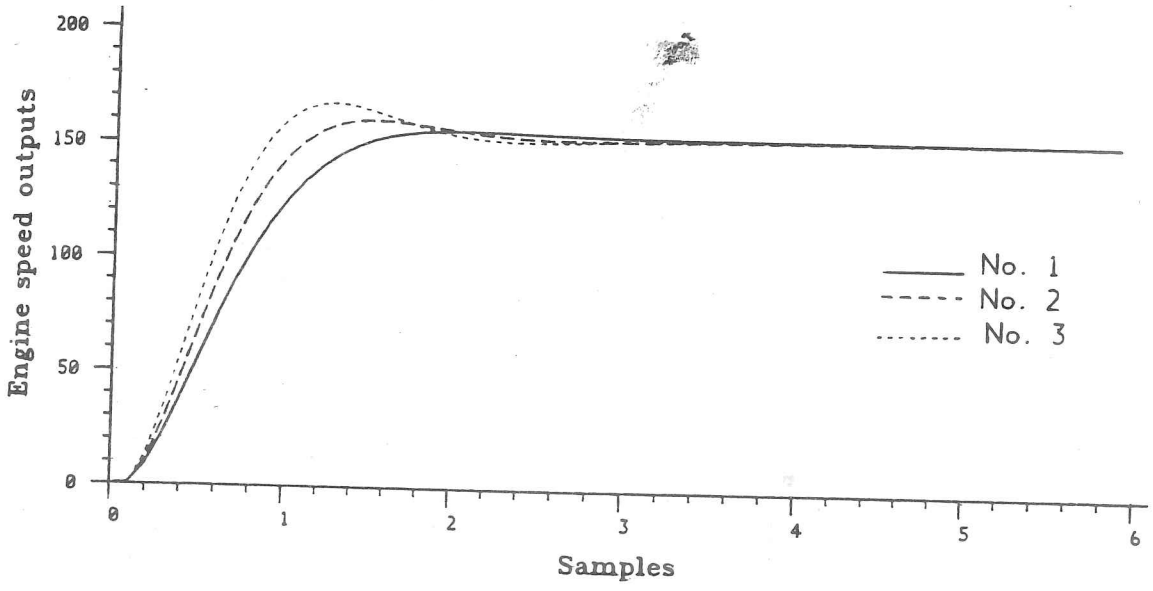

Fig. 4.9 Simulation results of engine speed outputs with different controllers

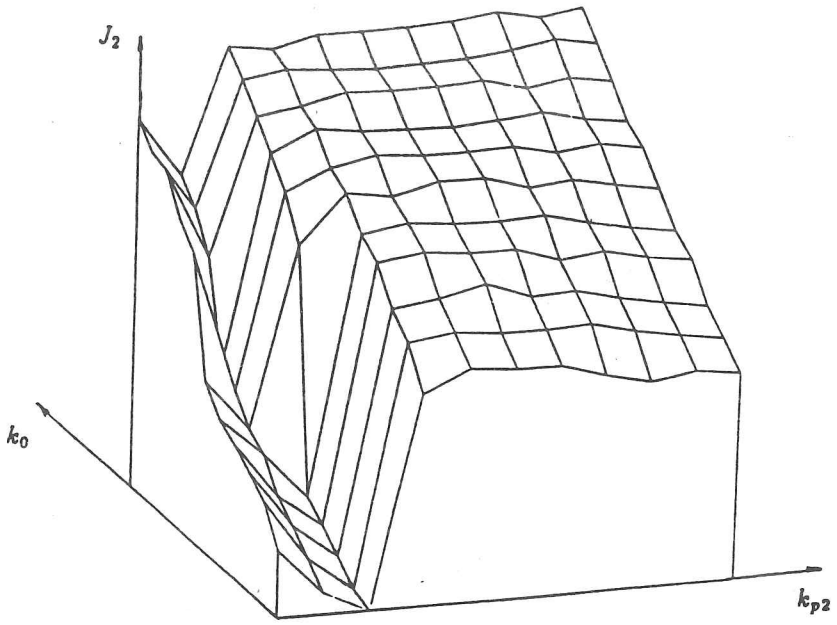

Fig. 4.10.a Result of J_2 against the variations of k_0 and k_{p2} (system 1)

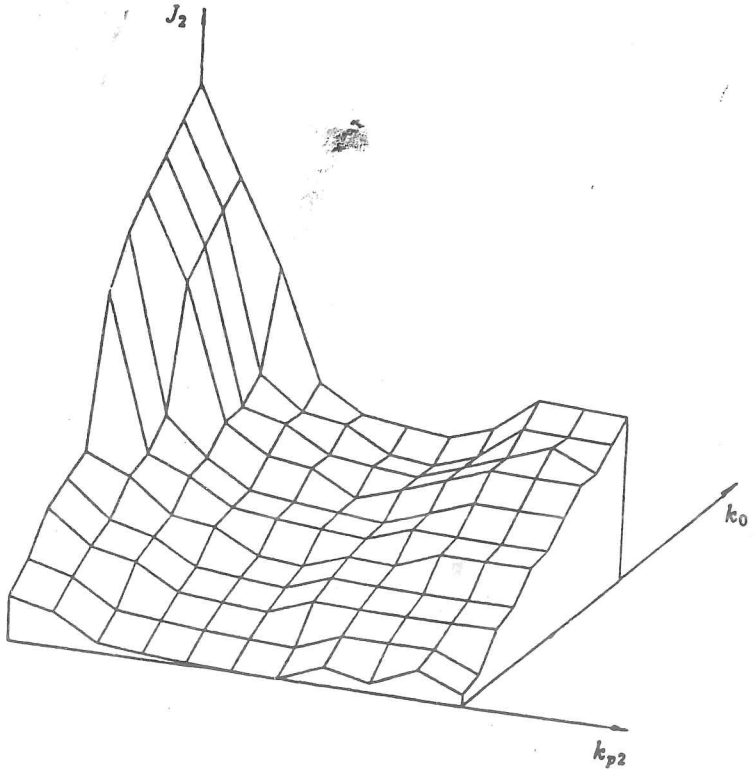

Fig. 4.10.b Result of J_2 against the variations of k_0 and k_{p2} (system 2)

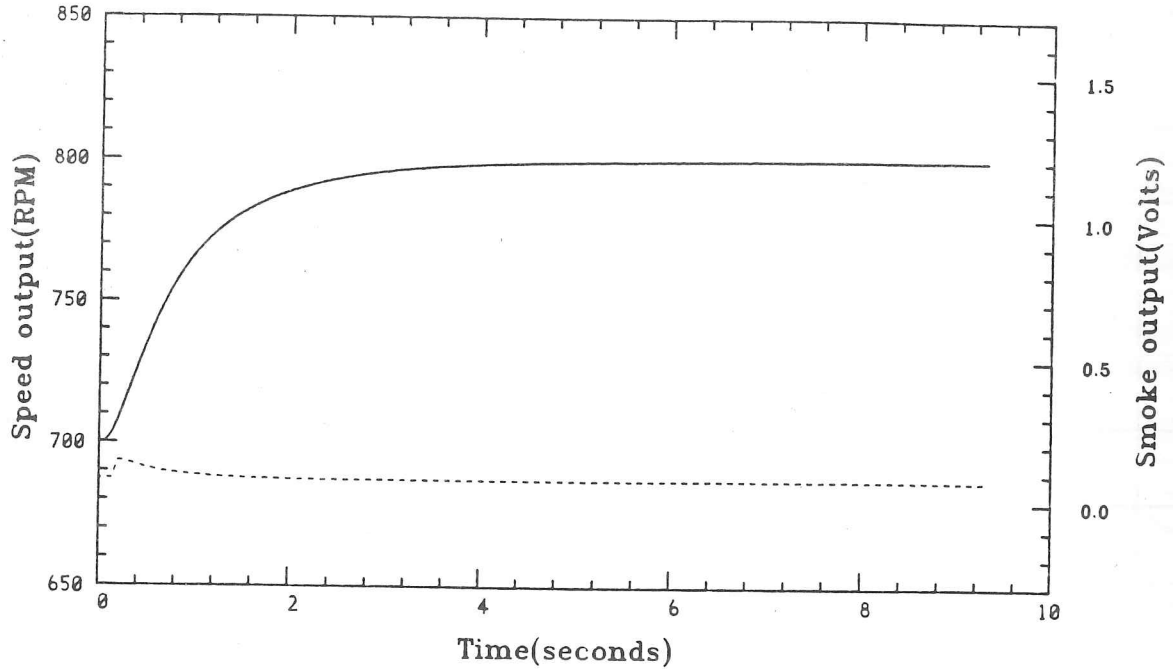

Fig. 4.11 Simulation of engine speed and smoke outputs in system 1

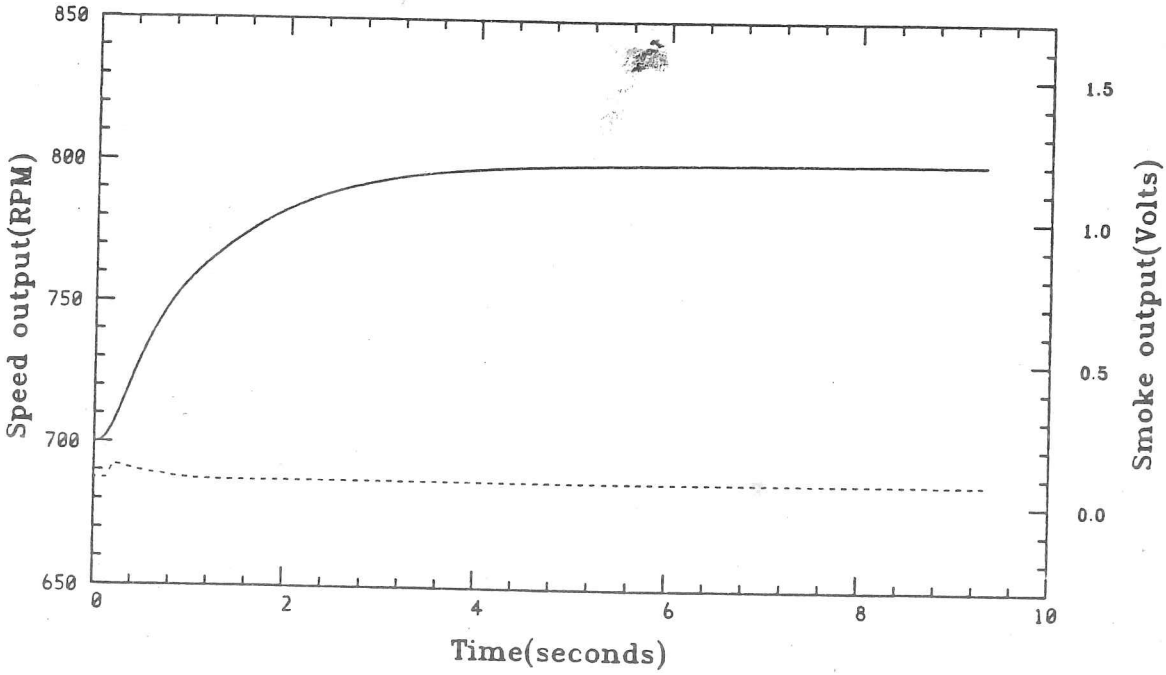

Fig. 4.12 Simulation of engine speed and smoke outputs in system 2

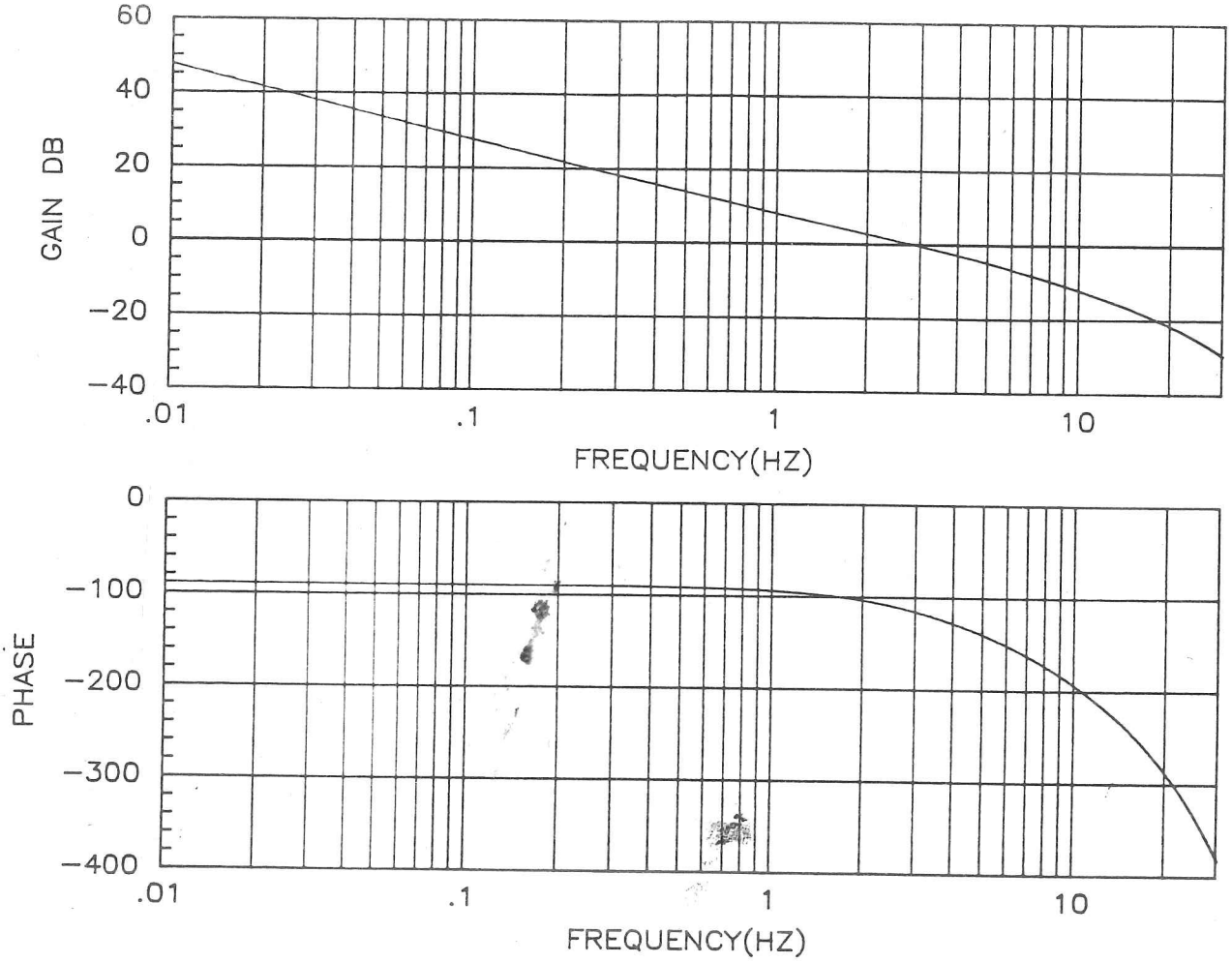

Fig. 4.13.a Bode diagram of system 1

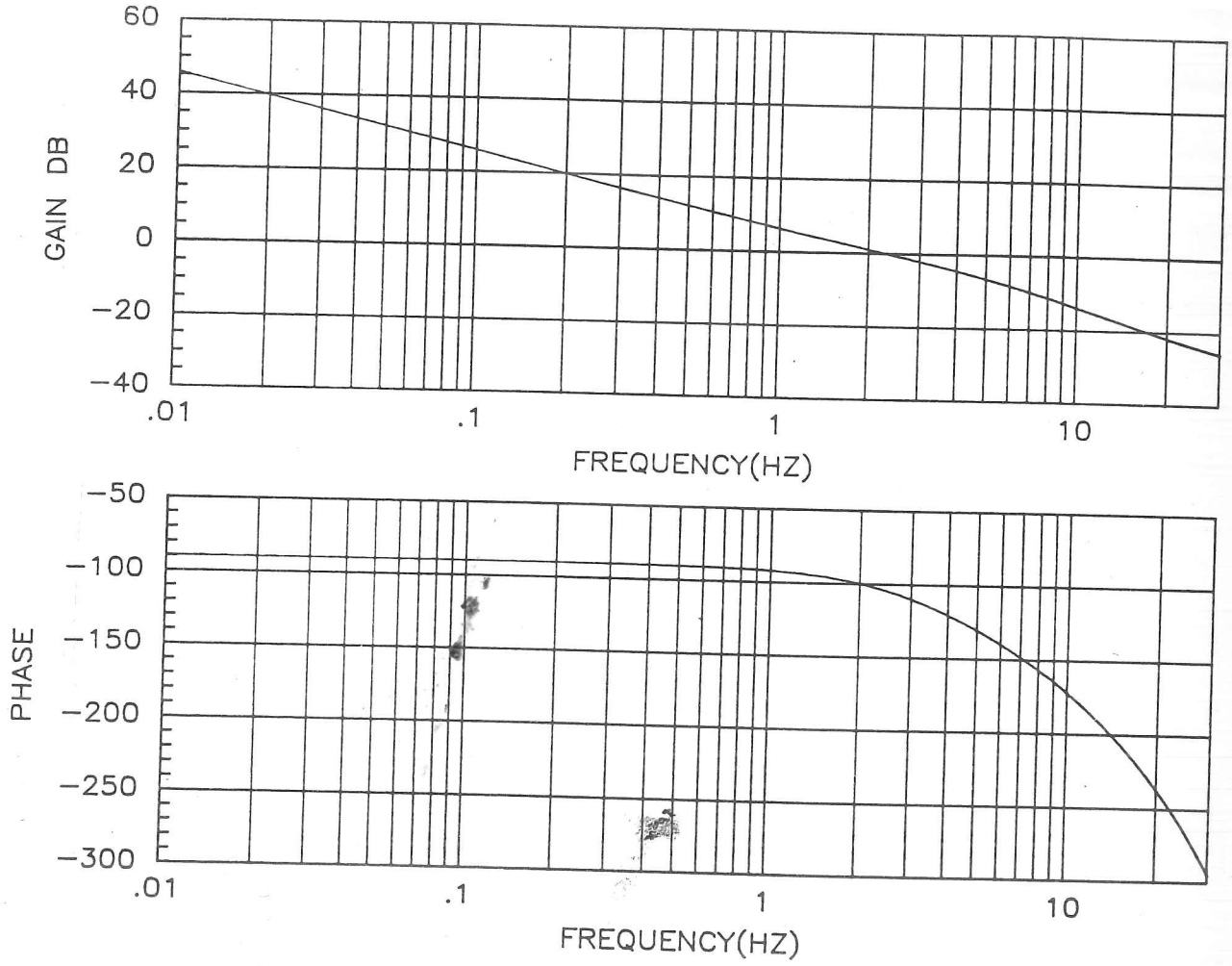

Fig. 4.13.b Bode diagram of system 2

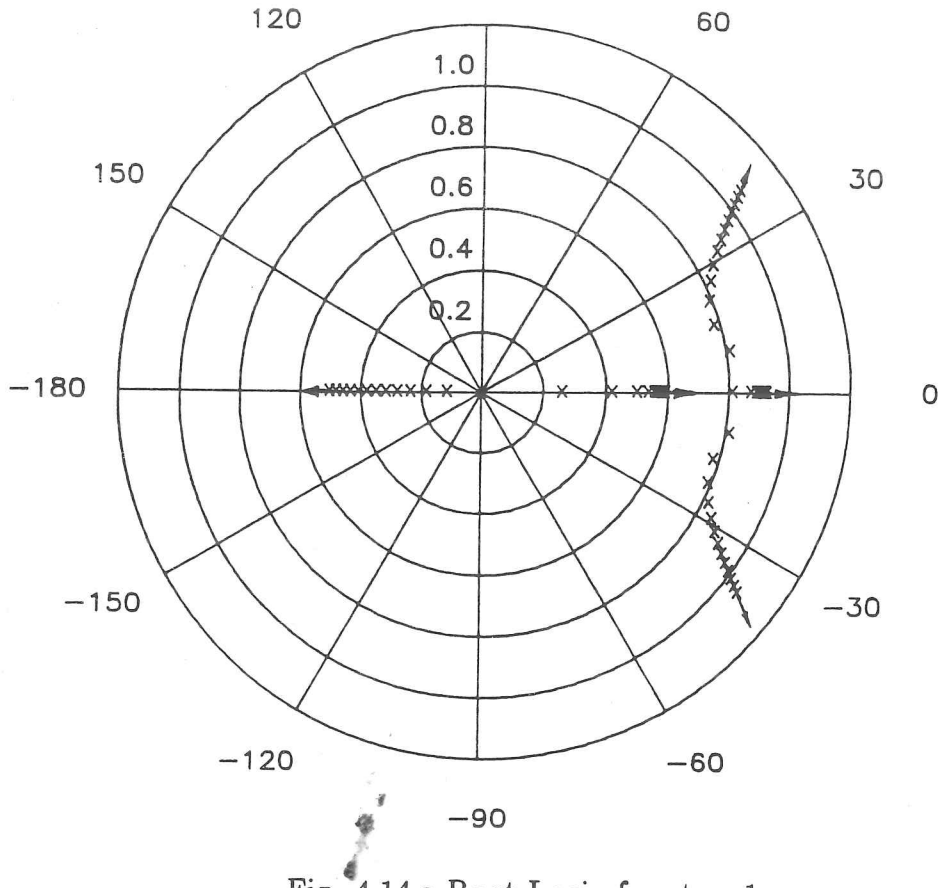

Fig. 4.14.a Root Loci of system 1

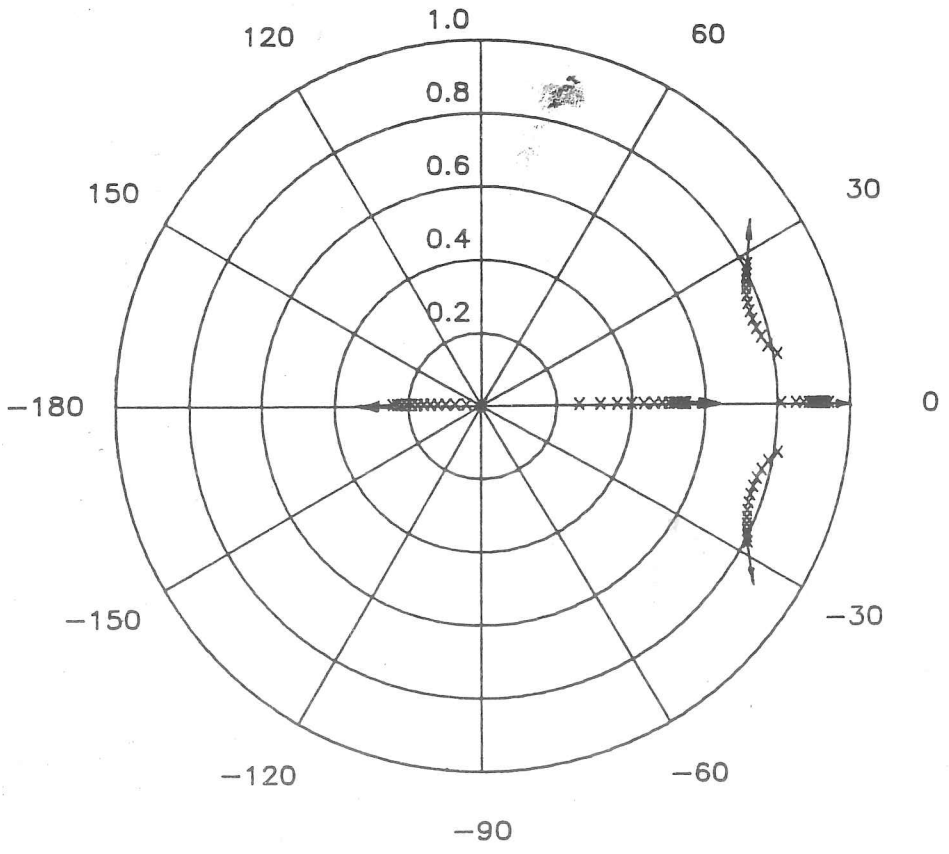

Fig. 4.14.b Root Loci of system 2

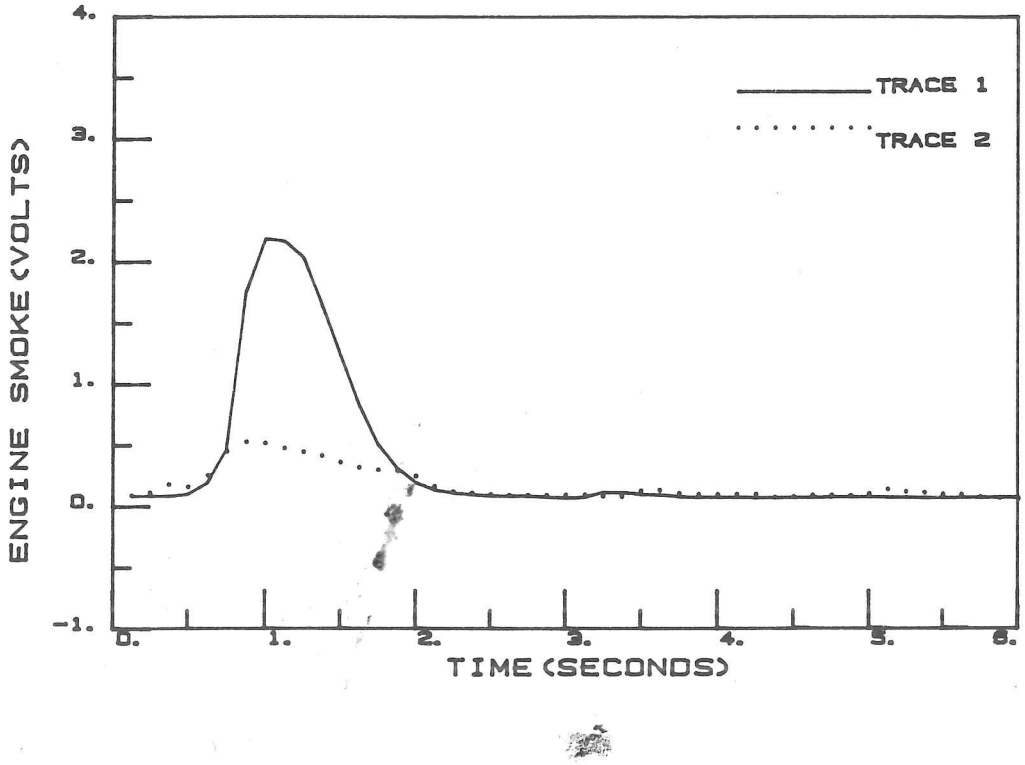

Fig. 4.15 Test results of engine smoke with and without smoke control

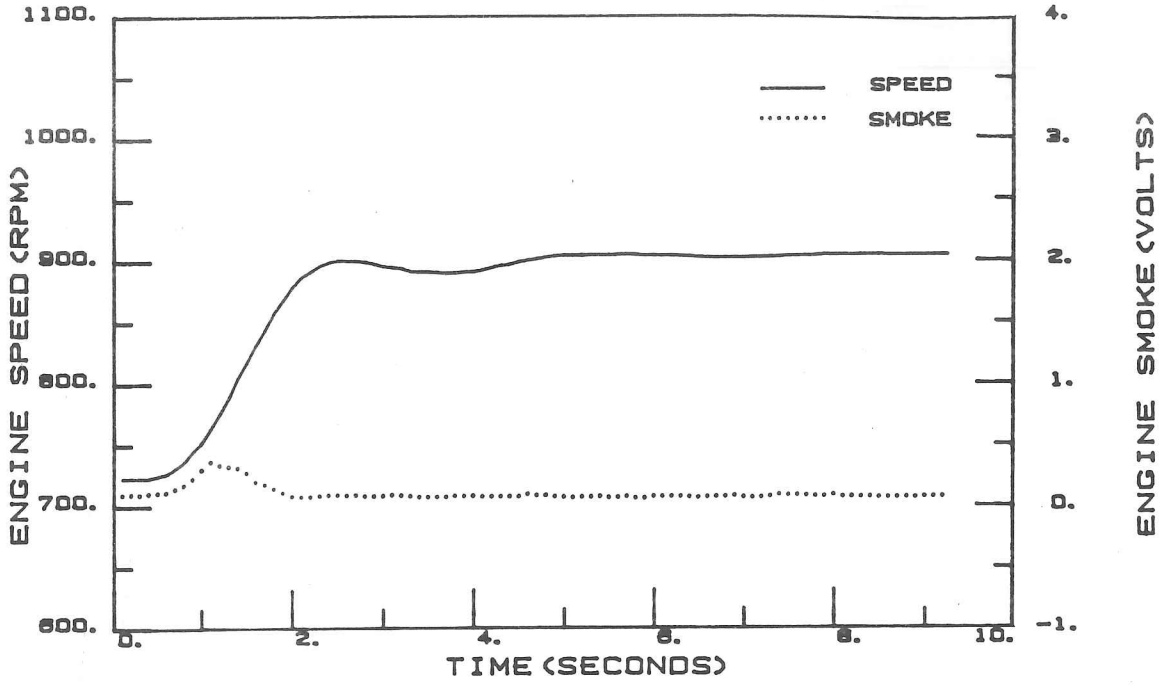

Fig. 4.16 Test results of control system

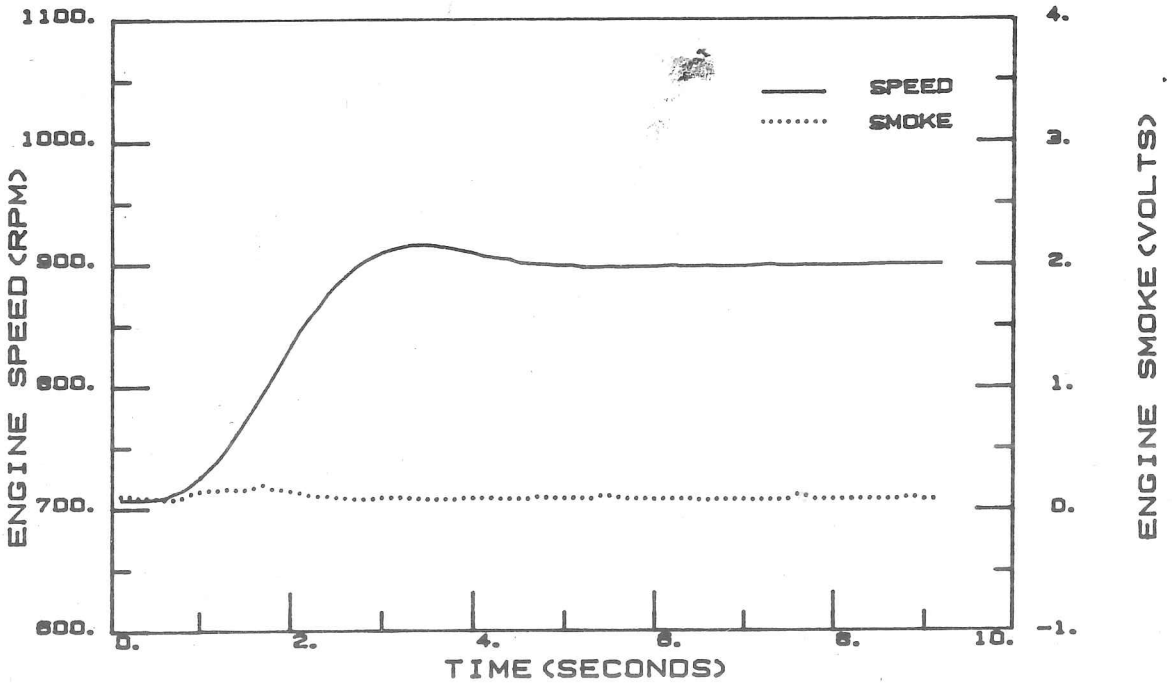

Fig. 4.17 Test results of control system

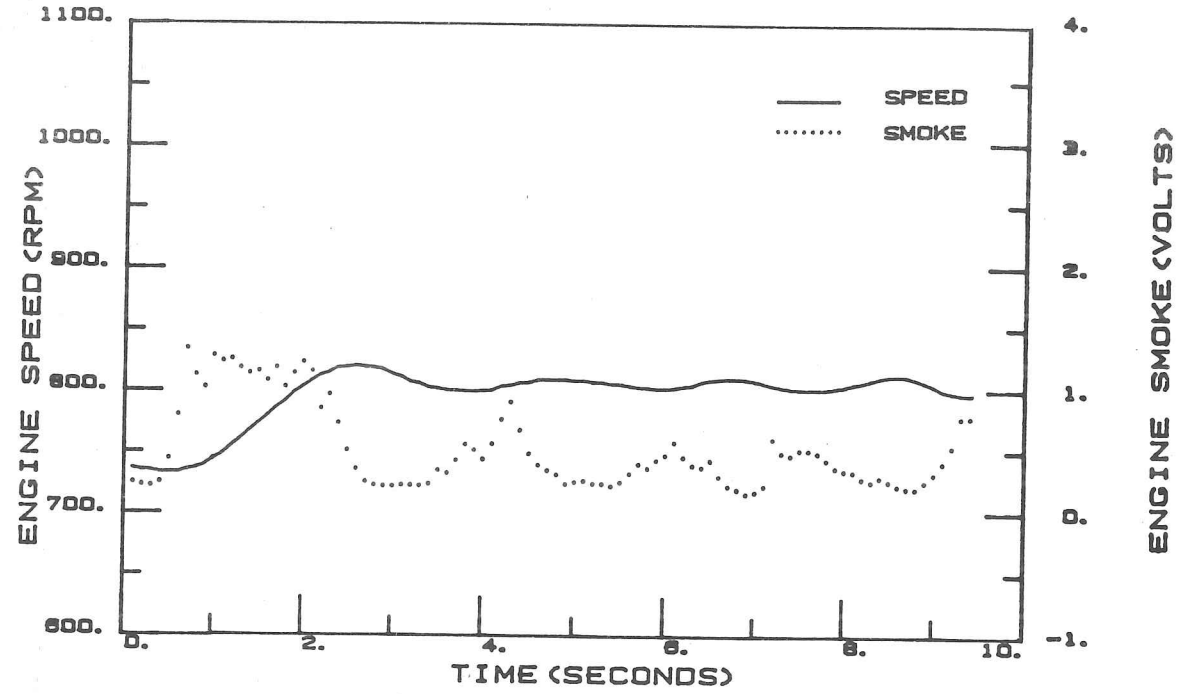

Fig. 4.18 Test results of control system

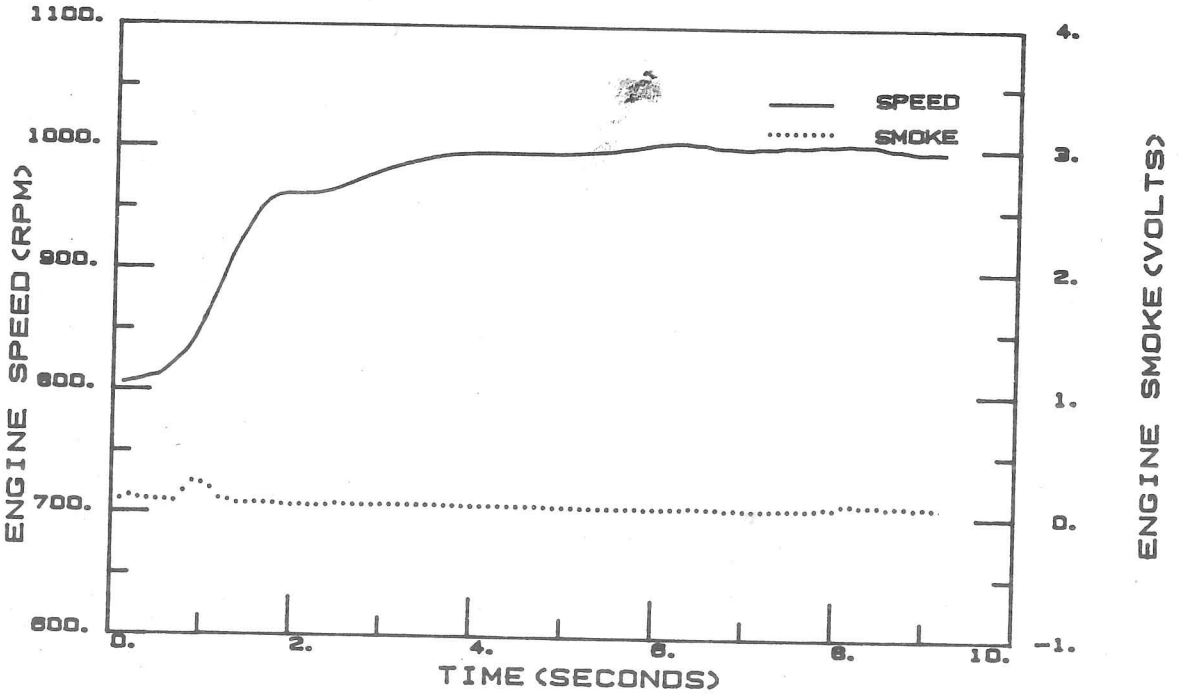

Fig. 4.19 Test results of control system

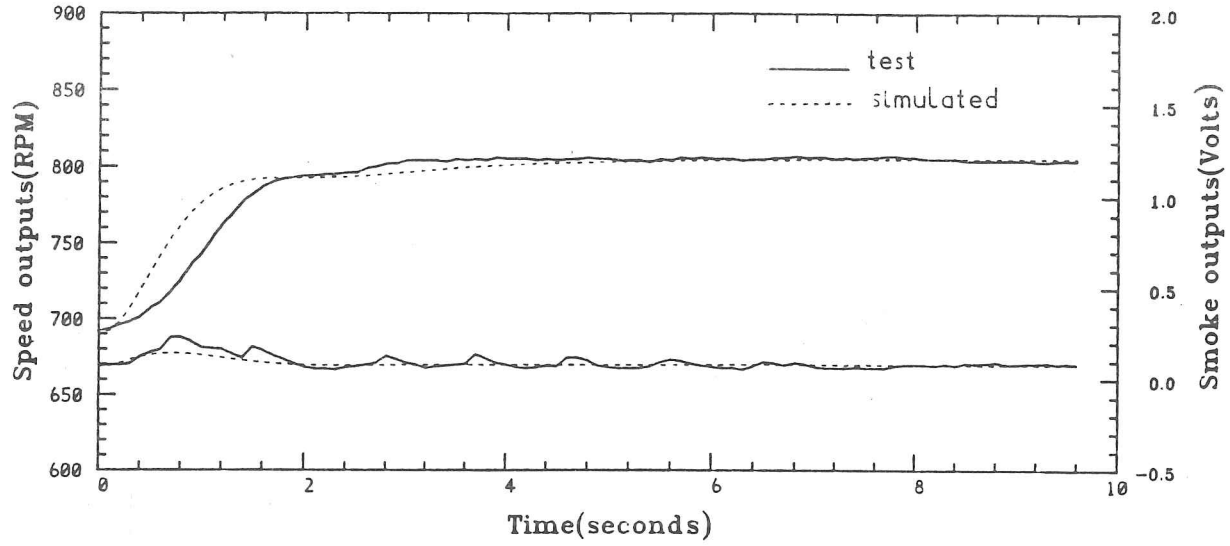

Fig. 4.20 Comparison of the test and simulated results of control system

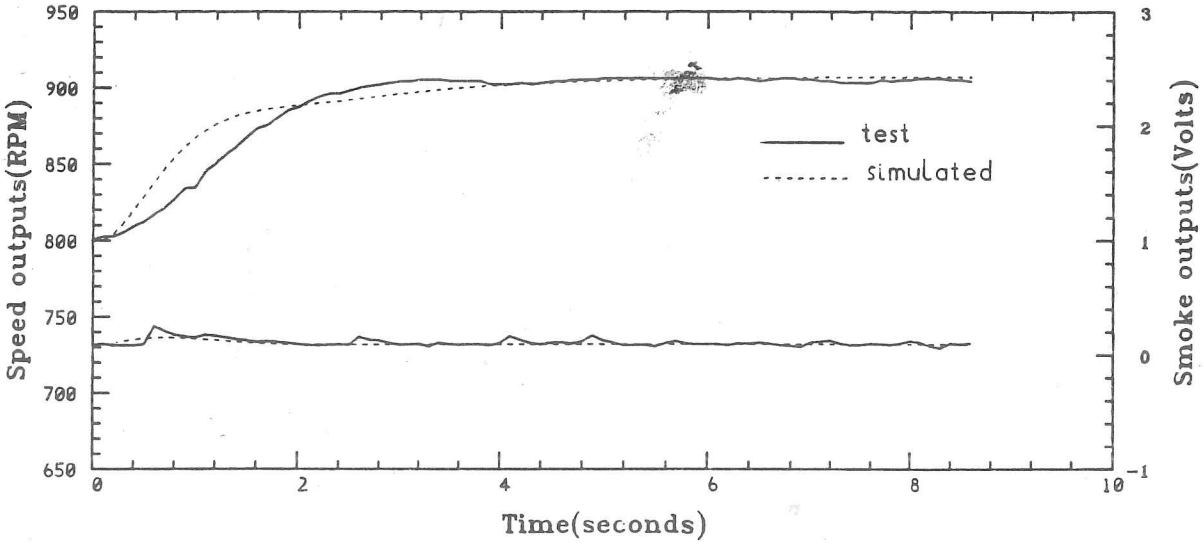

Fig. 4.21 Comparison of the test and simulated results of control system

Chapter Five

Application of self-tuning control

5.1 Introduction

Conventional control theory usually deals with dynamic systems whose mathematical representations are completely known. In contrast to this, adaptive control refers to the control of partially known systems. There has been an increasing interest in adaptive control which can be attributed to the fact that there is invariably some uncertainty in the dynamic characteristic of most practical systems. The tools of conventional control theory, even when used efficiently in the design of controllers for such systems, are inadequate for achieving satisfactory performance in the entire range over which the characteristics of the system may vary. Hence some type of monitoring of the system's behaviour, followed by the adjustment of the control actuation, is needed and this is referred to as adaptive control.

Adaptive control is a generalisation of classical feedback control in systems where the controller uses a linear control law. Some or all of the coefficients of the linear control law are automatically adjusted in response to on-line measurements of process or disturbance variables[H4].

There are three classes of adaptive control: self-tuning, model-reference and sub-optimal[H4]. Self-tuning control is, in a sense, the simplest adaptive control algorithm derivable from the point of view of discrete time stochastic control theory. In this approach, the identification is simplified by making the assumption that all the coefficients of C in equation(3.2) are zero except for c_0 which has the value of unity[H4].

$$C(q^{-1}) = 1$$

Additionally, the algorithms which self-tuning uses for control are made as simple and easily-implementable as possible.

Results of the modelling described in Chapter 3 and the non-adaptive control in Chapter 4 showed that the parameters in the engine's transfer functions changed with the speed-load conditions. The desired engine performance determined by a controller with fixed parameters can be realized for a particular engine condition but not over a wide range unless the parameters of the controller are varied with the variation of the engine model.

The nonlinearity of the transfer function of fuel rack-to-smoke, the nonlinear gain between the output and input and time delay, was shown in Chapter 3. For a process dominated by nonlinear characteristics, it is probably better to use a nonlinear model rather than an approximate linear model if this is realizable. This means that the parameters of $A(z^{-1})$, $B(z^{-1})$ in the model expressed by equation(3.2) of Chapter 3 vary with different amplitudes of the inputs. In a digital control system, this nonlinear model can be expressed in the form of a linear one in each time interval:

$$\begin{aligned}
\text{When } \; t = t_1, \quad & A_{t_1}(z^{-1})y(t_1) = B_{t_1}u(t_1) + C_{t_1}v(t_1) \\
t = t_2, \quad & A_{t_2}(z^{-1})y(t_2) = B_{t_2}u(t_2) + C_{t_2}v(t_2) \\
\vdots \qquad & \qquad \vdots \\
t = t_m, \quad & A_{t_m}(z^{-1})y(t_m) = B_{t_m}u(t_m) + C_{t_m}v(t_m)
\end{aligned}$$

The parameters, A_t and B_t, can be identified by an estimator which is normally a component of a self-tuning control system.

The problems mentioned above explore the necessity of utilizing self-tuning controllers in the engine control system. The aim of the work described in this Chapter is to investigate application of the self-tuning control to the engine system.

Fig. 5.1 represents a self-tuning scheme as applied to this engine control. As shown in the figure, the self-tuning control system consists of five parts: controlled plant — engine; on-line estimator; calculation of the coefficients in control algorithm; controller and smoke predictor. The basic philosophy of this approach was to estimate the engine speed and smoke models, calculate the coefficients of the controller with the estimated parameters, predict the smoke outputs and readjust the actuation signal to the fuel rack to protect against the high level smoke. The self-tuning control algorithms were used to control the engine speed. The output of the controller is readjusted by the output of the smoke predictor when the predicted smoke was higher than the required one.

This chapter is organized as follows: Section 5.2 states the on-line identification algorithm. Section 5.3 describes the smoke predictor and two control algorithms: one is pole assignment aimed to achieve the desired response of the control system, the other is PI self-tuning control aimed to extend the capability of a conventional PI controller. In Section 5.4 the self-tuning control execution when the control algorithms were implemented on a real engine are described. Finally, in Section 5.5 and 5.6 the self-tuning trials carried out on the engine are presented, the discussion of the test results will emphasise how they meet the objects of the control designs.

5.2 On-line parameter estimate

5.2.1 Selection of the identification algorithm

The Least Squares method is generally superior in terms of convergence rate compared with projection method, and it is known to provide extremely rapid initial convergence. However the estimator with this method switches off as the algorithm gain approaches zero and the advantage is lost[G2]. A related cause of difficulties arises when the least square method is used on a system which has an external disturbance — when a disturbance does occur the gain of the least-square estimator has become so high that the estimates vary rapidly, and the control exercised over the next few sample intervals is poor. This phenomenon is due to the use of a forgetting factor which is less than one.

A projection algorithm has the advantage of relative simplicity, and the algorithm gain does not go to zero, therefore it can automatically track varying parameters. This algorithm is also known as the normalized least-mean-squares (NLMS) [G2].

In contrast to the off-line case, the on-line case deals with sequential data, which requires that the parameter estimates be recursively updated within the time limit imposed by the sampling rate. Thus in many applications, it is necessary to use a relatively simple algorithm to meet the imposed time constraint.

With consideration of the simplicity of the estimate algorithm and the sensitivity of the estimator to the disturbance, NLMS algorithm was chosen for on-line parameter estimate in a self-tuning control system.

5.2.2 Normalized Least-mean-squares(NLMS) algorithm

The input-output characteristic of a linear dynamic system can be described by model which takes the form as that in Chapter 3:

$$y(t+1) = \phi(t)\theta + v(t+1) \tag{5.1}$$

where $y(t+1)$ denotes the system output at time $t+1$

$\phi(t)$ denotes a vector that is a function of $y(t), y(t-1), \ldots,$

$u(t-nd), u(t-nd-1), \ldots, v(t)$

θ denotes a parameter vector (unknown),

$\theta = [a_1, a_2, \ldots, a_{na}, b_0, b_1, \ldots, b_{nb-1}, 1]'$

v denotes the white noise sequence

na and nb define the degree of the model

nd defines the time delay

The estimate of $\theta(t)$ at each step is given by[G2]:

$$\hat{\theta}(t) = \hat{\theta}(t-1) + \frac{\alpha\phi(t-1)}{\beta + \phi'(t-1)\phi(t-1)}[y(t) - \hat{y}(t-1)] \tag{5.2}$$

where $\beta > 0; 0 < \alpha < 2$, β is a small constant applied to avoid division by zero.

This algorithm can be extended to the multi-variable case[G2]. In this case, the model representation becomes

$$\mathbf{Y}(t+1) = \Phi'(t) \cdot \Theta + \mathbf{V}(t+1)$$

where $\mathbf{Y}(t+1)$ is a $m \times m$ matrix of outputs

$\Phi(t)$ is a $n \times m$ matrix of past values of $\{y(t)\}$ and $\{u(t)\}$

Θ is a $n \times m$ matrix of parameters

$\mathbf{V}(t)$ is a $m \times m$ matrix of noise on outputs

The estimation of Θ becomes

$$\hat{\Theta}(t) = \hat{\Theta}(t-1) + \frac{\Phi(t-1)[\mathbf{Y}(t) - \Phi'(t-1) \cdot \Theta(t-1)] \cdot \bar{\alpha}}{\bar{\beta} + \Phi'(t-1) \cdot \Phi(t-1)}$$

with $\hat{\Theta}(0)$ given. Here $\bar{\alpha}$ and $\bar{\beta}$ are $m \times m$ diagonal matrices and $0 < \alpha_{ii} < 2$, $\beta_{ii} > 0$.

The estimation with the NLMS algorithm consists of the following steps:

1. $\mathbf{E}(t) = \mathbf{Y}(t) - \Phi'(t-1)\hat{\Theta}(t-1)$ — compute prediction errors
2. $\hat{\Theta}(t) = \hat{\Theta}(t-1) + \mathbf{W}(t-1) \cdot \mathbf{E}(t)$ — update parameters
3. $\hat{\mathbf{V}}(t) = \mathbf{Y}(t) - \Phi'(t-1)\hat{\Theta}(t)$ — compute residual errors
4. Form $\Phi(t)$ using $y(t), u(t)$ and $v(t)$
5. $\mathbf{W}(t) = \dfrac{\Phi(t) \cdot \bar{\alpha}}{\bar{\beta} + \Phi'(t) \cdot \Phi(t)}$ — update estimate gain

5.2.3 The structure of the models for engine control

In Chapter 3, the predicted output was a function of the system input, output and the estimated parameters

$$\hat{y}(t+1) = \{\hat{\theta}(t), \phi(t)\}$$

As shown in Fig. 3.10, the agreement between the actual and predicted outputs was acceptable when the speed model was in the simplest form — first order. For the sake of producing an estimation as simply and quickly as possible, the on-line estimate was

supplied by a first order speed-to-fuel rack model and a second order smoke-to-fuel rack model.

The determination of the time delay, $Nd1$ in speed model and $nd2$ in smoke model required the knowledge of off-line identification in Chapter 3: $nd1 = 1$, $nd2 = 2$. So the transfer function of speed-to-fuel rack used in on-line estimate was

$$y_1(t+1) = a_{1(1)}y_1(t) + b_{0(1)}u(t-nd1) + v_1(t+1)$$

And the transfer function of smoke-to-fuel rack was

$$y_2(t+1) = a_{1(2)}y_2(t) + a_{2(2)}y_2(t-1) + b_{0(2)}u(t-nd2) + v_2(t+1)$$

The matrices as used for on-line identification were formed as

$$\Upsilon(t) = \begin{pmatrix} y_1(t) & 0 \\ 0 & y_2(t) \end{pmatrix}$$

$$\Theta(t) = \begin{pmatrix} a_{1(1)} & 0 \\ b_{0(1)} & 0 \\ 0 & a_{1(2)} \\ 0 & a_{2(2)} \\ 0 & b_{0(2)} \end{pmatrix}$$

$$\Phi'(t) = \begin{pmatrix} y_1(t) & u(t-nd1) & 0 & 0 & 0 \\ 0 & 0 & y_2(t) & y_2(t-1) & u(t-nd2) \end{pmatrix}$$

5.2.4 Determination of the factor matrices $\bar{\alpha}$ and $\bar{\beta}$ in equation (5.1)

The elements of $\bar{\alpha}$ and $\bar{\beta}$ denote the algorithm gain of the regression matrix $\Phi(t)$. They are constant weightings attributed to the previous data at the current system parameter estimates. Normally the choice of the elements of $\bar{\alpha}$ and $\bar{\beta}$ are chosen in the range of: $0 < \alpha_{ii} < 2$, $\beta_{ii} > 0$. In order to find the proper $\bar{\alpha}$ and $\bar{\beta}$, estimation process was simulated on the computer. This off-line estimation used the test data taken from the real engine to be controlled, i.e., the data used for identification in Chapter 3. The value index was the mean square error between the real output $y(t)$ and the predicted output $\hat{y}(t)$.

In terms of the mean square errors between the simulated and test results, it was found that the minimum mean square errors could be obtained when

$$\bar{\alpha} = \begin{pmatrix} 1.12 & 0 \\ 0 & 0.91 \end{pmatrix}$$

Fig. 5.2.a shows the residual error at 90 samples of speed outputs and Fig. 5.2.b the sum of the squared errors between predicted and real speed outputs over 90 samples. The initial values of the estimated parameters are zeros. As shown in Fig. 5.2.a, after 40 samples the residual error damps down around zero and the sum of the prediction errors in Fig. 5.2.b increases more slowly.

Similarly, the errors of smoke outputs in the estimation process are shown in Fig. 5.3.a and 5.3.b. The residual error becomes much smaller around the 18th sample and damps down around zero after, but the errors of the smoke outputs oscillate around zero more than those of speed outputs. Also the sum of the predicted errors increases more obviously after 40 iterations when compared with that of speed predicted errors.

5.2.5 Comparison of predicted and real outputs with NLMS algorithm

Fig. 5.4.a shows the estimated parameters of speed-to-fuel rack model over 95 samples. The speed model is first order with initial value: $a_{1(1)} = 0.9$ and $b_{0(1)} = 0.2$. The comparison of predicted and real speed outputs in the estimate process is shown in Fig. 5.4.b. Both traces are very close especially after 40 iterations. The smoke model is second order and has initial values of the parameters: $a_{1(2)} = 1.6$, $a_{2(2)} = -0.4$ and $b_{0(2)} = 0.3$. Based on this initialization, the estimated parameters in the smoke model are shown in Fig. 5.5.a, and in Fig. 5.5.b is the comparison of the predicted and real smoke outputs in the corresponding estimate process. The tendencies of the two smoke traces are very similar even though the difference between them is more than that of the compared speed outputs.

5.3 Control algorithms

This section describes two control algorithms and the smoke predictor. The control algorithm of pole-assignment was used for achieving the desired response of engine speed, and PI self-tuning for extending the ability of conventional PI controller.

5.3.1 Pole assignment self-tuning control

As long as the parameter estimates of $\hat{A}(z^{-1}), \hat{B}(z^{-1})$ have been obtained, control with pole assignment algorithm is applied using

$$F(z^{-1})u(t) = -D(z^{-1})y(t) + H(z^{-1})r(t) \tag{5.3}$$

where $F(z^{-1}), D(z^{-1})$ and $H(z^{-1})$ are polynomials in z^{-1} and $r(t)$ is the required signal[H4].

A common requirement for the closed loop is that the steady-state error should be zero. There are several approaches to the problem of constant offsets. The simplest and commonly used way to date is to insert an integrator into the loop after the self-tuner which effectively computes increments in the control signal. Then, $F(z^{-1})$ becomes,

$$F(z^{-1}) = F'(z^{-1}) \cdot \frac{z-1}{z}$$

Hence, equation (5.3) becomes

$$u(t) = \frac{1}{F'(z^{-1})} \cdot \frac{z}{z-1} \cdot [-D(z^{-1})y(t) + H(z^{-1})r(t)]$$

$$u(t) = \frac{A(z^{-1})}{B(z^{-1})} y(t)$$

$$A(z^{-1})y(t) = z^{-nd}B(z^{-1}) \cdot \frac{1}{F'(z^{-1})} \cdot \frac{z}{z-1} \cdot [-D(z^{-1})y(t) + H(z^{-1})r(t)]$$

$$y(t) = \frac{z^{-nd+1}B(z^{-1})H(z^{-1})}{(z-1)A(z^{-1})F'(z^{-1}) + z^{-nd+1}B(z^{-1})D(z^{-1})} r(t)$$

To set the zero-offset at the steady-state,

$$\left(\frac{z^{-nd+1}B(z^{-1})H(z^{-1})}{(z-1)A(z^{-1})F'(z^{-1}) + z^{-nd+1}B(z^{-1})D(z^{-1})} \right)_{z=1} = 1$$

the $D(z^{-1})$ and $H(z^{-1})$ must be chosen as

$$H(z^{-1}) = D(z^{-1})$$

The characteristic equation of the closed-loop system can then be shown as

$$A(z^{-1})F(z^{-1}) + z^{-nd}B(z^{-1})H(z^{-1}) = 0$$

$F(z^{-1})$ and $H(z^{-1})$ can be obtained from the resolution to

$$A(z^{-1})F(z^{-1}) + z^{-nd}B(z^{-1})H(z^{-1}) = T(z^{-1}) \tag{5.4}$$

where the polynomial $T(z^{-1})$ specifies the desired closed-loop pole positions.

In the engine control system under study the actuation input is $u(t)$ and speed output is $y_1(t)$, then equation (5.3) becomes,

$$F(z^{-1})u(t) = H(z^{-1})[y_1(t) - r_1(t)]$$

where $\quad F(z^{-1}) = 1 + f_1 z^{-1} + \cdots + f_{nf} z^{nf}$

$$H(z^{-1}) = h_0 + h_1 z^{-1} + \cdots + h_{nh} z^{nh}$$

$F(z^{-1})$ and $H(z^{-1})$ can be determined from following equation

$$A(z^{-1})F(z^{-1}) + B(z^{-1})H(z^{-1}) = T(z^{-1}) \tag{5.5}$$

where

$$A(z^{-1}) = 1 + a_{1(1)} z^{-1}$$

$$z^{-nd} B(z^{-1}) = b_{0(1)} z^{-1}$$

n_f and n_h are selected as

$$n_f = n_{b(1)} - 1$$

$$n_h = n_{a(1)} - 1$$

As $n_a = 2$ and $n_b = 1$, constructing the polynomial $T(z^{-1})$ involves the positioning of two poles,

$$T(z^{-1}) = (1 - p_1 z^{-1})(1 - p_2 z^{-1})$$

p_i defines the designed pole position. Two poles in $T(z^{-1})$ were selected on line and the best values, in terms of the response of engine speed to speed requirement and effect of smoke control, were found to be $z_1 = 0.75$, $z_2 = 0.1$. The results with these poles assigned will be shown later in section 5.5.

5.3.2 Self-tuning PI controller

The non-adaptive proportional-integral(PI) controllers were designed on the basis of one engine operating point as described in Chapter 4. The results in Chapter 4 show that the non-adaptive PI controller was very effective when the engine load was not heavy and the range of the engine operations is not wide.

Some engines operate under a wide range of speed and load, the parameters of the engine models vary with the engine operation conditions. The PI controller in Chapter 4 was designed based on the transfer functions at engine condition of 800RPM and 30Nm. The results in Fig. 4.17 showed that the controller could not keep to perform well when the engine speed was as high as 1000RPM. To ensure a specified dynamic response independent of variation of the parameters, the PI self-tuning was called for.

The design of the self-tuning PI controller was aimed at keeping the controller's behaviours always as good as the best one of the non-adaptive controller. The algorithm of the self-tuning PI controller will be described as following.

In the speed feedback loop of the engine control system, the transfer function of fuel rack-to-speed was:

$$G_1(z^{-1}) = \frac{b_{0(1)}}{z - p_{1(1)}}$$

and the transfer function of PI controller was

$$C_1(z^{-1}) = \frac{(k_{p1} + k_{i1})z - k_{p1}}{z - 1}$$

The transfer function of the closed loop was

$$\frac{Y_1(z^{-1})}{R_1(z^{-1})} = \frac{C_1(z^{-1})G_1(z^{-1})}{1 + C_1(z^{-1})G_1(z^{-1})}$$

$$\text{or} \quad \frac{Y_1(z^{-1})}{R_1(z^{-1})} = \frac{b_{0(1)}[(k_{p1} + k_{i1})z - k_{p1}]}{z^2 - [1 + p_{1(1)} - b_{0(1)}(k_{p1} + k_{i1})]z + p_{1(1)} - b_{0(1)}k_{p1}} \tag{5.6}$$

Let the desired $Y_1(z^{-1})$ be $Y_{1d}(z^{-1})$

$$\frac{Y_{1d}(z^{-1})}{R_1(z^{-1})} = \frac{p_1 z + p_2}{z^2 + q_1 z + q_2} \tag{5.7}$$

With a comparison of the equation (5.6) and (5.7), two gains in PI controller were determined from the coefficients q_1 and q_2 in the reference model, then

$$\left.\begin{aligned} q_1 &= -\left[1 + p_{1(1)} - b_{0(1)}(k_{p1} + ki1)\right] \\ q_2 &= p_{1(1)} - b_{0(1)} k_{p1} \end{aligned}\right\} \tag{5.8}$$

Referring to the controller designed in Chapter 4, in which the optimal value of k_{p1} and k_{i1} were $k_{p1} = 3.75$ and $k_{i1} = 0.25$. $p_{1(1)}$ and $b_{0(1)}$ were obtained from the off-line estimate using the test data acquired at the corresponding engine condition of 800RPM and 30Nm torque. Then q_1 and q_2 were predetermined from equation (5.8).

With the predetermined q_1 and q_2, k_{p1} and k_{i1} were calculated in each sample interval by

$$k_{p1} = \frac{\hat{p}_{1(1)} - q_2}{\hat{b}_{0(1)}}$$

$$k_{i1} = -k_{p1} + \frac{1 + q_1 + \hat{p}_{1(1)}}{\hat{b}_{0(1)}}$$

5.3.3 Predictor for smoke output in the forward loop

The model of smoke-to-fuel rack in a discrete form includes a pure time delay which is represented as two sample intervals, $nd = 2$. During the initial period of engine acceleration, the control actuation can not influence the smoke output until two sample intervals later. Thus the high smoke will be unprotected if the controller cannot resolve the problem caused by pure time delay. On another hand, time delay affects the system stability and sensitivity, which must be considered in controller design.

Marshall[M3] described different methods to design the time-delay systems. One approach to designing feedback controllers for this kind of system is to insert a predictor

into the feedback loop. The signal, $\hat{y}(t)$, being a predicted version of the output signal is used as a feedback signal removing the effect of time delay to generation of the actuation signal, $u(t)$.

The use of the predictors in discrete-time minimum variance control was considered by Astrom in his book[A8]; in particular he pioneered the polynomial approach to designing predictors. The presentation in this book is a continuous-time analogue of this method.

In this engine control system with self-tuning algorithm, the predictor was used to predict the smoke level with the results of the on-line estimation. The purpose of the smoke prediction was to deduce the system output two sample intervals into the future and identify the nonlinear gain of the smoke model in each sample interval as mentioned in section 1.

The model of smoke-to-fuel rack in a discrete form is as shown below,

at time t,

$$y_2(t) = a_{1(2)}y(t-1) + a_{2(2)}y(t-2) + b_{0(2)}u(t-nd2)$$

here $nd2 = 2$,

$$\hat{y}_2(t+2) = \hat{a}_{1(2)}\hat{y}(t+1) + \hat{a}_{2(2)}y(t) + \hat{b}_{0(2)}u(t)$$

$$\hat{y}_2(t+1) = \hat{a}_{1(2)}y(t) + \hat{a}_{2(2)}y(t-1) + \hat{b}_{0(2)}u(t-1)$$

Thus, the predicted smoke output two steps ahead is

$$\hat{y}_2(t+2) = (\hat{a}^2_{1(2)} + \hat{a}_{2(2)})y_2(t) + \hat{a}_{1(2)}\hat{a}_{2(2)}y(t-1) + b_{0(2)}[u(t) + \hat{a}_{1(2)}u(t-1)]$$

The smoke predictor was incorporated into the forward loop. The predicted smoke output $\hat{y}_2(t+2)$ was fed back to the controller to adjust the generated actuation signal $u(t)$ for smoke protection. The error between the required smoke and predicted smoke

was amplified by a proportional gain, and then the actuation input was adjusted by this processed error.

5.4 Control test procedure

In this section, the structure of the self-tuning control program will be introduced. The test procedure involving the initialisation, engine test conditions and the control executing will be described.

5.4.1 Data logging, on-line observation and adaptation

The self-tuning control program used in the diesel engine control experiments reads from an analogue to digital converter, generates the set points(demands), calculates and applies actuation signal through a digital to analog converter. With a self-tuning algorithm, the control program is required to estimate the parameters of the models necessary for the engine control system and calculate the coefficients of the control law with the results of the estimates.

Points in the data streams can be recorded, checked or adapted on-line. The data logging contains the following variables:

number of sample points

sample time (relative to the initial sample time)

measured engine speed ($y_1(t)$, RPM)

measured engine smoke ($y_2(t)$, Volts)

command signal to fuel rack ($u(t)$, Volts)

The following variables can be observed by giving the command on the keyboard:

estimated parameters in the transfer functions

coefficients of the controllers

engine speed requirement

engine smoke requirement

measured engine speed (displayed with new value at each step)

measured engine smoke (displayed with new value at each step)

Adaptation can be done on-line to the following variables:

engine speed requirement

engine smoke requirement

coefficients of the controllers

5.4.2 Physical constraints

During the control process, the physical limitation of the system must be taken into account. Control saturation is one of the most usual factors. The limits of the control signal in the control program must fall within the system limits and must be reflected back to the estimator. As described in section 5.3 and 5.4, an integrator is essential for avoiding a big offset of the steady-state speed output. The control signal outputting from the D/A converter to fuel rack is sequenced as following:

1) calculate differential command signal $\delta u(t)$

2) integrate $u(t) = u(t-1) + \delta u(t)$

3) limit $u(t)$ and apply it

4) Store $u(t)$ for the next estimation and control step

Also, an engine speed-demand limit is imposed such that the measurement of the engine speed is within the scale of A/D converter (-10Volts to +10Volts).

5.4.3 Initialization

1. Model initialization

The control algorithms described in the previous sections were straight forward applications of the self-tuning regulators, where the parameters were estimated. In order to improve the estimation, reasonable initialization of the parameters in the models were supplied to the self-tuning controller. An approximate models, determined from the off-line estimation, was inserted into the scheme. Approximate parameters of the models fed forward the initial values of the parameters in the estimator.

2. Initial operation condition

When the self-tuning controller starts to work on an engine system, large oscillations of engine speed or other engine outputs may appear due to the large tuning in transients. To avoid this happening, the problem was tracked by running the engine with the non-adaptive PI controller until the parameter estimate had settled. Then the finished condition of the non-adaptive controller was used as the starting condition of the self-tuning controller.

5.4.4 Description of the test Conditions

The purpose of implementing the self-tuning controllers directly on the real engine was to investigate the transient response of these controllers and the possibility of applying self-tuning control to I.C. Engines.

The diesel engine self-tuning experiments were designed with this objective. Aiming to the different problems addressed by different self-tuning algorithms, test con-

ditions were chosen as those in which the control performances were problematically mentioned in section 5.1.

The self-tuning controller with the pole-assignment algorithm was mainly tested with heavy load engine conditions. The requirements of engine speed were similar to those in Chapter 4. i.e. speed range was from 700 to 900RPM, the speed step was 100RPM or 200RPM. The smoke requirements were the levels at corresponding steady-state engine conditions.

The PI self-tuning controller was tested at the same engine conditions at which the non-adaptive PI controller exhibited some disadvantages. With the combined use of a smoke predictor and an estimator, this self-tuning algorithm was only tested at a few engine conditions with light loads.

5.4.5 Combination of identification and control

Based on the previous description of the component parts, the control execution which was a combination of the system identification and self-tuning control algorithms can be described as follows,

1. the input $u(t)$, speed output $y_1(t)$ and smoke output $y_2(t)$ were sampled at each time interval;

2. data from the previous samples were used to estimate the parameters of the models with Normalized Least-Mean-Squares algorithm;

3. the improved estimates of the system models were then used to calculate the coefficients of the controllers, predict the engine smoke and then adjust the output of the controllers.

4. the actuation signal determined by the control law was sent out.

This combined self-tuning algorithm continued executing the sequence of steps $1 \sim 4$ at each sample interval, and the system was under the correct control corresponding to the specified algorithms.

5.5 Experimental results of the pole-assignment control

To study the performance of the pole-assignment self-tuner, alternative pole positions in the characteristic equation $T(z^{-1}) = 0$ were tested. The polynomial $T(z^{-1})$ involved the positioning of two poles. These were selected on-line, and the best values in terms of rise time, percentage overshoot, settling time and smoke errors were found to be $z = 0.1$ and $z = 0.75$.

Assigning fast pole can achieve fast response of engine speed to fuel rack, but may not match the smoke control. Fig. 5.6 shows the control results with

$$T(z^{-1}) = (1 - 0.1z^{-1})(1 - 0.55z^{-1})$$

The engine speed was increased from 800 to 900 RPM and the initial torque for an engine speed 800RPM was 60Nm. The (a) in Fig. 5.6 shows the speed and the smoke results when the control of the smoke was switched off. The speed response is fast (rise time 0.8s and settling time 1.9s), but the smoke 'puff' appears. When the smoke control was undertaken, as shown in the (b) of Fig. 5.6, the fast response of engine speed does not match the smoke control, and then produces the oscillation of the speed trace. Fig. 5.7.a, in contrast, shows that the slow movement of the fuel rack, generated by two slow poles, 0.85 and 0.75 in $T(z^{-1})$, causes no high smoke level but a noticeable lag in the speed response.

The results in Fig. 5.7.b were obtained with a characteristic equation

$$T(z^{-1}) = (1 - 0.1z^{-1})(1 - 0.75z^{-1})$$

This shows that the smoke is detected with the predictor and controller. The speed is increasing smoothly with rise time 1.5s and settling time 2.3s. This is the best result among those with different characteristic equations desired.

The pole-assignment controller was also tested at light-load engine conditions. Fig. 5.8 shows the results when the engine speed was required to increase from 700 to 900RPM and from 800 to 1000RPM. The initial torque was 24Nm. The good speed responses and smoke detection were similar to those results of the non-adaptive controller described in Chapter 4. However, poor behaviour of this controller happened occasionally. The results of two equivalent engine operating conditions in Fig. 5.9 show that the speed trace in (b) cannot settle down. This visible oscillations was resulted from the de-tuning between the real engine system and the estimated model.

Fig. 5.10 shows a satisfactory action of the parameter estimator with NLMS algorithm in a control process. The results displayed in this figure were obtained when the engine speed was controlled by the pole-assignment self-tuning controller to increase from 800 to 1000RPM. The initial torque of this test was 36Nm. As show in the figure, the estimator traces the variation of the parameters in the models very quickly (within 6 samples) and smoothly.

5.6 Experimental results of the PI self-tuning control

As mentioned above, the PI controller was applied in order to resolve the control problems caused by parameter variation in the models. This controller was tested at light-load conditions with engine speed in the range of 700 to 1000RPM.

Fig. 5.11 shows the control results with PI self-tuning controller. The three speed points of requirements were 800, 900, and 100RPM respectively. The initial engine speed was about 650RPM and the initial torque was 36Nm. The parameters in the

speed and smoke models were estimated in each time interval. The estimated model of smoke-to-fuel rack was used to predict smoke level two steps in advance, and the coefficients in controllers were calculated from the estimated parameters of speed-to-fuel rack transfer function. The adjusted controller maintained the desired control performance in spite of the variation on engine conditions. Compared with the results of non-adaptive PI controller in Fig. 5.12, the oscillation of the speed trace is removed when the engine speed is required to increase from 900 to 1000RPM.

Fig. 5.13 shows the control results with the same controller for the same engine conditions as in Fig. 5.12. The control performance is satisfactory when the engine speed is increased from 700 to 800RPM or 900 to 1000RPM, but not when speed from 800 to 900RPM. The oscillation of the speed trace was still due to the de-tuning between actual engine model and the model estimated. As also shown in the figure, the smoke level is not detected very well in the first a few seconds of this test cycle since the estimated model is less accurate and smoke prediction is deviate much from the real smoke level.

5.7 Conclusions

The pole assignment self-tuning controller was designed to achieve the desired engine speed response, while the smoke predictor was designed to solved to problems caused by the time delay between the input and smoke output. As shown in the test results, the engine control system with a pole assignment self-tuner and a smoke predictor reached the objectives of the control design and was able to control both speed and smoke when engine torque was high(50–60Nm). This cannot be realized with only the non-adaptive controllers.

The PI self-tuning controller was mainly used to solve the problem caused by the

variation of the coefficients in the transfer functions with the engine conditions. In Chapter 4, the PI controller with fixed gains showed good control behaviour when the engine was accelerated from 700 to 900RPM, but it could not kept working well when the engine speed was higher due to the variation of the parameters in the speed model. In contrast of this, the test results of the PI self-tuning controller demonstrated the control system with this controller could span a wider range of engine speed, thus expended the ability of the PI controller with fixed gains.

The primary aim of this control system was to control the engine speed and smoke during transients. Both the non-adaptive controller and self-tuning controller behaved well during transients with light loads and in the speed range of 700–900RPM. However, when it settled down to the steady-state conditions, the engine's performance with self-tuning controller was worse than that with a non-adaptive controller. The speed traces with the self-tuning controller looked more oscillatory since the coefficients in the controller were calculated from the estimated models which were sometimes de-tuned from the real engine models.

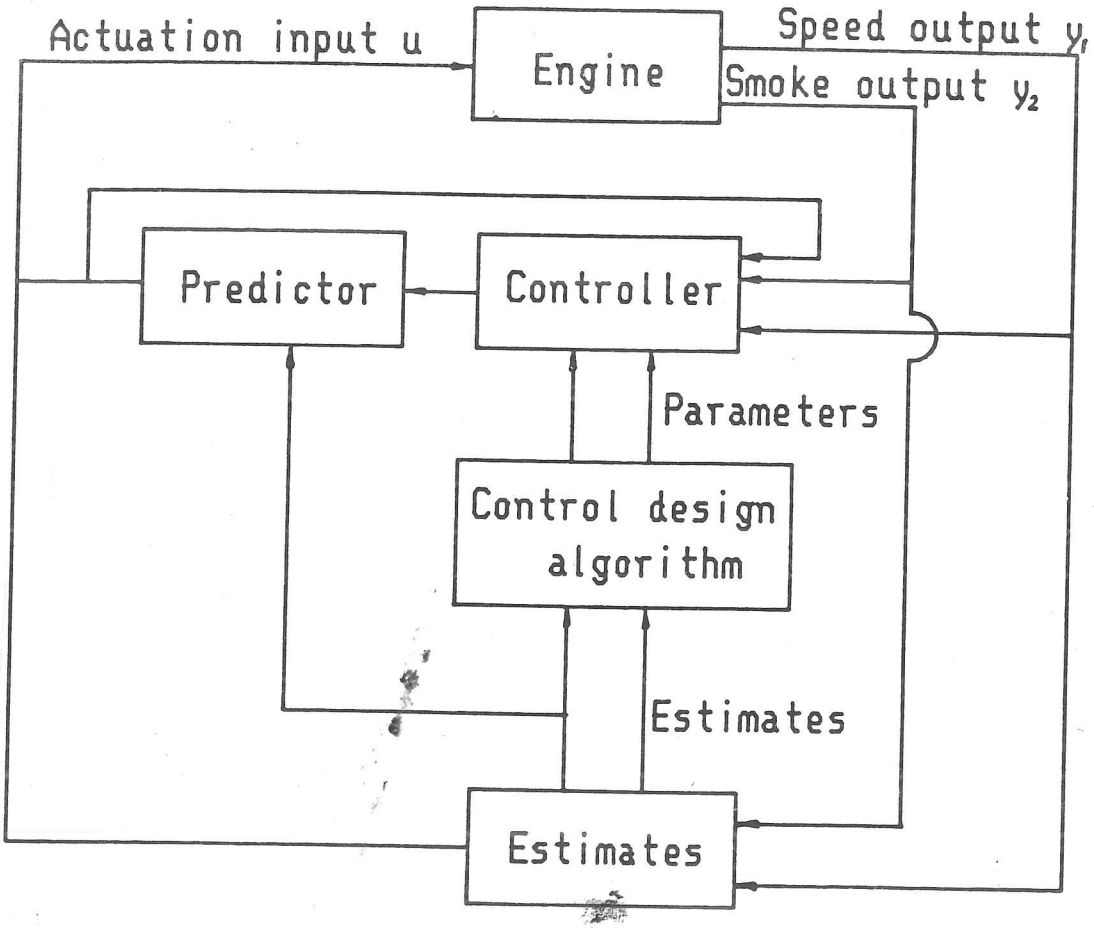

Fig. 5.1 The scheme of the self-tuning engine control system

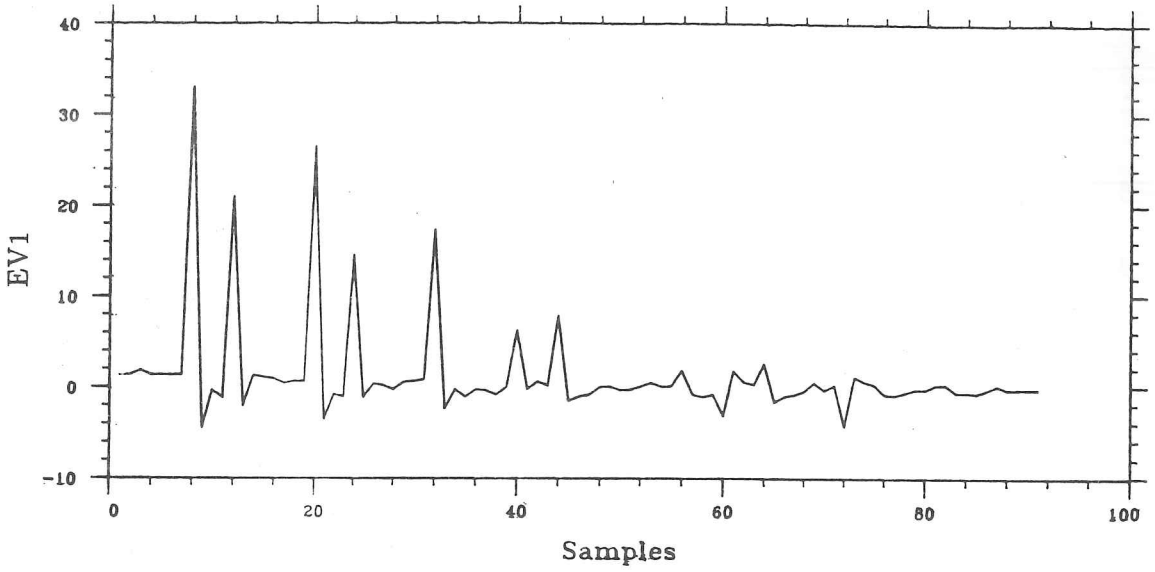

Fig. 5.2.a The residual errors of the speed outputs in the estimate process

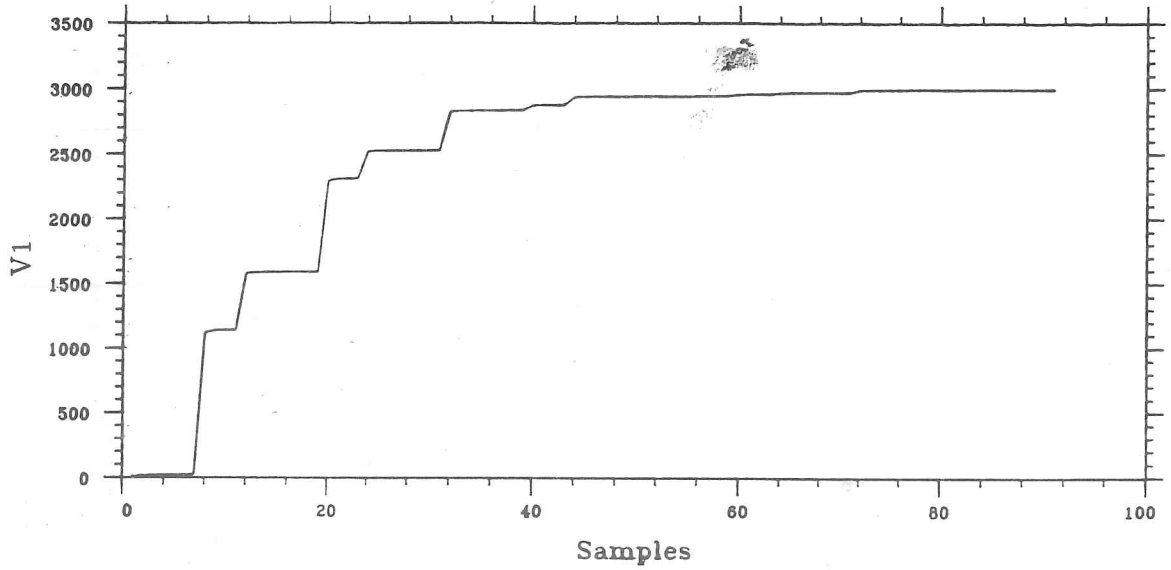

Fig. 5.2.b The sum of the squared errors between the predicted and real speed outputs in the estimate process

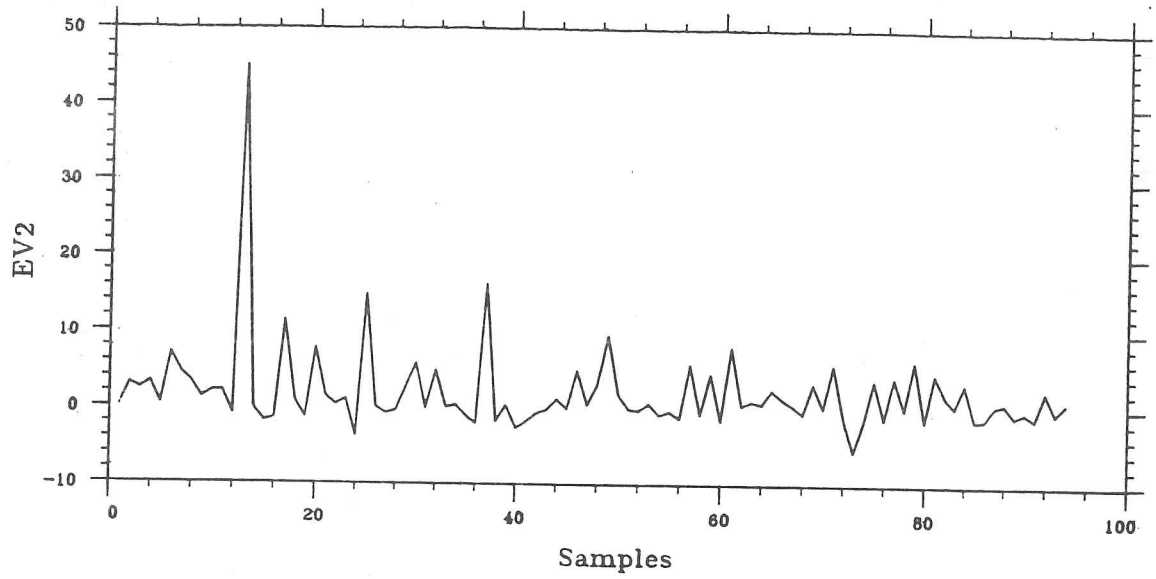

Fig. 5.3.a The residual errors of the smoke outputs in the estimate process

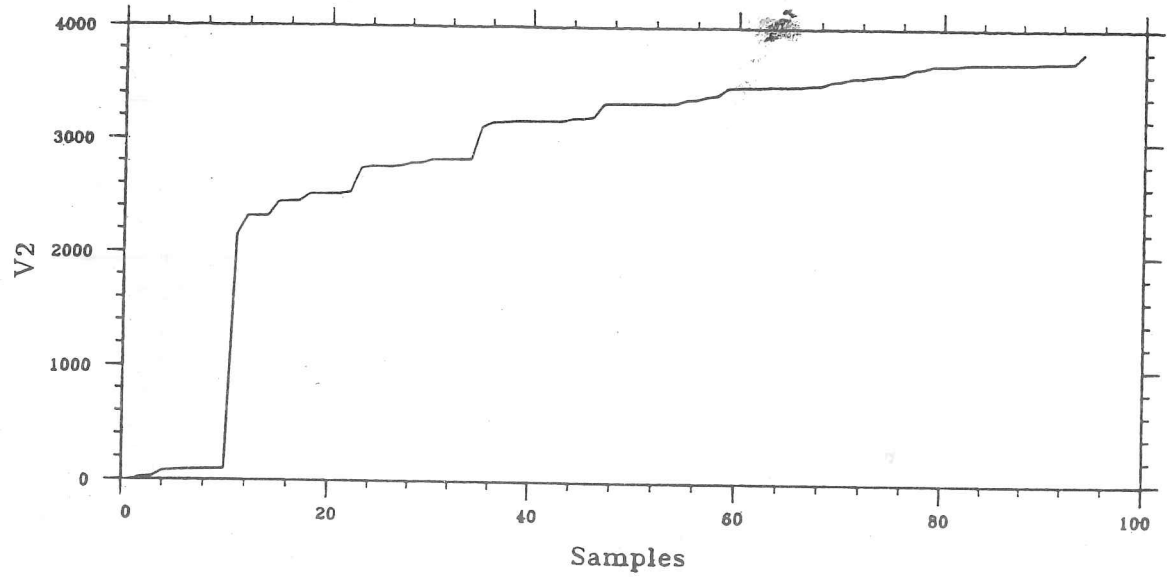

Fig 5.3.b The sum of the squared errors between the predicted and real smoke outputs in the estimate process

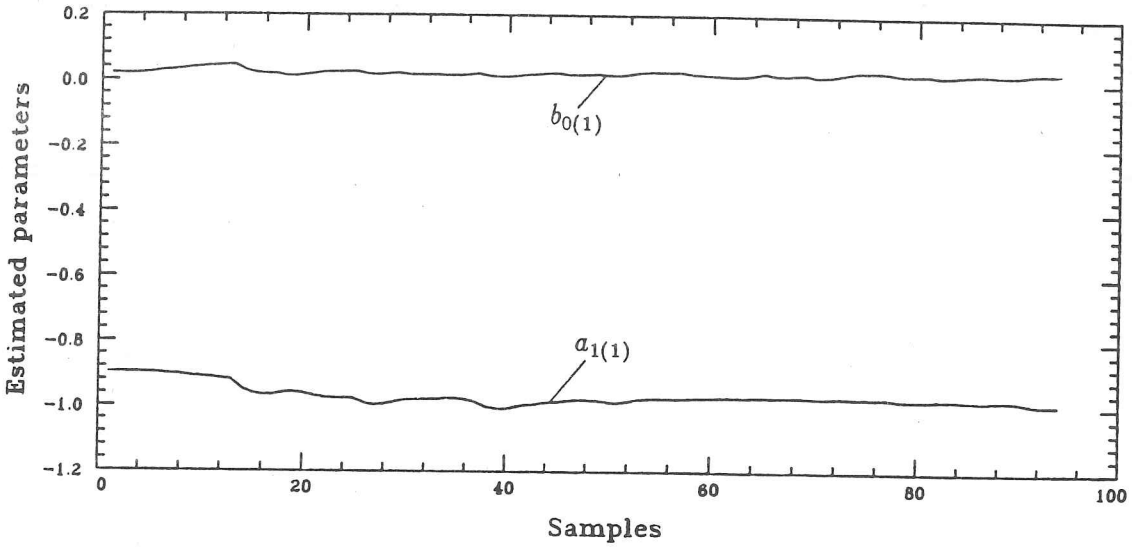

Fig. 5.4.a The estimated parameters of speed-to-fuel rack model

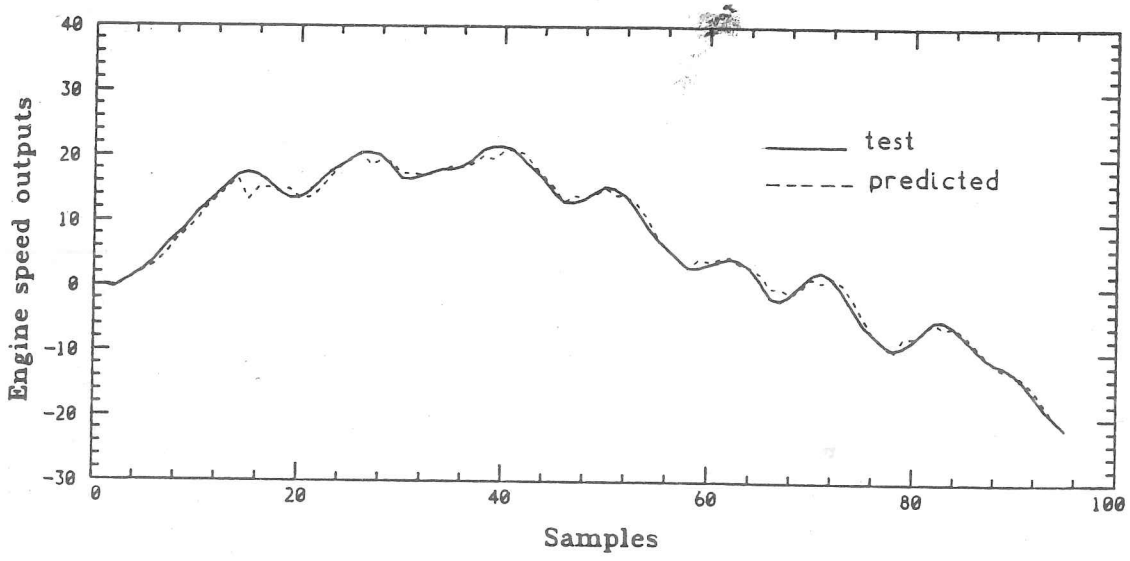

Fig. 5.4.b Comparison of the predicted and real speed outputs

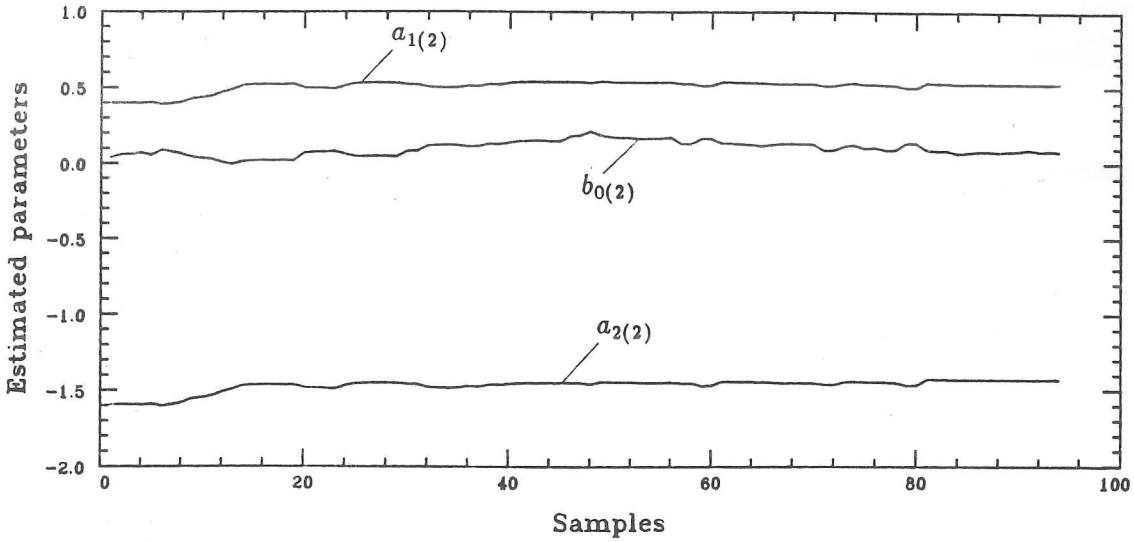

Fig. 5.5.a The estimated parameters of smoke-to-fuel rack model

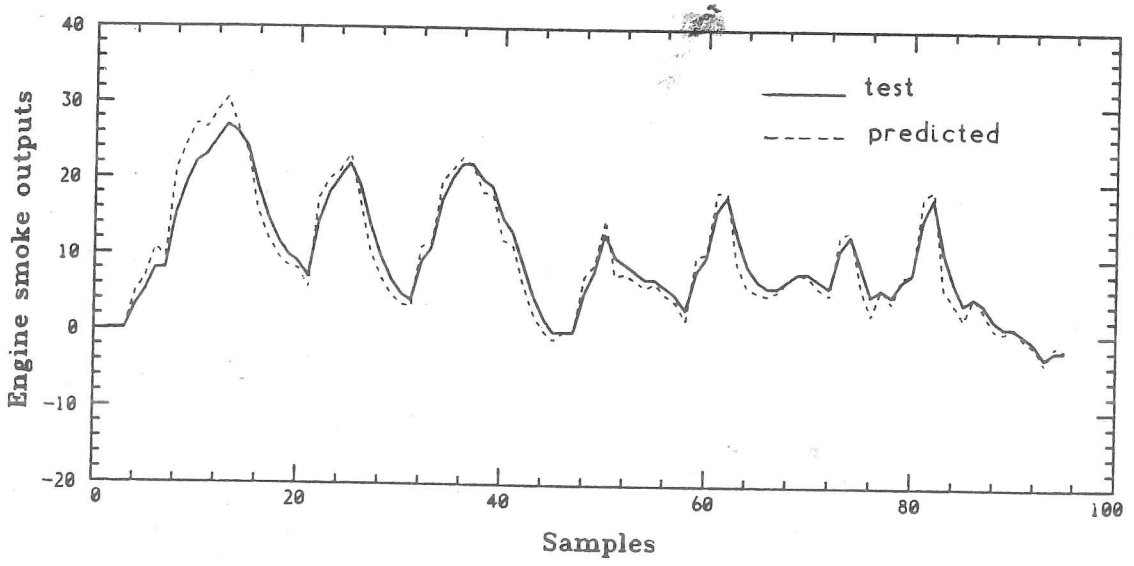

Fig. 5.5.b Comparison of the predicted and real smoke outputs

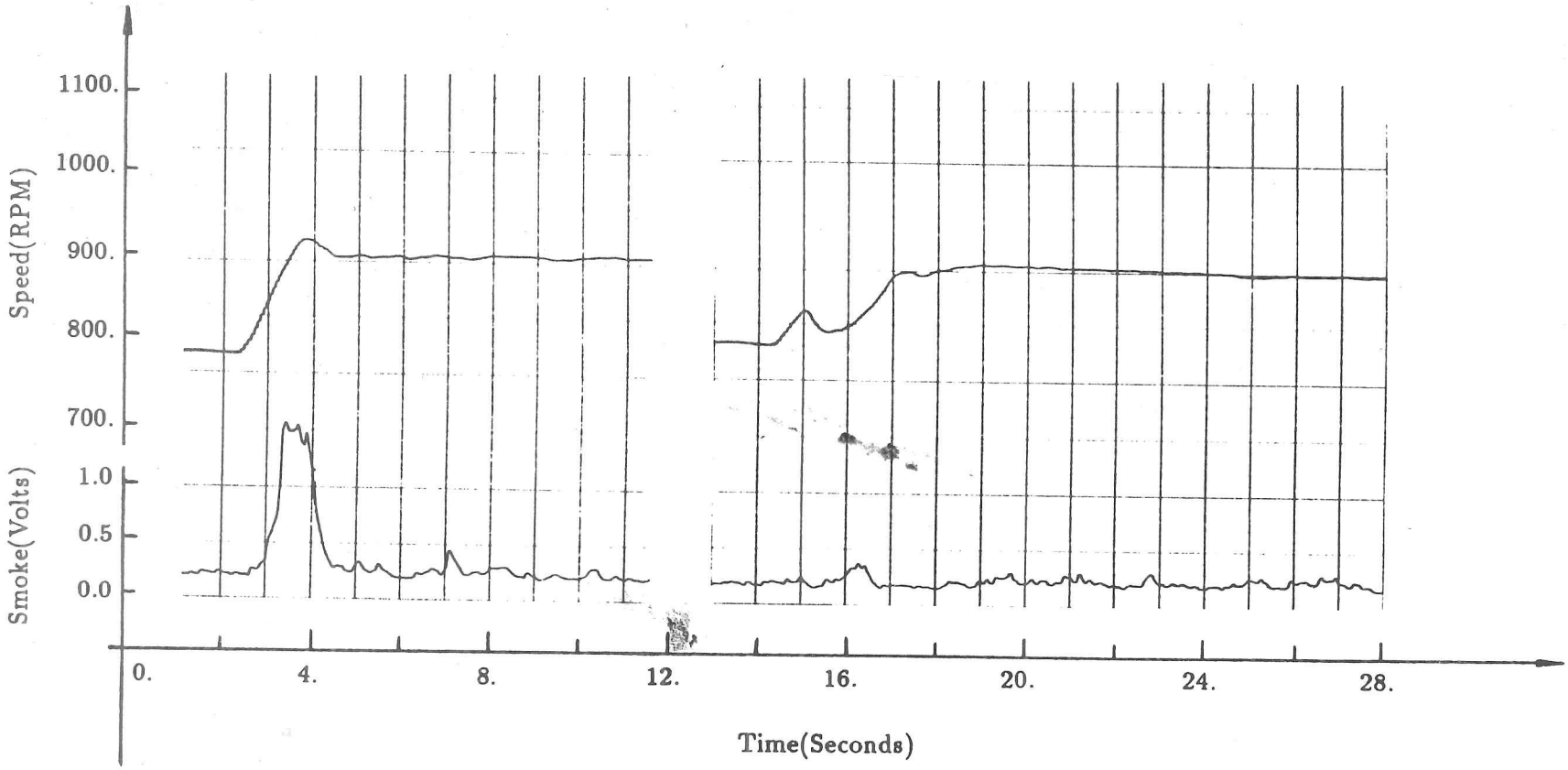

Fig. 5.6 Test results of the pole-assignment controller at heavy load engine condition; $T(z) = (z - 0.1)(z - 0.55)$

a. without smoke control; b. with smoke control

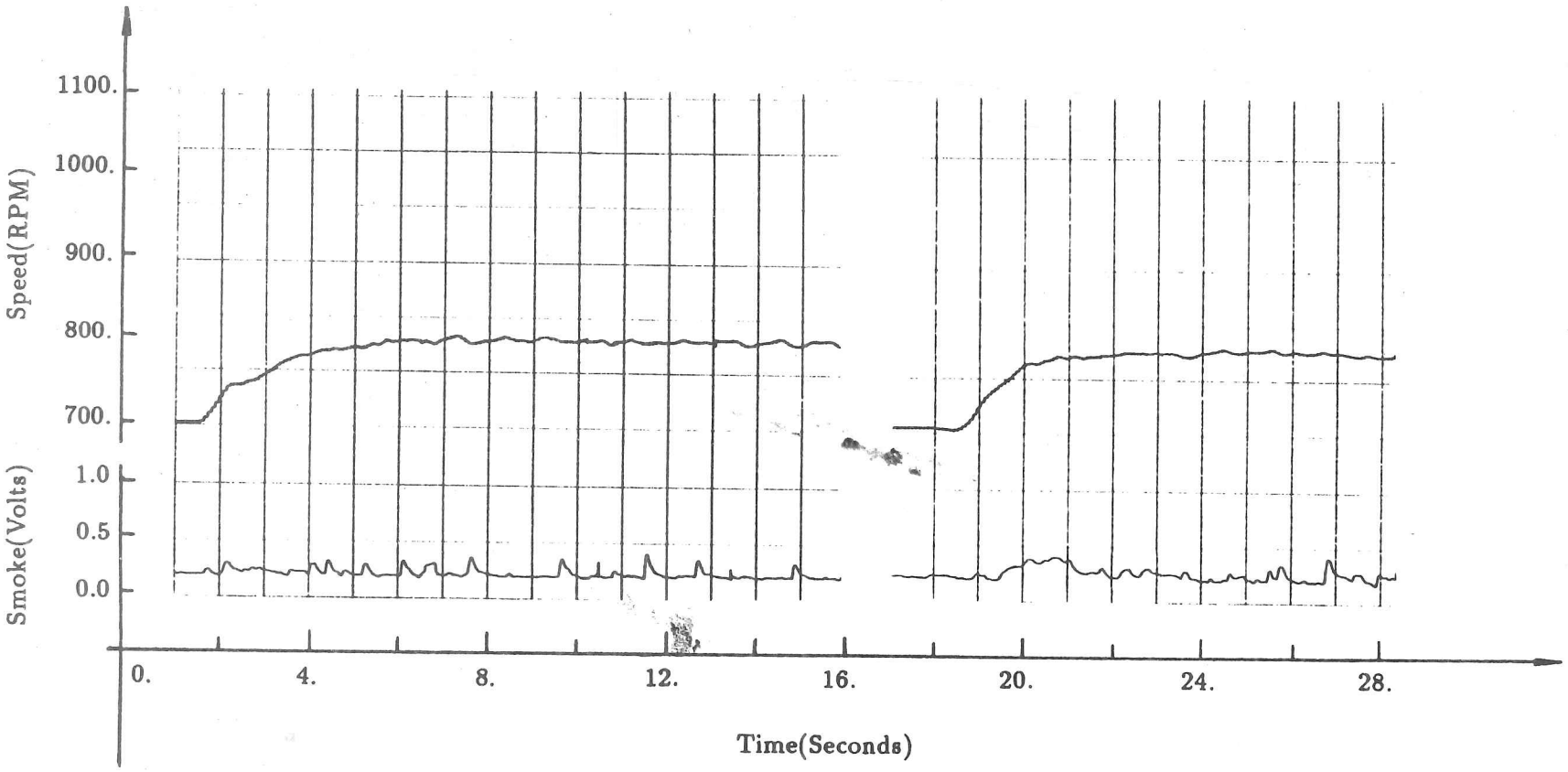

Fig. 5.7 Test results of the pole-assgnment controller at heavy load engine condition; a. $T(z) = (z - 0.75)(z - 0.85)$

b. $T(z) = (z - 0.1)(z - 0.75)$

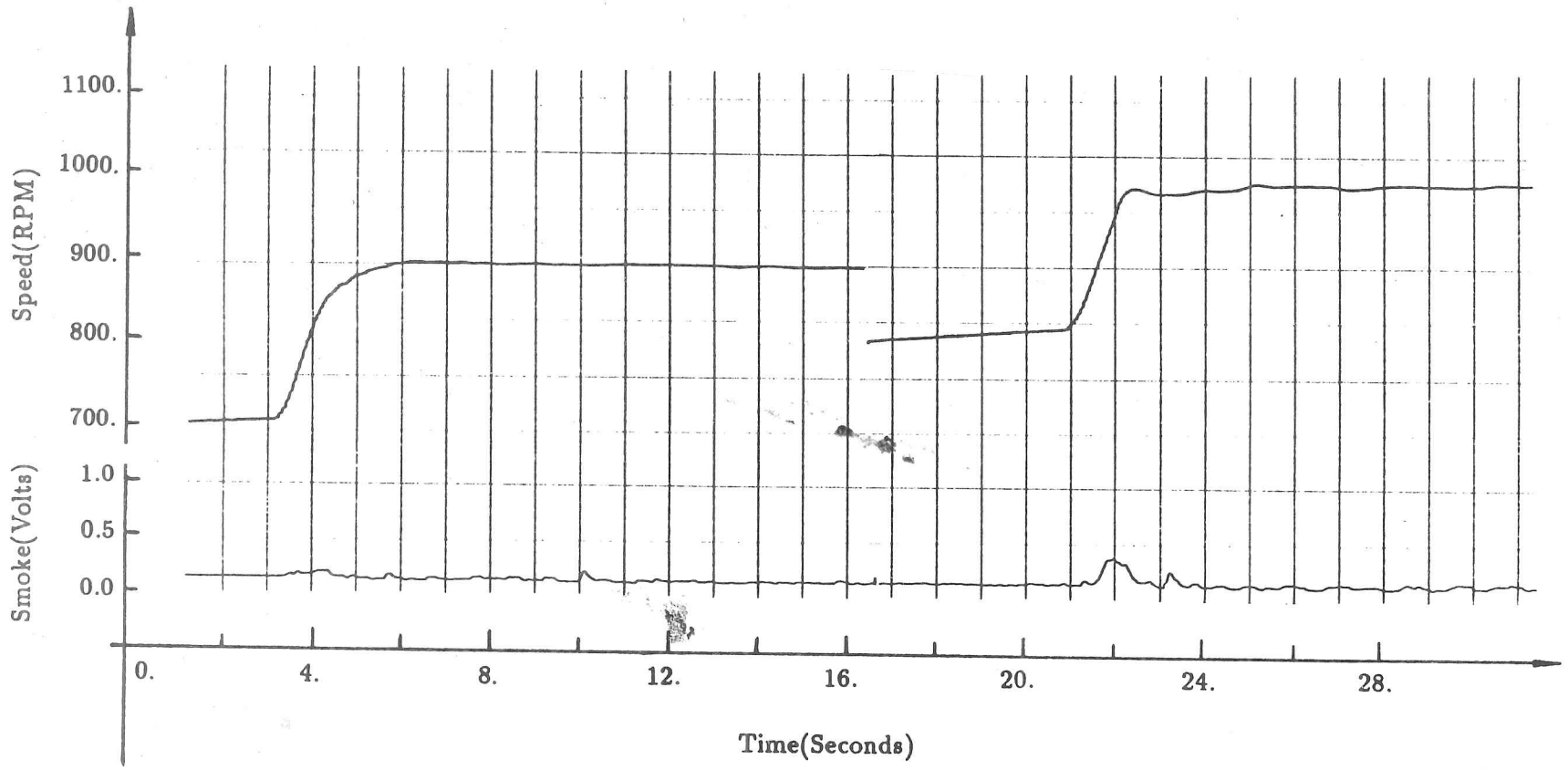

Fig. 5.8 Test results of the pole-assignment controller at light load engine condition; $T(z) = (z - 0.1)(z - 0.75)$

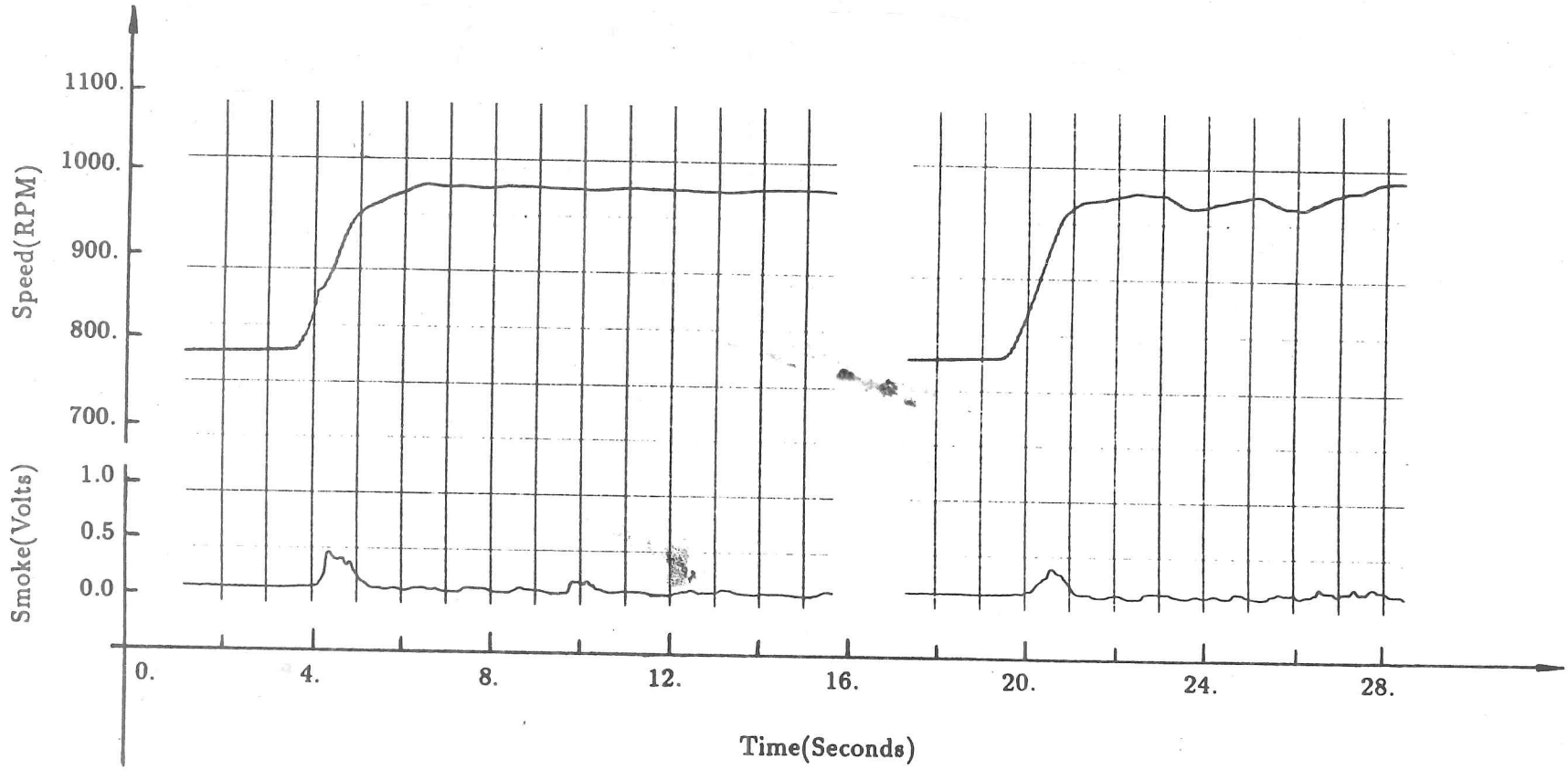

Fig. 5.9 Test results of the pole assignment controller at light load engine condition; $T(z) = (z - 0.1)(z - 0.75)$

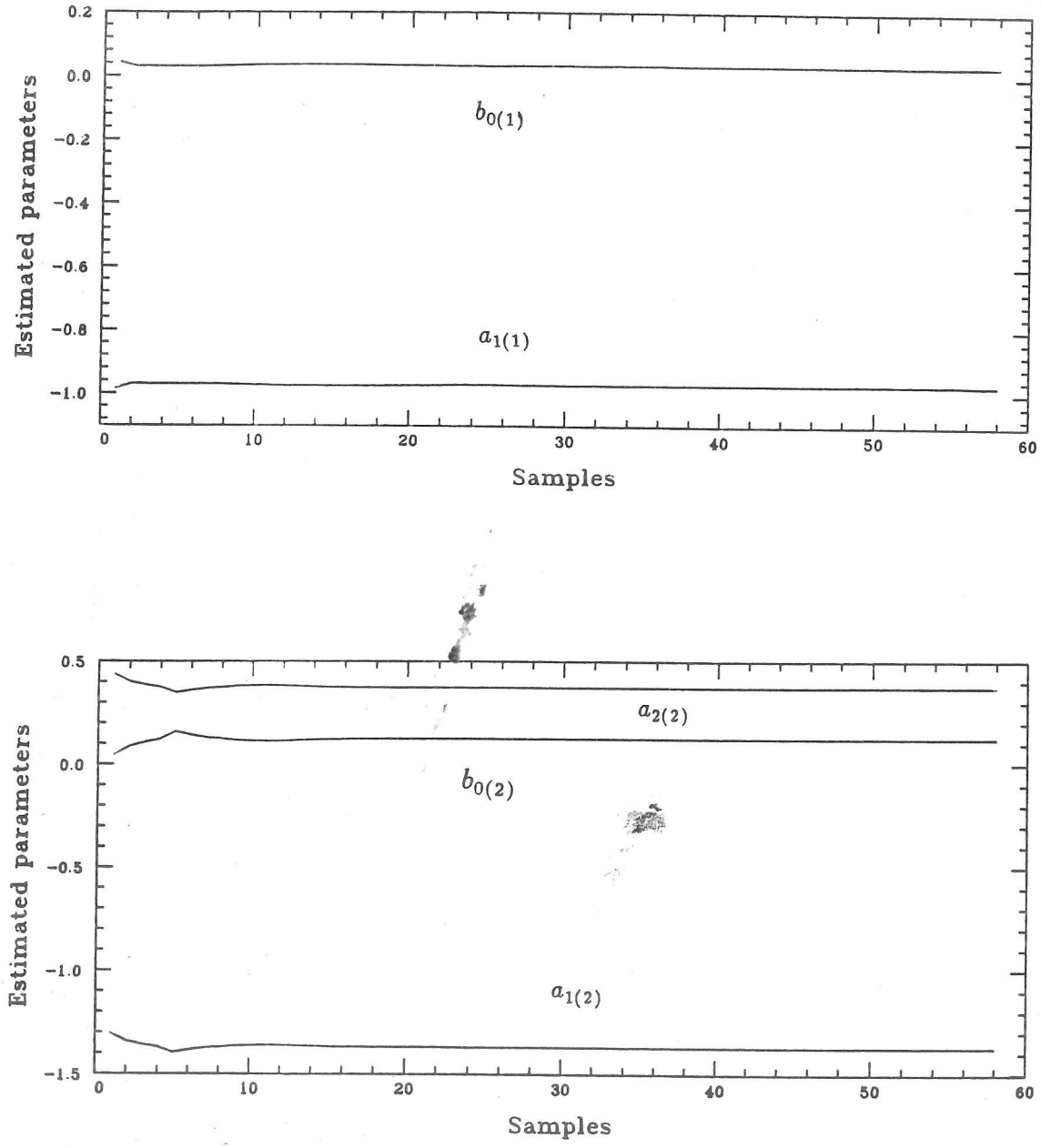

Fig. 5.10 Parameter estimate when the engine speed increases from 800 to 1000RPM with initial load of 36Nm

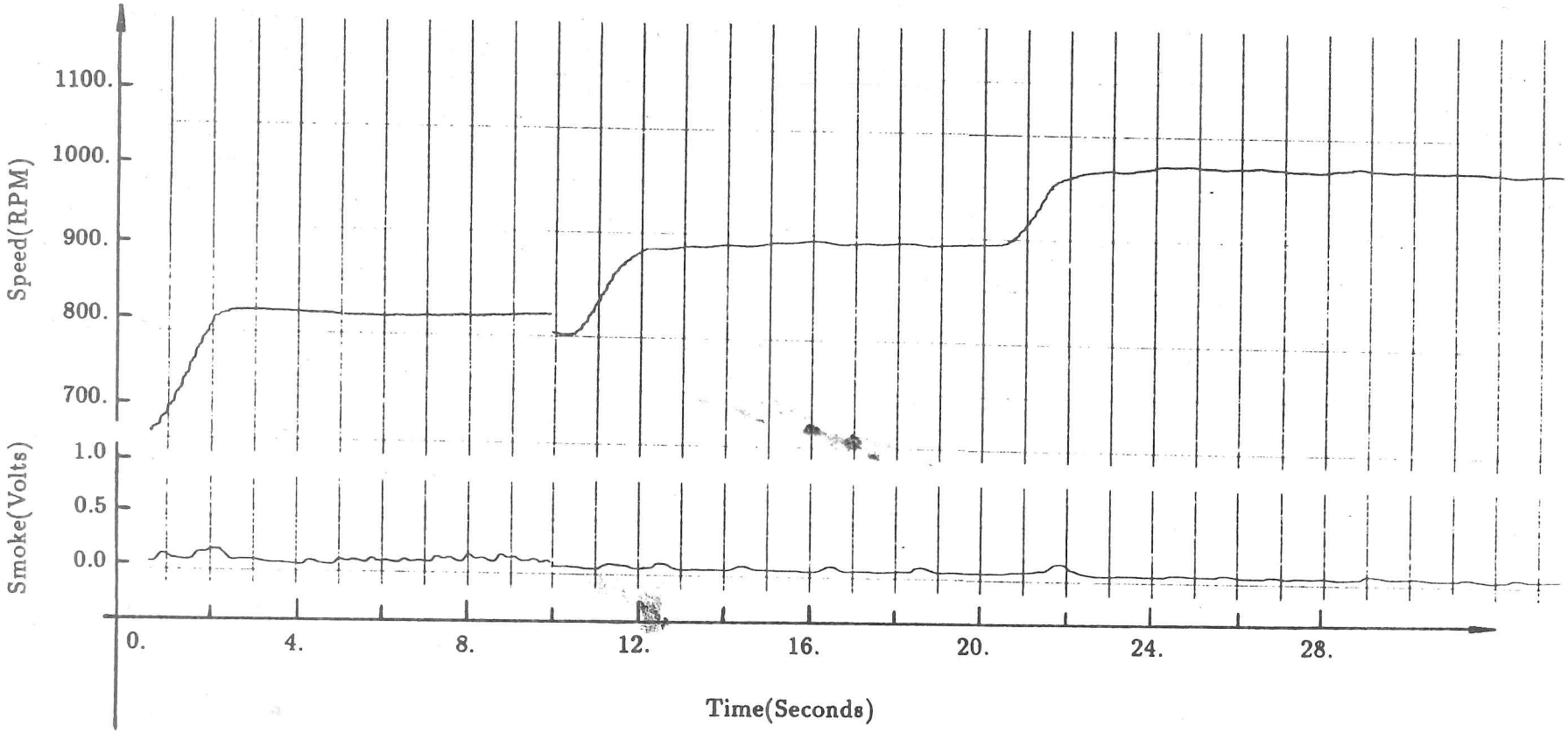

Fig. 5.11 Test results of the PI self-tuning controller

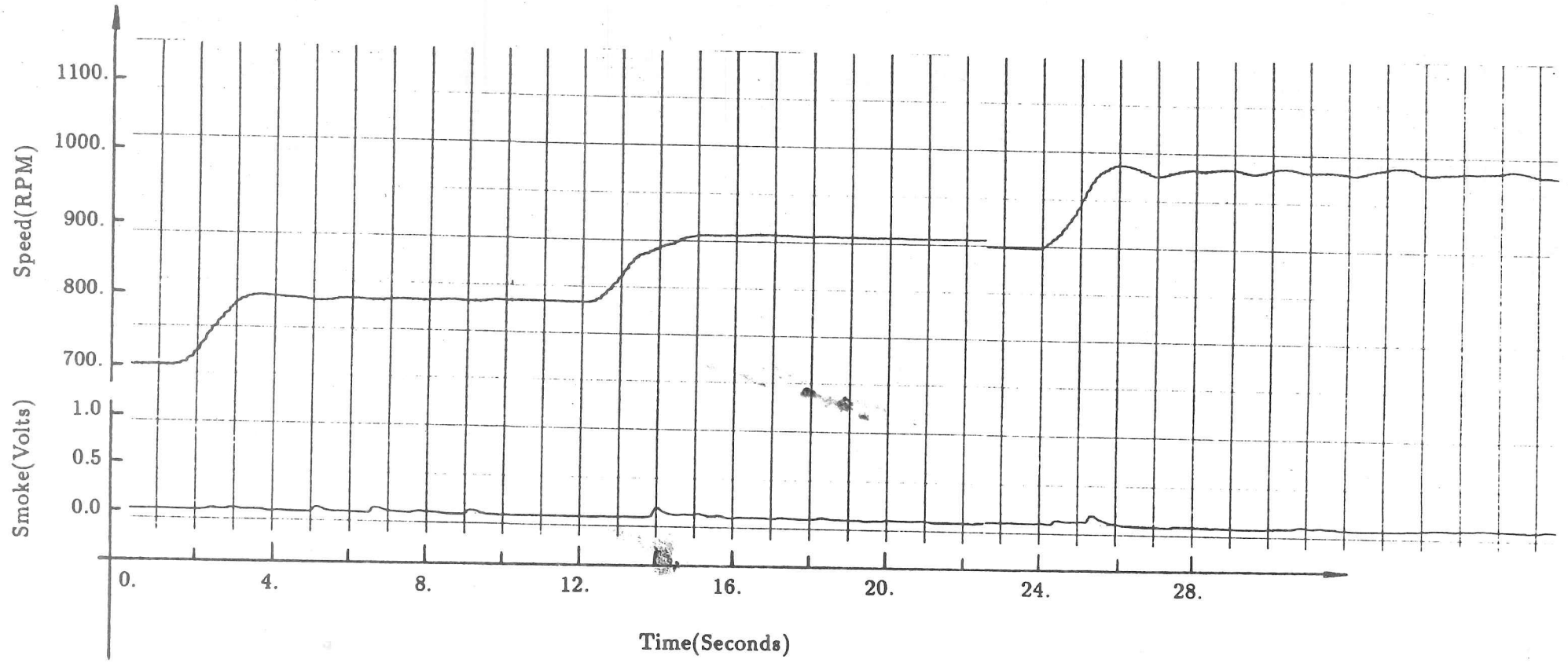

Fig. 5.12 Test results of the non-adaptive PI controller

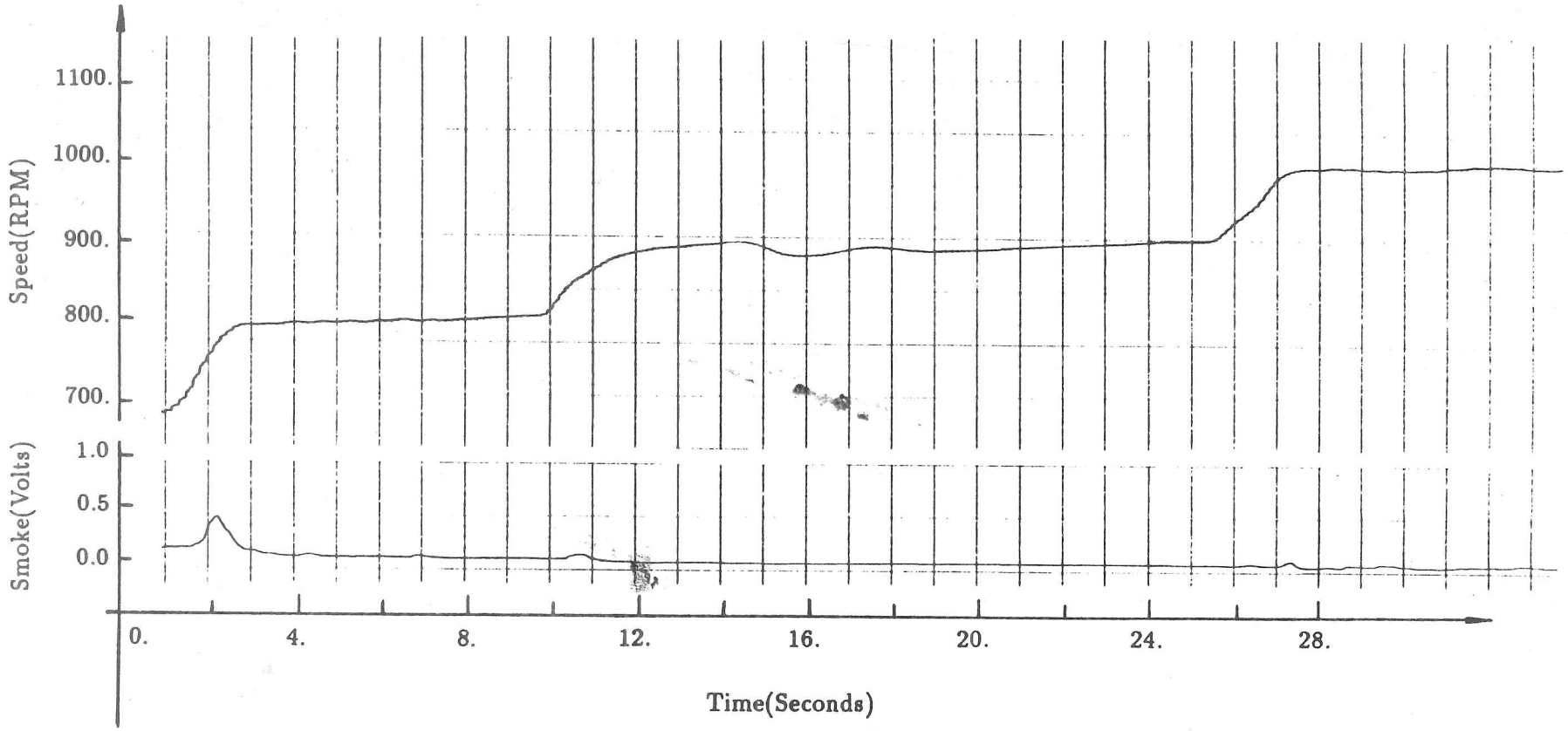

Fig. 5.13 Test results of the PI self-tuning controller

Chapter Six

Conclusions

6.1 Conclusions on the present work

The smoke signal from a sensor installed in the exhaust pipe of a diesel engine has been shown to be very useful in the detection of the smoke emission. A calibration coefficient of 0.87 confirms a good correlation between the Hartridge Units and the outputs of the smoke sensor.

The Recursive Least Square method associated with the synchronisation technique for data acquisition was successfully used for engine modelling.

Two models, speed-to-fuel rack and smoke-to-fuel rack, which were necessary for the control system design, were obtained. Initially the model of smoke-to-fuel rack was investigated with the experimental modelling techniques. It has been found that the model of smoke-to-fuel rack is nonlinear and very difficult to represent with a linear model, even of high order.

The controllers with non-adaptive parameters were very effective in reducing the smoke 'puff' at engine conditions with light loads.

The controllers designed with self-tuning algorithms could work to reach the control objective at engine conditions of heavy load or when the parameters of the models were varying due to the change of engine operation conditions. However, these self-tuning controllers are more complicated than those with fixed parameters and de-tuning might happen to distort the control behaviour. Further work is needed for perfecting this application.

The controllers were implemented on a real engine. The control algorithms were tested and the experimental results obtained demonstrated the the great benefits of the smoke sensor and the values of this engine control system.

6.2 Suggestions to the future work

Based on the present work on engine smoke control, further work can be suggested. This may be clarified into two areas: engine system identification and development of the controllers.

1. Engine system identification

a) Parameter estimate

In the work of engine modelling described in this thesis, the time interval of P.R.B.S. was synchronized with the engine revolution, and also with the sample time interval. The inherent problem with this method is that the sample frequency is fixed with respect to crankshaft angles but changed in time, so the amplitude of the P.R.B.S. has to be small enough to avoid much variation of speed output, i.e. sample time interval. Further work can be done on the data acquisition for parameter estimates with a fixed sample frequency. The sample frequency can be much higher but independent of the engine speed. The time one P.R.B.S. pulse takes can be longer than one or two engine cycles but each pulse still synchronized with the engine revolution. With this method, the discrete nature of the engine is taken into account, and the identified model will not be affected by the sample frequency of data acquisition.

b. Nonlinear modelling of the smoke-to-fuel rack model

The nonlinearity of the smoke-to-fuel model was investigated on a preliminary basis. More work can be done on the further investigation of the model's nonlinearity

and improving the model for more accurate engine smoke control.

2. Development of the engine smoke control system

a) More work can be proposed to improve the self-tuning controller for engine control.

b) Injection timing is a directly controllable parameter for smoke control. A variation in injection timing has a number of effects on engine smoke at steady-state engine conditions. A control system for the engine smoke detection at steady-state can be designed to adjust the injection timing with the feedback of the smoke level to obtain the minimum smoke output at different engine conditions.

c) For the optimal engine control, a smoke sensor can be used to join the integral control system for the sensing of the particle emission.

References

[A1] Aquino, C.F., "Transient A/F control characteristics of the 5 litre central Fuel Injection Engine", *SAE* 810494

[A2] Alkidas, A.C., and Cole, R.M., "Gaseous and particulate emissions from a single-cylinder divided-chamber diesel engine", *SAE* 831288

[A3] Alkidas, A.C., "Relationships between smoke measurement and particulate measurements", *SAE* 840412

[A4] Auiler, J.E., Zbrozek, J.D., and Blumberg, P.N., "Optimization of automotive engine calibration for better fuel economy — methods and applications" *SAE* 770076

[A5] Astrom, K.J., and Eykhoff, P., "System identification — a survey", *Automatica* , Vol. 7, pp. 123–162, 1971

[A6] Astrom, K.J., and Wittenmark, B., "On self-tuning regulators", *Automatica*, Vol. 9,pp. 185-199, 1973

[A7] Astrom, K.J., Borrison, U., Ljung, L., and Wittenmark, B., "Theory and application of self-tuning regulators", *Automatica* , Vol. 13, pp.457-476, 1977

[A8] Astrom, K.J., *Introduction to Stochastic Control Theory*, Academic Press, 1970

[B1] Benson, R.S., Whitehouse, N.D., "Internal combustion engines", Oxford, Pergamon, 1979

[B2] Boccadoro, Y., and Kizer, T., "Adaptive spark control with knock detection", *SAE* 840447

[B3] Broome, D., and Khan, I.M., "The mechanisms of soot release from combustion of Hydrocarbon fuels with particular reference to the diesel engine", *Conference on Air Pollution Control in Transport, Proc. Instn. Mech. Engrs.* , 185(1971)

[B4] Brown, D.G., and Thompson, S., "A novel approach to engine torque speed control", *SAE* 831302

[C1] Cassidy, J.F., "Electronic closed loop control for the automobile", *SAE* 740014

[C2] Cassidy, J.F., "A computerized on-line approach to calculating optimum engine calibration", *SAE* 770078

[C3] Cassidy, J.F., Athans, M., and Lee, W.H., "On the design of electronic automotive engine controls using Linear Quadratic control theory", *IEEE Transaction on Automatic Control*, Vol. AC-25, No. 5, October 1980, pp. 901-912

[C4] Chaudhuri, B., Schwabel, R.J., and Voelkle, L.H., "Speed control integrated into the powertrain computer", *SAE* 860480

[C5] Chang, M. and Sell J. A., "A linear model of engine torque and Carbon Monoxide emissions", *SAE* 830427

[C6] Clarke, D.W., and Gawthrop, P.J., "Self-tuning controller", *Proc. IEE.* Vol. 122, No. 9, 1975, pp. 929-934

[C7] Clarke, D.W., and Gawthrop, P.J., "Self-tuning control", *Proc. IEE.* Vol. 126, No. 6, 1979, pp. 633-640

[C8] Clarke, D.W., "PID algorithms and their computer implementation", *Thans Inst M C* Vol. 6, No. 6, Oct-Dec, 1984

[C9] Cohen, A. I., Randall K.W., Tether, C.D., VanVoorhies, K.L., and Tennant, J.A., "Optimal control of cold automobile engines", *SAE* 840544

[C10] Collings, N., Baker, N., Wolber, W.G., "Real-time smoke sensor for diesel engines", *SAE* 860157

[C11] Collings, N., Hong, G. and Baker, N.J., "Diesel smoke transient control using a real-time smoke sensor", *SAE* 871629

[C12] Cross, R.K., Lakra, P., and O'Neill, C.G., "Electronic fuel injection equipment for controlled combustion in diesel engines", *SAE* 810258

[D1] Dehghani, M.M.A., and Sehitoglu, H., "Optimization of engine controls using Geometric Programming", *SAE* 830429

[D2] Dohner, A.R., "Transient system optimization of an experimental engine control system over the federal emissions driving schedule", *SAE* 780286

[D3] Dobner, D.J., "A mathematical engine model for development of dynamic engine control", *SAE* 800054

[D4] Dobner, D.J., "Dynamic engine models for control development – Part I: nonlinear and linear model formulation", *Int. J. of Vehicle Design*, Special Publication SP4, 1983

[D5] Dorf, R.C., "Modern control system", Addison-Wesley Publishing Company

[E1] Eckard, D.W., and Serve, J.V., "Maintaining low exhaust emissions with turbocharged gas engine using a feedback air-fuel ratio control system", *ASME, Journal of Engineering for Gas Turbine and Power*, Vol. 109, October 1987

[E2] El-lbiary, Y., Jacobsen, R. and Leemhius, R., "Accurate speed control of motors using an Xpert mobile valve", *SAE* 871635

[F1] Flower, J.O., and Hazell, P.A., "Sampled-data theory applied to the modeling and control analysis of compression-ignition engines – Part I",

Int. J. Control, 1971, Vol. 13, No. 3, pp. 549-562

[F2] Flower, J.O., and Hazell, P.A., "Sampled-data theory applied to the modeling and control analysis of compression-ignition engines – Part II", *Int. J. Control*, 1971, Vol. 13, No. 4, pp. 609-623

[F3] Flower, J.O., Windett, G.P., and Forge, S.C., "Aspects of the frequency response testing of simple sampled system", *Int. J. Control*, 1971, Vol. 14, No. 5, pp. 881-896

[F4] Flower, J.O., and Windett, G.P., "Dynamic measurements of a large diesel engine using P.R.B.S. techniques", *Int. J. Control*, 1976, Vol. 24, No. 3

[F5] Franklin, G.F., Powell, J.D. and Emami-Naein, A. *Feedback control of dynamic systems* Addison-Wesley Publishing Company Inc., 1986

[G1] Gettel, L.E., Perry, G.C., Boisvert, J., and O'Sullivan, P.J., "Dual fuel engine control systems for transportation applications", *ASME, Journal of Engineering for Gas Turbines and Power*, Vol. 109, October 1987

[G2] Goodwin, G.C., and Sin, K.S., *Adaptive filtering prediction and control*, Englewood Cliffs, N.J., Prentice-Hall, 1984

[G3] Glikin, P.E., "Fuel injection in diesel engines", *Proc. Instn. Mech. Engrs.* Vol. 199, 1985

[G4] Gorille, I., "Electronic engine management at Bosch", *SAE* 840541

[G5] Greeves, G, and Wang, C.H.T. "Origins of diesel particulate mass emission", *SAE* 810260

[G6] Gupta, A.K., Mehta, P.S., and Gupta, C.P. "Model for predicting air-fuel mixing and combustion for direct injection diesel engine", *SAE* 860331

[H1] Haddad, S. and Watson, N., *Principles and performance in diesel engineering*, Ellis Horwood Ltd., 1984

[H2] Hamburg, D.R., and Shulman, M.A., "A closed-loop A/F control model for internal combustion engines", *SAE* 800826

[H3] Hamburg, D.R., and Klick, D., "The measurement and improvement of the transient A/F characteristics of an electronic fuel injection system", *SAE* 820766

[H4] Harris, C.J., and Billings, S.A., (Eds)., "Self-tuning and adaptive control: theory and applications (IEE Control Engineering series 15)", Peter Peregrinus Ltd, 1981

[H5] Henderson, P.T., Haddox, M.L. and Wells, D., "Diesel engine emissions: a timing control approach", *SAE* 871630

[H6] Hoard, J.W., and Berry, R.D., "New state of the art in engine controls", *SAE* 810061

[I1] Ikegani, M., Li, X., and Nakayama, Y., "Trend and origins of particulate and Hydrocarbon emission from a direct-injection diesel engine", *SAE* 831290

[I2] Ikeura, K., Hosaka, A., and Yano, T., "Microprocessor control bring about better fuel economy with good drivability", *SAE* 800056

[J1] Jacquot, R.G., *Modern digital control systems*, Marcel Dekker, INC., New York and Basel, 1981

[K1] Kam, W.Y., Tham, M.T., Morris, A.J., and Warwick, K., *IFAC Synposium on Identification and System Parameter Estimation*, 1985

[K2] Khan, I.M., "Formation and Combustion of Carbon in a diesel engine", *Proc. Instn. Mech. Engrs.* , 184, Part 3J, 36(1969-70)

[K3] Khan, I.M., Greeves, G., and Probert, D.M., "Prediction of soot and Nitric Oxide concentrations in diesel engine exhaust", *Conference on Air Pollution Control in Transport, Proc. Instn. Mech. Engrs.* , 205(1971)

[K4] Khan, I.M., Greeves, G., and Wang, C.H.T., "Factors affecting smoke and gaseous emissions from direct injection engines and a method of calculation", *SAE* 730169

[K5] Kittelson, D.B. and Collings, N., "Origin of the response of electrostatic particle probes", *SAE* 870476

[K6] Koivo, H.N., "A multivariable self-tuning controller", *Automatica*, Vol. 16, pp. 351-366

[K7] Kyriakides, S.C., and Dent, J.C., "Phenomenological diesel combustion model including smoke and NO emissions", *SAE* 860330

[L1] Laurent, H., Ang, L., and Daly, P., "Integrated engine control – the next step in electronic engine technology", *SAE* 840540

[L2] Leigh, J.R., *Applied digital control*, Prentice-Hall International, UK, LTD, 1985

[L3] Li, X., Inagaki, H., Miwa, K., and Ikegami, M., "Fuel effects on particulate and hydrocarbon emissions from a direct-injection diesel engine", *JSAE Review*, Vol. 8, No. 1

[M1] MacFarlane, A.G.J., "A survey of some recent results in linear multivariable feedback theory", *Automatica*, Vol. 8, pp. 455-492

[M2] MacFarlane, A.G.J., (Ed.), *Complex variable methods for linear multivariable feedback systems*, London: Taylor and Francis, 1980

[M3] Marshell, J.E., *Control of time-delay system* (IEE Control Engineering Series 1), Stevenage, Peter Peregrinus, 1979

[M4] Michelberger, P., Boker, J., Keresztes, A., and Varlaki, P., "Identification of a multivariable linear model for road vehicle(bus) dynamics from test data", *Int. J. of Vehicle Design*, Vol. 8, No. 1, 1987

[M5] Mihele, W.P., and Citron, S.J., "An adaptive idle mode control system", *SAE* 840443

[M6] Millington, B.W., and French, C.C.J., "Diesel exhaust – a European viewpoint", *SAE* 660549

[M7] Miyagi, H., Nagase, M., Nakano, J., and Kobashi, M., "TOYOTA electronic control system for a diesel engine", *SAE* 830862

[M8] Moon, K.C., "Charging mechanism of submicro diesel particles", Ph.D. Thesis, submitted to the University of Minnesota, August 1984

[M9] Morris. R.L., Borcherts, R.H., Warlick, M.V., and Hopkinst, H.G., "Spark ignition engine model building – an identification approach to throttle-torque response", *Int. J. of Vehicle Design*, Vol. 3, No. 1, 1982

[N1] Narendra, K.S., and Monopoli, R.V., *Application of adaptive control*, Academic Press INC., 1980

[N2] Nisimura, Y., and Ishii, K., "Engine idle stability analysis and control", *SAE* 860415

[O1] Olsson, G., Cohen, A.I. and Rao, H.S., "An approach to Air-Fuel ratio control for automobile engines using self-tuning regulators", 0191-2216/81/0000-1431 *IEEE* 1981

[P1] Pipho, M.J., ambs, J.L. and Kittelson, D.B., "In-cylinder measurements of particulate formation in an direct injection diesel engine", *SAE* 860024

[P2] Powers, W.F., "Internal combustion engine control system research at Ford", 0191-2216/81/0000-1447 *IEEE* 1981

[P3] Prabhakar, R., Citron, S.J., Goodson, R.E., "Optimization of automotive engine fuel economy and emissions", *ASME, Journal of Dynamic Systems, Measurement and Control*, June 1977/109

[R1] Rao, H.S., Cohen, A.I., Tennant, J.A., and Voorhies, K.L.V., "Engine control optimization via nonlinear programming", *SAE* 790177

[R2] Reams, L.A., Wiemero, T.A., Levin, M.B., and Wade, W.R., "Capability of diesel electronic fuel control", *SAE* 820449

[R3] Ricardo and Co. Engineers(1927) Ltd., "Diesel research and special engine projects", Report on the preliminary investigation of the Ricardo electronic smokemeter, pp. 11658 (March 5, 1969)

[R4] Ricardo and Co. Engineers(1927) Ltd., "Development of electronic smokemeter", Summary, pp. 12924 (July 23, 1970)

[R5] Rillings, J.H., "Application of modern control theory to engine control", 0191-2216/81/0000-1439 *IEEE* 1981

[R6] Ring, H.J., "Diesel electronic engine emission controls", *SAE* 840545

[R7] Rillings, J.H., "Engine control system sensitivity", *SAE* 820386

[R8] Rumsey, A.F., and Powner, E.T., "Digital-computer control of vehicle in an automated transportation system", *Proc. Instn. Mech. Engrs.*, Vol. 120, No. 10, Oct. 1973

[S1] Schmidt, R.C., Carey, A.W., and Kamo, R., "Exhaust characteristics of automotive diesel",*SAE* 660550

[S2] Schumann, R., "Design and application of multivariable self-tuning controllers", *IFAC Symposium on Identification and System Parameter Estimation* 1985

[S3] Schwab, M., "Electronic control of a 4-speed automatic transmission with lock-up clutch", *SAE* 840448

[S4] Schwarzenbach, J. and Gill, K.F., *System modelling and control*, Edward Arnold, 1984

[S5] Sehweimer, G.W., "Ion probe in the exhaust manifold of diesel engines", *SAE* 860012

[S6] Sell, J.A., and Chang, M.F., "Closed-loop control of an engine's Carbon Monoxide emissions using an Infrared Diode Laser", *SAE* 820388

[S7] Shinoda, K., Koide, H., Kobayashi, F., Nagase, M., Okeda, S., Takata, M., and Nakano, J., "Development of new electronic control system for a diesel engine"*SAE* 860597

[S8] Simon, G.M., and Terrence L. S., "Diesel exhaust particulate control techniques for light-duty trucks", *SAE* 860137

[S9] Sobolak, S.J., "Simulation of the Ford vehicle speed control system", *SAE* 820777

[S10] Spring, G.S., and Patterson, D.J., *Engine emission*, PLenum Press, New York–London, 1973

[S11] Stivender, D.L., "Engine air control-basis on a vehicular systems control hierarchy", *SAE* 780346

[S12] Sweet, L.M., "Control systems for automotive vehicle fuel economy: a literature review", *ASME Journal of Dynamic Systems, Measurement and Control*, September 1981, Vol. 103/173

[S13] Sweet, L.M., "Automotive application of modern control theory", *SAE* 820913

[T1] Takahashi, T., Ueno, T., Yamamoto, A., and Sanbuichi, H., "A simple engine model for idle speed control", *SAE* 850291

[T2] Toyada, T., Inoue, T., and Aoki, K., "Single point electronic injection system", *SAE* 820902

[T3] Trenne, M.U. and Ires, A.P., "closed loop design for electronic diesel injection system", *SAE* 820447

[T4] Tsai, S.C., and Goyal, M.R., "Dynamic turbocharged diesel engine model for control analysis and design" *SAE* 860455

[V1] Van De Vegte, J., "Classical design of two-by-two systems", *Int. J. Control*, Vol. 35, No. 3, pp. 477-489, 1982

[V2] Vergear, H.C., Lawson, A., Jones, W.M., and Robinson, W., "Development of an emission control system for two-stroke diesel powered transient coaches", *SAE* 860133

[W1] Waiz, L., Wessel, W., and Berger, J., "Progress in electronic diesel control", *SAE* 840442

[W2] Warwick, K., "Simplified parameter adaptive control" *Optimal Control Applications and Methods*, Vol. 8, 37-48(1987)

[W3] Welbourn, D.B., Robert, D.K., and Fuller, R.A., "Governing of compression-ignition oil engines", *Proc. Instn. Mech. Engrs.*, Vol. 173, No. 22, 1959

[W4] Wellstead, P.E., and Zanker, P., "Techniques of self-tuning", Control System Centre report No. 432, UMIST, 1978 UMIST

[W5] Wellstead, P.E., "Self-tuning digital control systems: the pole-zero assignment approach", Control System Centre report No. 490, UMIST, 1980

[W6] Wessel, W.G., "A strategy for optimization of diesel fuel injection system", *SAE* 790036

[W7] Widdershoven, J. and Pischinger, F., "Possibilities of particle reduction for diesel engines", *SAE* 860013

[W8] Windett, G.P., and Flower, J.O., "Sampled-data frequency response measurement of a large diesel engine", *Int. J. Control*, Vol. 19, No. 6, 1974, pp.1069-1086

[W9] Wolber, W.G., "Automotive engine control sensors' 80", *SAE* 800121

[Y1] Yaegashi, T., Ohashi, M., Kawobe, K., and Mizuno, I., "Development of computer-aided experiment system for electronic controlled engines",

JSAE Review, Vol. 7, No. 1, ISSN 0389-4304

[Y2] Yuan, Z., "On PID self-tuning regulators and its practical applications", *IFAC Synposium on Identification and System Parameter Estimation* 1985

[Z1] Zames, G., "Feedback, minimax sensitivity, and optimal robustness", *IEEE Transactions on Automatic Control*, Vol. AC-28, No. 5, May 1983

[Z2] Zanker, P.M., and Wellstead, P.E., "On self-tuning diesel engine governors", Control System Centre report No. 422, UMIST, 1978

Appendix A

Analysis of the steady-state error of the engine speed

The steady-state speed error of the engine control system is

$$e_{ss} = \lim_{z\to 1}(z-1)[Y_1(z^{-1}) - R_1(z^{-1})]$$

$$= \lim_{z\to 1}(z-1)\left(\frac{Y_1(z^{-1})}{R_1(z^{-1})} - 1\right)\cdot R_1(z^{-1})$$

$$R_1(z^{-1}) = \frac{z}{z-1}$$

$$e_{ss} = \lim_{z\to 1}(z-1)\left(\frac{Y_1(z^{-1})}{R_1(z^{-1})} - 1\right)\cdot\frac{z}{z-1}$$

$$= \lim_{z\to 1}\left(\frac{Y_1(z^{-1})}{R_1(z^{-1})} - 1\right)$$

1) The steady-state speed error of the system 1

$$\frac{Y_1(z^{-1})}{R_1(z^{-1})} - 1 = \frac{C_1(z^{-1})G_1(z^{-1})}{1 + C_1(z^{-1})G_1(z^{-1}) + C_1(z^{-1})C_2(z^{-1})G_2(z^{-1})} - 1$$

$$= \frac{k_0\frac{z-f_0}{z-1}\cdot\frac{b_{0(1)}z}{(z-p_{1(1)})(z-p_{1(2)})}}{1 + k_0\frac{z-f_0}{z-1}\frac{b_{0(1)}z}{(z-p_{1(1)})(z-p_{1(2)})} + k_{p2}k_0\frac{z-f_0}{z-1}\frac{b_{0(2)}}{(z-p_{2(1)})(z-p_{2(2)})}} - 1$$

$$= \frac{k_0(z-f_0)\frac{b_{0(1)}z}{(z-p_{1(1)})(z-p_{1(2)})}}{(z-1)+k_0\frac{b_{0(1)}z(z-f_0)}{(z-p_{1(1)})(z-p_{1(2)})}+k_{p2}k_0\frac{b_{0(2)}(z-f_0)}{(z-p_{2(1)})(z-p_{2(2)})}} - 1$$

$$e_{ss} = \lim_{z\to 1}\left(\frac{Y_1(z^{-1})}{R_1(z^{-1})} - 1\right) = 0$$

2) The steady-state speed error of system 2

$$\frac{Y_1(z^{-1})}{R_1(z^{-1})} - 1 = \frac{C_1(z^{-1})G_1(z^{-1})}{1+C_1(z^{-1})G_1(z^{-1})+C_2(z^{-1})G_2(z^{-1})} - 1$$

$$= \frac{k_0\frac{z-f_0}{z-1}\cdot\frac{b_{0(1)}z}{(z-p_{1(1)})(z-p_{1(2)})}}{1+k_0\frac{z-f_0}{z-1}\frac{b_{0(1)}z}{(z-p_{1(1)})(z-p_{1(2)})}+k_{p2}\frac{b_{0(2)}}{(z-p_{2(1)})(z-p_{2(2)})}} - 1$$

$$= \frac{k_0(z-f_0)\frac{b_{0(1)}z}{(z-p_{1(1)})(z-p_{1(2)})}}{(z-1)+k_0\frac{b_{0(1)}z(z-f_0)}{(z-p_{1(1)})(z-p_{1(2)})}+k_{p2}(z-1)\frac{b_{0(2)}}{(z-p_{2(1)})(z-p_{2(2)})}} - 1$$

$$e_{ss} = \lim_{z\to 1}\left(\frac{Y_1(z^{-1})}{R_1(z^{-1})} - 1\right) = 0$$